UNIVERSITY OF OKLAHOMA

GRADUATE COLLEGE

CHROMOSOME ORGANIZATION AND SEGREGATION IN PSEUDOMONAS AERUGINOSA

A DISSERTATION

SUBMITTED TO THE GRADUATE FACULTY

in partial fulfillment of the requirements for the

Degree of

DOCTOR OF PHILOSOPHY

By

BIJIT KUMAR BHOWMIK
Norman, Oklahoma
2017

CHROMOSOME ORGANIZATION AND SEGREGATION IN PSEUDOMONAS AERUGINOSA

A DISSERTATION APPROVED FOR THE
DEPARTMENT OF CHEMISTRY AND BIOCHEMISTRY

BY

_____
Dr. Valentin V. Rybenkov, Chair

_____
Dr. Elena Zgurskaya

_____
Dr. Rakhi Rajan

_____
Dr. Christina Bourne

_____
Dr. Marc Libault

© Copyright by BIJIT KUMAR BHOWMIK 2017
All Rights Reserved.

Acknowledgements

At the culmination of my graduate study, I would like to express my sincere gratitude to all of my family and friends for their continuous support and encouragement. Without their help this would never be possible.

I especially want to thank Dr. Rybenkov for his guidance, patience and support throughout my graduate studies. He not only taught me how designing new experiments but has also encouraged me to think through particular problems with great scientific insight. His guidance and encouragement has helped me to develop into a better scientist. I also want to extend my gratitude to my graduate committee members Dr. Zgurskaya, Dr. Rajan, Dr. Bourne and Dr. Libault for all of their time, attention and encouragement. Additionally, I would like to thank Dr. Schroeder and Dr. Hansmann for their valuable feedback during my graduate studies.

I would like to thank my lab members Dr. Petrushenko, Dr. Sarkar, Dr. Weeks, and Dr. Krishnamoorthy for sharing their knowledge and experience. I would like to specially thank Dr. Zhao for allowing me to use his experimental data. I also want to thank Dr. Benjamin Smith for helping me with microscopy as well as my colleagues, Dr. Wolloscheck, April Clevenger, Viridiana Herrera and Casey Stevens for sharing their knowledge and enthusiasm.

Finally, I want to express my deepest thanks to my parents and my fiancée Koel Biswas for their love, blessings, support, patience and sacrifice.

Table of Contents

List of Tables

List of Figures

Abstract

The faithful propagation of genetic information from a mother to its progeny is one of the most fundamental aspects of life. Encoding the entirety of an organisms' genetic information onto chromosomes poses a unique set of problems that cells are required to overcome for proper genetic flow. In bacteria, one or more DNA molecules are condensed almost 1000-fold in order to fit within the small vicinity of a single cell. While undergoing significant compaction, the chromosome must also retain its accessibility in order to perform various DNA dependent processes. Although several key elements of chromosome organization have been identified, our knowledge regarding this process remains limited. In order to maintain genetic integrity, newly replicated chromosomes must faithfully segregate into daughter cells before the completion of cell division. Unlike in eukaryotes, chromosome replication and segregation in bacteria occur concurrently. How a bacterial chromosome maintains coordination between replication, segregation, and cell division is still unclear. The role of chromosome organization in segregation is also not fully understood. Therefore, it is of the utmost importance to acquire a better understanding of these complex biological processes which will in-turn illuminate our comprehension of the most basic and fundamental aspects of life. Elucidation of such processes will enable the potential to better manipulate chromosomes which can have various applications including but not limited to anti-microbial drug discovery, anti-cancer therapy, and creating programmable artificial cells.

This study investigated chromosome segregation in an opportunistic human pathogen, *Pseudomonas aeruginosa*. *Pseudomonas* related infections are one of the major causes of death in newly born babies, burn victims, cystic fibrosis patients, and patients with suppressed immune system. The ability of this organism to differentiate into different morphological states allows it to survive in various ecological niches. Its intrinsic multi-drug resistance and ability to form biofilms make it difficult to control. With the emergence of multi-drug resistant strains of *Pseudomonas aeruginosa,* the discovery of new drugs is imperative in order to prevent further transmission of this organism. A better understanding of chromosome dynamics can help identify and exploit novel drug targets.

To determine the segregation pattern in the *P. aeruginosa* strain PAO1, a fluorescent repressor-operator system was used. The data indicate that the PAO1 chromosome is longitudinally organized between the origin of replication site, *oriC* to the sister chromosome resolution site, *dif*. In PAO1, both replication and segregation initiate at *oriC* and progress bidirectionally. Interestingly, chromosome segregation but not replication ends at the *dif* site. Proteins of the condensin family play a major role in global chromosome organization in both prokaryotes and eukaryotes. In *Pseudomonas aeruginosa,* two different families of condensins are present: MksBEF and SMC-ScpAB. These two proteins localize on different regions of the chromosome and differentially affect chromosome segregation. Finally, the study uncovered a novel co-ordination between condensin mediated global chromosome organization and ParAB*S*

mediated chromosome segregation, where the presence of at least one of them is necessary for cell viability.

Summary

DNA serves as the primary molecule for the storage and propagation of genetic information. The enormous length of the chromosomal DNA poses a unique set of problems. A single human cell contains approximately 3 meters of double stranded DNA within a nucleus of about 6 μm. It is still unclear how this long thread of DNA is organized within such small confines while maintaining its individuality [1], and is capable of performing several key biological functions. In eukaryotes, each DNA molecule is condensed 10,000 to 20,000-fold, forming chromosomes. Multiple histone and non-histone proteins contribute to this compaction [2, 3]. Although relatively small in length, bacterial DNA also needs to overcome similar problems in order to condense its >1 mm long DNA into a cell which is approximately 2-4 μm long [4].

While the circular DNA in bacteria needs to be compacted about a 1000-fold, it also needs to maintain a certain degree of flexibility to allow various cellular machineries access to the genetic information which it encodes. Bacterial cells achieve this by organizing the chromosome into several dynamic structures. Meanwhile, chromosomes need to be segregated faithfully after replication so that each daughter cell can inherit a single copy of the entire genome. Therefore, harmony between global chromosome organization and chromosome segregation is vital for proper maintenance and transfer of genetic information. At the same time, these two events also require coordination with chromosome replication and the cell cycle for maintaining the proper chain of events.

It is often instructive to distinguish three levels of complexities in organization of bacterial chromosome. The first level of organization is achieved by small DNA binding proteins known as Nucleoid Associated Proteins (NAPs). These proteins organize DNA by binding, bending and wrapping it around themselves [5, 6]. At the second level, DNA is organized into giant loops around a protein scaffold. Condensins and cohesins play a major role in this global chromosome organization [7]. Finally, the chromosome is organized at the subcellular level, where each locus of the chromosome occupies a specific region inside the cell [8]. This spatial organization of the chromosome is maintained throughout the cell cycle. This level of organization has only recently been recognized and is presently under intense investigation. [9]. Subcellular organization of chromosome is of particular interest because it is deeply interlinked with chromosome segregation, a fundamental cellular process that ensures correct inheritance of genetic information by daughter cells. Indeed, chromosome segregation reproduces global chromosomal layout whereas perturbation in chromosomal layout is often detrimental to cell viability [10].

In this study, we explored the idea that condensins not only establish global folding of the chromosome but also play a key role in facilitating subcellular positioning and segregation of the chromosome. This idea is based on the observation that deletion of condensins results in both chromosome decondensation and missegregation [11-13]. To test this idea, we investigated the roles of condensins in *Pseudomonas aeruginosa.*

P. aeruginosa is an opportunistic human pathogen that is responsible for high mortality in newly born babies, burn victims and cystic fibrosis patients. It is one of the most common hospital acquired pathogens and causes serious diseases in patients recovering from surgery or having a compromised immune system. Emergence of multi-drug resistant strains of *Pseudomonas aeruginosa* has become a serious human health issue worldwide [14, 15]. Therefore, understanding the underlying mechanism of chromosome organization and segregation can provide us with novel methods to control infections caused by this pathogen.

The second benefit of using *P. aeruginosa* for this study is that it harbors condensins of two different families: a canonical SMC-ScpAB and a recently discovered condensin MksBEF [16]. The role of MksBEF in chromosome organization is yet to be established. Remarkably, SMC-ScpAB and MksBEF were found to support different morphological states. SMC-ScpAB facilitates planktonic growth whereas, MksBEF promotes sessile growth [17]. This suggest that a causative link might exist between chromosome organization and cell physiology in *P. aeruginosa*.

For this study, we used the *P. aeruginosa* strain PAO1. The chromosome of PAO1 is asymmetrically organized into two arms between the origin of replication site (*oriC*) and the sister-chromosome dimer resolution site (*dif*) [18]. These two sites have special roles in chromosome replication and segregation. In model laboratory bacteria *E. coli* and *B. subtilis*, *oriC* and *dif* are located opposite to each other, generating a symmetrically oriented chromosome [19,

20]. In these bacteria, both replication and segregation take place concomitantly. Both processes start at the *oriC* locus and end at *dif*. However, many bacteria, similar to PAO1, carry an asymmetric chromosome; no such organism has been previously studied for replication and segregation. Therefore, studying PAO1 chromosome will also help us to better understand the coordination between replication and segregation.

Finally, this system also allows us to answer a fundamental biological question: what are the driving forces for chromosome segregation? Currently, three systems are postulated as the driving forces in segregation [21, 22]. The first one is condensins, which condense the chromosomes and help maintain them topologically unlinked. The second system is the ParAB*S* system, which is required for proper positioning of newly replicated chromosome. The third force is entropy, which can segregate chromosomes if another mechanism that topologically separates sister chromosomes is present. These three forces interact with each other. In particular, SMC proteins are recruited to *parS* sites in a ParB dependent manner [23, 24]. As a result, deducing relative contributions of these three forces is difficult. As we will show later, delineating the driving forces in chromosome segregation is possible in *P. aeruginosa*, owing to the presence of two different condensins along with the ParAB*S* system.

In this study, we explored the chromosomal layout and segregation in *P. aeruginosa* strain PAO1. To this end, various segments on the chromosome were tagged with multiple *tetO* sequences and visualized by expressing a fluorescently labelled TetR protein that binds to these sequences. The role of two condensins

in chromosome segregation and global chromosomal layout was then determined by analyzing the segregation pattern in condensin mutants. We also determined the role of the ParAB*S* system in maintaining global chromosomal layout by monitoring the segregation pattern of *oriC* in ParB mutants. Finally, the role of entropy (or other yet undocumented factors) in chromosome organization was determined by sequentially removing condensins and ParB.

Our results indicate that the chromosome of PAO1 is longitudinally oriented between *oriC* and *dif*. Both replication and segregation initiate from the *oriC* locus and move bidirectionally along the arms. Interestingly, we found that chromosome segregation finishes at the asymmetrically located *dif* locus. Additionally, we uncovered the presence of two domains in the longer left arm. Analysis of our segregation and replication data indicates that segregation proceeds discontinuously along the chromosomal arms, while replication proceeds with equal rates on both arms. In contrast to segregation, chromosome replication terminates at a location opposite to *oriC.* This reveals that there is no obvious coordination between chromosome replication and segregation at the terminus region. Furthermore, this result demonstrates a special role for *dif* locus in chromosome segregation.

SMC and MksB both play distinct roles in chromosome organization and segregation. Both of them contribute to overall compactness of the chromosome however, their roles are different. We demonstrated that SMC and MksB are localized to different parts of the chromosome. This suggests that these proteins have their own preferential binding sites. SMC binds close to the *oriC* locus,

whereas MksB binds to a different chromosomal region and remains close to mid-cell. Our results also indicate that both MksB and SMC are required to condense the bulk of the chromosome. We also found that SMC has a special role in tethering the *dif* proximal locus.

These results support our hypothesis that condensin mediated global chromosome organization is required for proper chromosome segregation. Interestingly, simultaneous deletion of condensins and ParB is lethal for the cell. This result supports our second hypothesis that entropy by itself is not sufficient and requires either a condensin or ParB for cell viability.

In a separate line of enquiry, we wanted to determine the biochemical activities of eukaryotic condensins. To this end, we expressed and purified SMC subunits of the human condensin using a Baculovirus expression system. This system utilizes insect cells to express eukaryotic proteins. In humans, two different condensins are present, condensins I and II. Each of them is composed of five subunits. Both of them share the same pair of SMC subunits: SMC2 and SMC4. Activity of condensins is attributed to the SMC proteins, whereas the non-SMC proteins play a regulatory role [25]. Although SMC4 was not able to be expressed within this system, the SMC2 subunit of human condensin was readily expressed and purified. The purified SMC2 possess characteristic DNA binding activity. However, expression of SMC4 was never detected. The inability to express SMC4 subunits suggest that SMC2 alone cannot stabilize the SMC4 proteins and that the co-expression of SMC4 with other non-SMC subunits is

necessary. Overall, we found that the purified SMC2 possess characteristic DNA binding activity typical for condensins.

CHAPTER 1: Introduction

This chapter describes the major players involved in chromosome organization and segregation focusing primarily on the bacterial chromosome. The main focus of this thesis is to determine the coordination between global chromosome organization and chromosome segregation in the opportunistic human pathogen *Pseudomonas aeruginosa.* Additionally, due to the highly conserved nature of condensins in organizing the chromosome, both prokaryotic and eukaryotic condensins will be described.

1.1 Chromosome organization in bacteria

Visualization and characterization of eukaryotic chromosomal dynamics was achieved in great detail by the 1880s [26]. However, the actual organization of bacterial DNA remained a mystery until 1930s. The demonstration of discrete bodies of the bacterial chromosome was achieved by staining the chromosome using DNA specific dyes, which led to the discovery of the nucleoid. This discovery changed the perception of the bacterial chromosome from an amorphous structure to a complex and highly organized physical object [27, 28]. Isolation and characterization of several small nucleoid associated proteins reveled their involvement in local chromosomal arrangements [29]. Electron micrographs of nucleoid spreads later revealed a higher order structure with giant DNA loops which extended from a central protein scaffold [30, 31]. Finally, the

visualization of fluorescently labelled bacterial chromosomes within live cells, led to the discovery of its dynamic subcellular organization [32, 33].

1.1.A. Local chromosome organization by nucleoid associated proteins

Nucleoid associated proteins act by binding relatively non-specifically across the chromosome and subsequently wrapping, bending or bridging chromosomal segments. The first two nucleoid proteins isolated from *E. coli* were H-NS (Histone-like Nucleoid Structuring protein) and HU (Heat Unstable protein) [34]. Several other proteins were isolated soon after from purified nucleoids and collectively named Nucleoid Associated Proteins (NAPs). Biochemical characterization of the twelve major NAPs has revealed that their DNA binding, bridging, bending and wrapping activities modulates local chromosomal structure [29, 35]. These twelve NAPs, are HU, IHF, FIS, H-NS, Lrp, CbpA, CbpB, DnaA, Dps, Hfq, IciA and StpA.

HU (Heat Unstable) proteins are made of two subunits: HUα and Huβ. Approximately 60,000 copies of each monomer is present in *E. coli* and depending on their growth stages, HU can exist as both homodimers or heterodimers [36, 37]. HU binds preferentially to distorted regions of DNA, nicks, bends, and three or four-way junctions. Interestingly, rather than introducing one new bend, HU recognizes and stabilizes pre-existing DNA bends [38-40]. A bending angle of 0° to 180° with an average of 100° was determined for the nicked DNA-HU complex in different organisms [40-42]. At low HU

concentrations, DNA is compacted, however, at high HU concentrations, it becomes extended [42, 43]. In the presence of topoisomerase I, HU generally induces negative DNA supercoils in plasmid DNA [44]. Putting it all together, HU binds at different regions on DNA and stabilizes them, thus mainlining local compaction of the chromosome.

IHF (Integration Host Factor) proteins share significant amino acid similarity with HU proteins, but unlike HU, IHF binds to a well-conserved nucleotide sequence and introduces a 180° turn within that DNA segment [45]. Similar to HU, IHF is also composed of an α-subunit and a β-subunit and has a copy number of approximately 20,000 dimers per cell [37]. The αβ heterodimeric form is the predominant form, although both αα and ββ forms are also biologically active [46]. The consensus DNA binding site for IHF contains three characteristic sequences: two conserved segments of DNA 5′-TATCAA-3′ and 5′-TTG-3′, and a 6-base pair with an A-tract. The center of the U-turn is positioned at the 5′ end of the TATCAA consensus site [47]. By introducing these U-shaped bends, IHF affects chromosome replication initiation and regulates transcription [48-50].

FIS (factor for inversion stimulation) proteins are made of two identical subunits, each of them contains a putative helix-turn-helix (HTH) domain. These HTH domains are used to bind and bend DNA segments [51]. FIS recognizes a poorly conserved 17 bp long, AT rich DNA binding site [52]. However, nonspecific binding to DNA can be observed, often leading to branch formations in supercoiled DNA [53]. Depending on the substrate DNA, FIS introduces a bend with a bending angle between 50° to 90° [54, 55]. Interestingly, FIS can both

suppress or activate transcription, depending on its binding site relative to that of RNA polymerase [56, 57]. This dual role correlates excellently with its expression level during different phases of cell growth. This protein express at a very high level (approximately 50,000 copies per cell) during the exponential phase [58]. During this phase, FIS activates multitudes of genes involved in translation which are required during fast cell growth. At the onset of the stationary phase, FIS levels drop (about 500 copies per cell) which leads to the removal of its inhibitory control of a gene encoding RpoS. RpoS then reprograms RNA polymerase to express genes that are required for adaptation to slower cell growth [59-62].

H-NS (histone-like nucleoid-structuring) are small (15kDa) proteins, which are present in abundance (about 20,000 copies per cell) within various species of bacteria, and acts as a global transcriptional repressor [63-66]. This protein consists of an N-terminal oligomerization domain, a C-terminal DNA binding domain and a flexible linker domain that connects these two domains [67-69]. Dimeric H-NS proteins form a DNA-H-NS-DNA complex, thus bridging and stabilizing DNA segments [70]. H-NS also constrains negative supercoiling of DNA, which facilitates DNA bridging and loop formation [66, 71, 72]. Transcriptional downregulation by H-NS is modulated by its interaction with the haemolysin expression-modulating (Hha)/YdgT family of proteins [73, 74] . However, how the Hha/YdgT proteins regulate H-NS function is still unknown.

Lrp (Lipoprotein receptor-related) proteins are small low molecular weight proteins that act as a regulatory element for several genes including genes involved in nutrient uptake, amino acid metabolism and microbial virulence.

Depending on the target promoter, Lrp can activate, suppress or remain unaffected by leucine [75]. Lrp is present in about 3000 copies per cell and can exist in diverse oligomeric states [76, 77]. Its dimeric form bridges different segments of DNA in a manner similar to H-NS: Lrp dimers bound to one segment of DNA interact with another Lrp dimer bound to a different segment of DNA [78, 79]. This kind of interaction can stabilize DNA loops and influence global chromosome organization. Lrp proteins can also form an octameric structure, around which DNA can be wrapped; similar to the nucleosomes present in eukaryotes. These kind of structures are often found at the promoter region and acts as a repressor [80, 81].

Other NAPs isolated from the bacterial nucleoid include CbpA, CbpB, DnaA, Dps, Fis, Hfq, IciA, StpA, and SMC complexes [29, 35]. Proteins of the SMC family were later found in archaea and eukaryotes. A detailed description about these proteins are provided later in this thesis.

1.1.B. Global chromosome organization and the SMC complex

In last few decades, proteins of the Structural Maintenance of Chromosome (SMC) family have emerged as major players of global chromosome organization in all kingdoms of life. MukB, the first protein of the SMC family, was identified during the screening of *E. coli* mutants which produced anucleate cells [12]. Soon thereafter, proteins of the SMC family were found in other organisms including archaea and eukaryotes [82-84]. Notably, one

of the applied approaches involved fractionation of *Xenopus* chromosome scaffold. This scaffold can be observed in histone depleted mitotic chromosomes, indicating that SMC proteins play a structural role in chromosome organization. Two major components of the chromosome scaffold proved to be topoisomerase II and ScII, an SMC protein [3, 85, 86]. This finding suggested a structural role for SMC proteins in chromosome organization.

Molecular architecture of SMC proteins

Each SMC protein has five distinct domains [87]. The globular N-terminal and C-terminal domains contain two canonical nucleotide binding motifs; Walker A (G-X-S/T-G-X-G-K-S/T-S/T) and Walker B (h-h-h-h-D, where h is a hydrophobic amino acid). While the Walker A motif is essential for ATP binding, the Walker B motif is required for ATP hydrolysis. The C-terminal domain carries the signature C-motif and D-loop, required for stabilizing the binding and hydrolysis of ATP. Between these two globular domains are two long α- helices which are connected by a third globular domain. An SMC monomer folds back onto itself by forming an anti-parallel coiled-coil domain, thus generating an ABC-type ATPase site at the 'head' domain and a globular 'hinge' domain (Figure 1-1A). Two monomers of SMC protein associate with each other through the hinge domain, forming a homodimer (prokaryotes) or a heterodimer (eukaryotes). Formation of the dimer also results in the formation of two functional ABC-type ATPases at the head domain (Figure 1-1B) [88]. Various conformations of SMC dimers have been observed through electron microscopy, including V-shaped, I-shaped and a ring-like structure [89, 90]. Although SMC proteins of different

organisms share very little sequence identity, they all share this common secondary and tertiary structure. Dimers of SMC proteins interact with two other non-SMC proteins, a kleisin and a kite protein, to form a functional condensin complex.

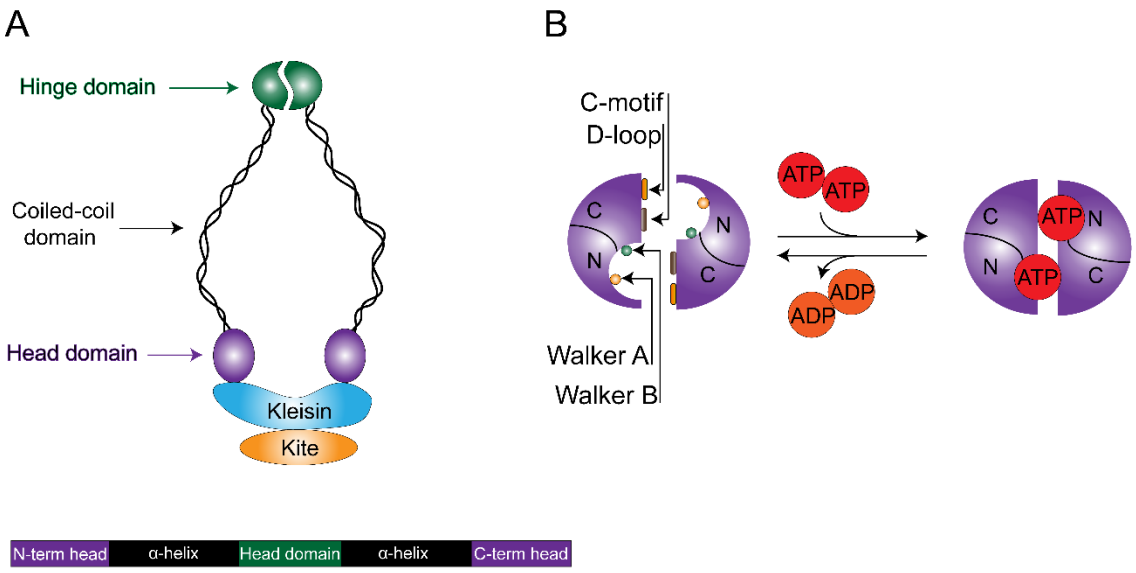

Figure 1-1: Architecture of condensins. (A) Schematic representation of condensins. Each SMC monomer is made of two globular domains, two α-helix and a third globular hinge domain between them. Each monomer folds back onto itself forming a functional ABC-type ATPase head domain. Two monomers associate with each other through the hinge forming an SMC dimer. Association with kleisin and kite subunits is required for condensin activity. (B) Engagement of the two head domains of the SMC dimer forms two ATPase domains. For each ATPase domain, the N-terminal and C-terminal domain of a monomer carries the Walker A and Walker B motif respectively. The C-terminal domain of the second monomer carries the C-motif and D-loop. Hydrolysis of two ATP molecules lead to the disengagement of the head domains.

The SMC family

In bacteria, three families of condensins have been found: SMC-ScpAB, MukBEF and a MksBEF. In these complexes, SMC, MukB and MksB belong to the SMC family, ScpA, MukF and MksF belong to the Kleisin family and ScpB, MukE and MksE belong to the Kite family [91]. The first condensin identified, MukBEF was originally discovered in *E.coli* and later identified in different enterobacteriaceae and γ-proteobacteria [12, 13, 92, 93]. All three subunits of MukBEF are expressed from a single operon, where they are located in the order of *mukF-mukE-mukB* [16]. The second family of condensins, SMC-ScpAB was later discovered in various bacteria and archaea, where, *smc* is encoded separately from *scpA* and *scpB* [94, 95]. MksBEF in *P. aeruginosa,* is also encoded in a single operon where these three genes are organized in the order of *mksF-mksE-mksB* [16]. The Mks2BEF condensin, found in the virulent *P. aeruginosa* strain PA14, encodes an additional uncharacterized MksG protein within a single operon [16].

In eukaryotes, the SMC family consists of six different sub-classes of proteins (SMC 1-6) [96, 97]. SMC2 and SMC4 which interact with three non-SMC proteins (CAPD2, G and H) forming the condensin complex. This complex plays a vital role in chromosome assembly and segregation [84, 98]. In the cohesin complex, SMC1 and SMC3 binds with two other non-SMC proteins, Scc1 and Scc3. This complex is required for sister chromatid cohesion [82, 99]. A third SMC complex involved in DNA repair and checkpoint responses, consists of SMC5, SMC6 and Nse1-6. [100-102].

Activity of the SMC complex

How condensins organize the chromosome within bacteria is still unclear. The presence of condensins in the protein scaffold of isolated bacterial chromosomes indicates their involvement in chromosome structuring by stabilizing giant loops emanated from the scaffold. The biochemical activities of condensins also supports their role in scaffold formation [103]

Biochemical characterization of bacterial condensins revealed that their DNA binding activity resides in their SMC subunits [104]. Co-operative binding of these proteins to stretches of DNA promotes the formation of filamentous nucleoprotein complexes. Upon binding, the ability of condensins to capture distant DNA segments, allows the formation of a protein scaffold from which DNA loops are radiated outside the scaffold [103]. ATP and non-SMC subunits of condensins appear to play a regulatory role in DNA binding and bridging activity of SMC subunits [104].

Within cells, bacterial condensins form distinct clusters on the chromosome. The *E. coli* condensin, MukBEF is localized close to the *oriC* region which is located at the mid-cell region. As cells grow, the MukBEF cluster migrates to the quarter position along with the newly replicated *oriC* [105, 106]. The non-SMC subunits of MukBEF are required for this cluster formation, indicating that these proteins have a regulatory role in the proper loading of this condensin proximal to *oriC* [107]. The SMC-ScpAB complex from *Bacillus subtilis* and *Streptococcus pneumoniae* form clusters in the vicinity of a conserved *parS* sequence, which is located close to *oriC* [10, 24, 108]. In *B. subtilis* and *S.*

pneumoniae, recruitment of SMC to *parS* depends on the chromosome partitioning protein ParB [23, 24, 108].

1.1.C. Subcellular organization of bacterial chromosome

Finally, a third level of chromosome organization involves the subcellular organization of the entire chromosome inside of the cell. To determine the global layout of the chromosome and its dynamics during the cell cycle, the fluorescent repressor operator systems (FROS) [109] and fluorescence *in situ* hybridization (FISH) [110], are frequently used. Experiments carried out in various bacterial species revealed that chromosomal organization varies between species and can change depending on the growth phase or available nutrients.

Previous detailed studies of chromosome segregation and localization led to the discovery of macrodomains (MD) [110]. In *E. coli*, four macrodomains have been identified: Ori, Ter, Left and Right. Two less-structured regions have also been identified that flank the Ori macrodomain [111, 112]. Two DNA binding proteins have been implicated in the maintenance of the macrodomain organization in *E. coli.* The MatP protein recognizes a specific DNA sequence, *matS,* which is repeated 23 times within the 800 Kbp Ter domain. Binding of MatP to *matS* is necessary to maintain the Ter macrodomain [113-115]. A second DNA binding protein MaoP binds to a single specific DNA sequence, *maoS,* which is present in Ori macrodomain and is required for its maintenance [116].

Chromosomes in fast-growing *E. coli*, sporulating *Bacillus subtilis, Caulobacter crescentus, Myxococcus xanthus* and *Vibrio cholerae* tend to

assume the so-called *ori-ter* configuration, where the origin (*oriC*) is located at or close to the old cell pole and the terminus (*ter*) is located at the new cell pole [117-121]. Both chromosomal arms lie side-by-side in between them. Soon after replication, the origins are repositioned to the cell poles. As replication proceeds further, newly replicated DNA migrates sequentially and occupies specific positions inside the cell, while the un-replicated terminus migrates towards the mid-cell. Upon cell-division, the newly replicated terminus occupies the new cell pole, thus, restoring the *ori-ter* configuration in newly born cells (Figure 1-2, Left).

However, in slow growing conditions, the *E. coli* chromosome organizes itself into a left-*ori*-right configuration, where the origin (*oriC*) resides in the mid-cell region and the left and right arm occupy different cell halves. The terminus region (*ter)*, connecting two arms also occupies the mid-cell region. After replication, the newly formed origins migrate towards opposite cell quarters and the arms segregate to either side of the origin, restoring the left-*ori*-right configuration [122] (Figure 1-2, Right).

Interestingly, in *B. subtilis,* chromosomal organization depends on its developmental stage. During sporulation, the chromosome organizes itself into an *ori-ter* configuration. In contrast, during vegetative growth it alternates between an *ori-ter* and left-*ori*-right configuration [8, 123]. However, the precise mechanism used to generate and maintain the linear organization of the chromosome in still unknown. It is also unclear if a specific locus on the chromosome occupying a particular location inside the cell can provide a unique way to regulate the expression of certain genes. Finally, the biological

significance of maintaining transverse or longitudinal orientation and proteins responsible for this process are yet to be identified.

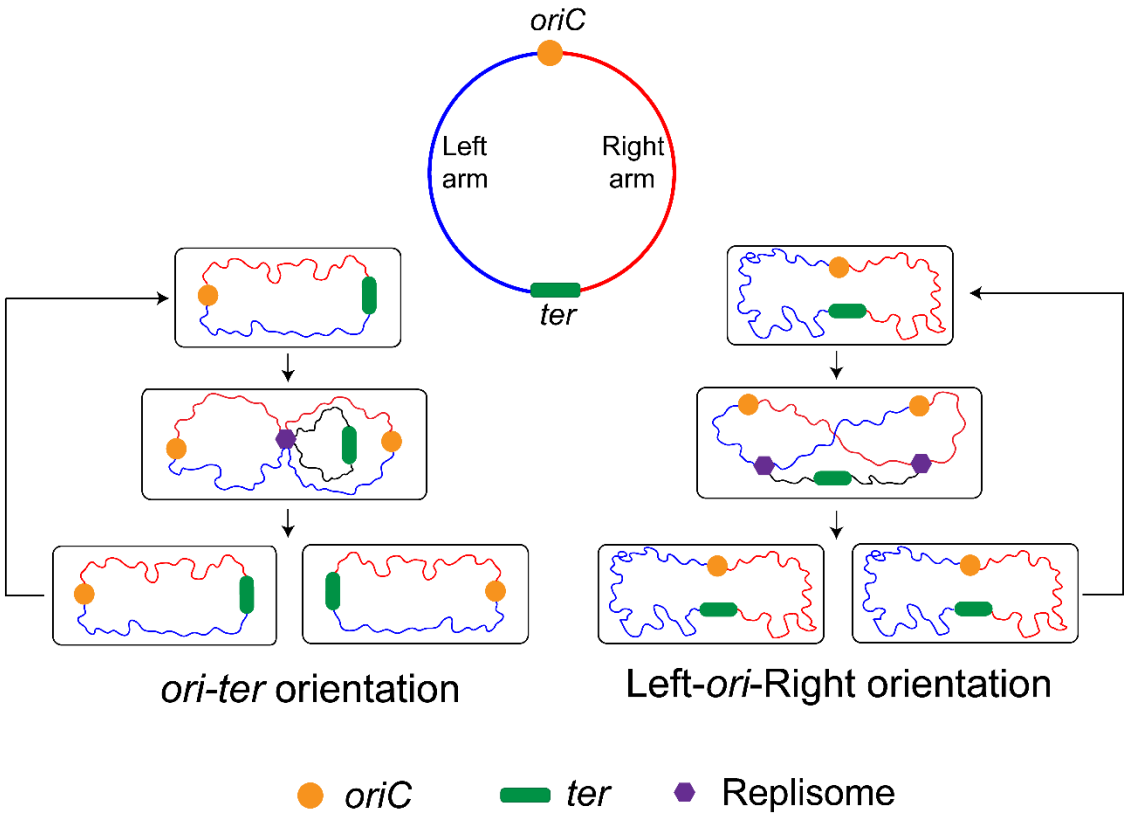

Figure 1-2: Global chromosomal layout in bacteria. Chromosome in bacteria, is organized between *oriC* and *ter.* Depending on species and growth conditions, chromosomes can have different orientations. In *ori-ter* orientation, *oriC* and *ter* are located at opposite cell-poles. Chromosomal arms run parallel to each other between *oriC* and ter. In Left-*ori*-Right orientation, both *oriC* and *ter* occupies the mid-cell and each arm occupies opposite cell halves.

1.2 Driving forces in chromosome segregation

Faithful segregation of the newly duplicated chromosome is essential to ensure that each daughter cell inherits a complete copy of the genome. Unlike eukaryotes, bacterial chromosome segregation takes place concomitantly with replication [22]. Several models have been postulated to illustrate the mechanism of chromosome segregation in bacteria [21]. However, these mechanisms are not mutually exclusive and likely cooperate in proper chromosome positioning.

1.2.A. ParAB*S* system in chromosome segregation

Chromosome segregation initiates from the origin-proximal region of the chromosome. The ParAB*S* partitioning system has been shown to actively segregate this region in various bacteria [124-128]. It comprises of three elements: the DNA binding protein ParB, which binds to *parS,* and a *cis*-acting centromere-like DNA sequence, which together forms a nucleoprotein complex. [126, 129, 130]. Finally, a Walker A-type ATPase, ParA is thought to provide the driving force for segregation of this nucleoprotein complex. Two different models have been postulated for ParAB*S* mediated chromosome segregation. According to the pulling model, ParA forms a filamentous structure away from the ParB:*parS* complex. The edge of this filamentous structure captures the ParB:*parS* complex and then retracts, pulling DNA with it. This kind of movement has been observed in *V. cholera* and *C. crescentus* [124, 131, 132]. According to the pushing model, ParA forms a filamentous structure in between the duplicated ParB:*parS* complex. The filament then grows in between them thus pushing the origins apart [133].

1.2.B. Entropic model of chromosome segregation

Although the ParAB*S* system is widespread in the bacterial kingdom, several bacterial species, including *E. coli,* lack a well-defined partitioning system [128]. According to the entropic model proposed by Jun and Molder, the inherent entropic force exerted by “self-avoiding” DNA polymers can contribute to the segregation of bacterial chromosomes following replication. [134, 135]. However, this model cannot fully explain the segregation process. In contrast to the main hypothesis of this model, chromosomes are self-adhering polymers and entropic force alone cannot explain how newly replicated origins dis-entangle themselves and occupy specific locations within the cell. This model also cannot explain how the linear organization of genes is achieved after segregation [136-138].

1.2.C. Extrusion-capture model

According to the extrusion-capture model proposed by Lemon and Grossman, the newly replicated chromosome is segregated, in part, by utilizing the energy released during DNA replication [139]. This model was suggested based on the observation that the DNA replication machinery is positioned in the center of the cell during chromosome replication and segregation. The replisome binds to the origin of replication in the mid-cell, pulls the rest of the template DNA towards the cell center, and after replication releases them towards opposite cell poles. Proper positioning of the replicated chromosome is then achieved by other positioning systems.

1.3 Chromosome architecture in *Pseudomonas aeruginosa*

P. aeruginosa is an opportunistic human pathogen responsible for serious nosocomial infections in new-borns, patients with impaired immunity, and burn victims and is a leading cause of morbidity in cystic fibrosis patients [140]. It is one of the most common hospital acquired pathogens and is responsible for high mortality rates in patients with ventilator-associated pneumonia [141, 142]. Intrinsic resistance to several common antibiotics as well as the emergence of multi-drug resistant strains of *P. aeruginosa* demands particular attention for identifying novel drug targets. Understanding the mechanism of basic cellular events such as chromosome replication and segregation has great potential for providing new means to control this organism.

The genome of wild type *Pseudomonas aeruginosa* and more than 200 other *Pseudomonas* strains and clinical isolates have been sequenced and now publicly available [143]. Analysis of their genomes has revealed that the chromosome of *P. aeruginosa* is approximately 30% larger than that of *E. coli* or *B. subtilis*. However, the greater size of this chromosome is not due to gene duplication, but instead is a result of greater gene complexity and horizontal transfer of genes from other bacteria and viruses [18, 144].

Several key chromosomal elements required for chromosomal replication and segregation in *P. aeruginosa,* have already been identified, including: the origin of replication *oriC* [145, 146], the sister chromosome resolution site *dif* [147] and the chromosomal partitioning system ParAB*S* [128, 129]. In *P. aeruginosa,* ten putative *parS* sites have been identified and four of them are located in close

vicinity to *oriC* [129]. Among these four *oriC* proximal *parS* sites, only one is required for proper chromosome segregation [10, 148]. Surprisingly, no *Ter*-Tus system has been identified in *P. aeruginosa*.

The chromosome of the *P. aeruginosa* strain PAO is longitudinally organized between *oriC* and *dif,* and located diametrically opposite to *oriC*. The chromosome of this strain lacks the reported inversion between *rrnA* and *rrnB* sites, located on opposite chromosomal arms [149]. This strain also contains partial deletions in PA4684 and PA4685 genes, which respectively, encode the non-SMC subunits MksF and MksE of the MksBEF condensin complex. [150]. As a result of this deletion, the MksBEF condensin is not functional in PAO. In this strain, segregation initiates from a single *parS* site located close to *oriC,* segregates bi-directionally and finishes at the *dif* locus. While the cell's replication machinery remains at the mid-cell region for the entire duration of cell cycle, the chromosome is pulled towards it prior to segregation [149].

CHAPTER 2: Methods

2.1 Construction of plasmids

To introduce chromosomal tags in the chromosome of *P. aeruginosa*, the pP30D-FRT-tetO-0069 plasmid was used (Figure 2-1) [149]. The backbone of this suicide vector contains the *oriT* region, the ColE1 origin of replication, the *aac1* gene (conferring resistance to gentamicin), and an array of 140 tetracycline operator (*tetO*) sequences. To insert this array into the desired locations on the chromosome, approximately 500 base pairs of a chromosomal segment was amplified by PCR. Both the plasmid and amplified product were then digested with HindIII/KpnI restriction enzymes (New England Biolabs) and the products were ligated together by phage T4 DNA ligase (New England Biolabs). The ligation mixture was then transformed into chemically competent DH5α cells and spread on LB-agar plates supplemented with gentamicin (30 μg/mL). Plasmids from individual colonies were then purified and correct constructs were identified by sequencing.

To construct the pPSV35Ap-TetR-CFP plasmid, DNA sequence harboring yGFP-ParBT1 was removed from pPSV35Ap-TetR-CFP-yGFP-ParBT1 plasmid using overlap excision PCR [149]. The resulting plasmid carries an in-frame DNA segment encoding the tetracycline repressor (TetR) protein fused with cyan fluorescent protein (CFP) at its C-terminal. Expression of this chimera is controlled by an IPTG-inducible lacUV5 promoter.

pPSV35Ap-TetR-mCherry was constructed by amplifying *tetR* gene from pPSV35Ap-TetR-CFP-yGFP-ParBT1 plasmid, and the gene encoding mCherry was amplified from the pUC18T-mini-Tn7T-Gm-mCherry plasmid. These two segments were then ligated by overlap extension PCR and cloned into the SacI/HindIII restriction sites of pPSV35Ap-TetR-CFP plasmid, thus replacing CFP with mCherry

To construct the deletion plasmid pEXG2-Δ*parB,* approximately 500 base pairs of chromosomal segments were amplified from both the upstream and downstream regions of *parB* gene (PA5562) by PCR. The PCR fragments were then ligated by overlap-extension PCR, and subsequently cloned between the HindIII/BamHI restriction sites of pEXG2 plasmid.

To replace the endogenous *smc* and *mksB* with DAS4-tagged versions, pEX18Ap-*smc*-DAS and pEX18Ap-*mksB*-DAS plasmids were constructed. To this end, approximately 500 base pairs of chromosomal segments from 3' ends of *smc* and *mksB* gene were amplified and nucleotide sequence encoding a DAS4 tag was introduced at their 3' end before the native stop codon. The resulting fragments were then cloned between the KpnI/BlpI restriction sites of the pEX18Ap-Δ*smc* and pEX18Ap-Δ*mksB* plasmids, respectively [17].

The complete list of plasmids is provided in Table 1.

2.2 Construction of strains

To integrate the *tetO* cassette at various positions in both wild type, Δ*mksB,* Δ*parB and* Δ*mksB* Δ*smc* genomes, the traditional conjugation method was used [151]. *E. coli* SM10(*λpir*) cells carrying the suicide vectors were mated with the recipient *P. aeruginosa* strains and successful transformants were selected by spreading on a Vogel-Bonner minimal medium (VBMM: 0.083 M Magnesium sulfate, 0.48 M citric acid monohydrate, 2.87 M dipotassium phosphate anhydrous, 1.28 M sodium ammonium phosphate) agar plates supplemented with 30 µg/mL gentamicin. Successful integration of *tetO* repeats was further verified by PCR. To incorporate the *tetO* cassette into the Δ*smc* chromosome, each suicide vector was first extracted from 50 mL of overnight culture of DH5α *E. coli* cells carrying those plasmids. Approximately 5 µL of concentrated plasmid (500 ng/ µL in Tris, pH 7.5) was transformed into Δ*smc* cells *via* electroporation, followed by an incubation of 4 hours in super optimal broth with catabolite repression medium (SOC) at 37 °C. Cells were then spread on an LB-agar plate supplemented with gentamicin (30 µg/mL) and successful transformation was then verified by PCR. To visualize these chromosomal markers, pPSV35Ap-TetR-CFP or pPSV35Ap-TetR-mCherry plasmid was introduced in *tetO* tagged cells via electroporation and transformants were selected on LB-agar plate supplemented with gentamicin (30 µg/mL) and carbenicillin (200 µg/mL).

To delete the *parB* gene, the parental *P. aeruginosa* strain PAO1 was mated with SM10(*λpir*) cells carrying the deletion plasmid pEXG2-Δ*parB.*

Merodiploid cells were then streaked on TYA plate (1% Bacto tryptone, 0.5%yeast extract and 1.5% agar) and incubated at 30 °C. single colonies were picked and checked for gentamicin sensitivity by replica-plating. Gentamicin sensitive colonies were picked and further verified for deletion by PCR analysis.

To construct cells for the DAS4 mediated degradation assay, the *sspB* gene (PA4427) was first deleted from Δ*parB* strain using the deletion plasmid pEXG2-Δ*sspB,* using allelic exchange method described previously. *smc* (PA1527) or *mksB* (PA4686) gene was then removed using pEX18-Δ*smc* and pEX18-Δ*mksB* plasmids donated by Dr. Hang Zhao. Finally, *mksB* gene was replaced with a DAS4-tagged version from Δ*parB* Δ*sspB* Δ*smc* cells using two-step allelic exchange method. A similar method was used to construct Δ*parB*Δ*sspB*Δ*mksB*-*smc*-DAS4 strain. Finally, a ∆*parB*∆*sspB*-*smc*-DAS4-*mksB*-DAS4 strain was constructed by successive replacement of *smc* and *mksB* with their DAS4 tagged versions.

To express human condensin subunits, the pFastBac™ Dual expression vector was used (Figure 2-2). This vector can express two proteins simultaneously from two strong viral promoters : a polyhedron promoter and a p10 promoter. Constructs used in these experiments are described in Table 1. Plasmids carrying the human *smc*2 and/or *smc*4 genes were transformed into *E. coli* DH10Bac competent cells (Invitrogen). Site-specific integration of the plasmid into the bacmid, located inside the DH10Bac cells, results in disruption of *lacZα* gene, thus generating white colonies when grown in LB-agar plates supplemented with 50 µg /mL kanamycin, 7 µg/mL

gentamicin, 10 µg/mL tetracycline,100 µg/mL X-gal, and 40 µg/mL IPTG. A single white colony was inoculated into 2 mL LB medium supplemented with 50 µg/mL kanamycin, 7 µg/mL gentamicin, and 10 µg/mL tetracycline. The recombinant bacmid was purified using a PureLink™ HiPure Plasmid Miniprep Kit (Invitrogen), following manufacturer's protocol. Successful integration was further verified using PCR.

A complete list of strains constructed is provided in Table 2 and 3.

2.3 Engineering the PAO1 genome through allelic replacement

To modify the genome of *P. aeruginosa* strain PAO1, two different suicide vectors (pEX18Ap and pEXG2) were used. These vectors harbor a ColE1 origin of replication, permitting replication in *E. coli* but not in *P. aeruginosa*. These vectors also contain the *oriT* region from RP4 plasmid, allowing the plasmids to be transferred from *E. coli* to *P. aeruginosa* by conjugation. They also contain an antibiotic resistance marker (*bla* in pEX18Ap, *aacC1* in pEXG2) used for selection and a functional *Bacillus subtilis sacB* gene used for plasmid curing. Plasmid maps are illustrated in Figure 2-3.

To introduce these plasmids, a bacterial conjugation method was employed [151]. For this purpose, the recipient *P. aeruginosa* strain and the donor *E. coli* strain SM10(*λpir*) hosting the suicide vectors were grown in LB medium at 37 °C until they reach an OD_{600} of 0.2. At this density, 5×10^7 donor SM10(*λpir*) cells and 2×10^8 receptor *P. aeruginosa* cells were harvested, resuspended in a total volume of 20 µL LB medium and spotted on a LB-agar

plate without any antibiotic. After incubating overnight at 37 °C, the cells were harvested and resuspended in 2 mL of 10 mM magnesium sulfate solution. Aliquots from this suspension were then spread on Vogel-Bonner minimal medium (VBMM: 0.083 M Magnesium sulfate, 0.48 M citric acid monohydrate, 2.87 M dipotassium phosphate anhydrous, 1.28 M sodium ammonium phosphate) agar plates supplemented with 30 µg/mL gentamicin. Single colonies were picked with a sterile toothpick and streaked onto a TYA plate (1% Bacto tryptone, 0.5%yeast extract and 1.5% agar) supplemented with 15% sucrose and incubated at 30 °C. The presence of *sacB* gene confers an acute sucrose sensitivity leading to bacterial cell death when grown on medium containing sucrose. Single colonies were then checked for sensitivity towards the particular antibiotic marker present on the vector backbone by streaking on an LB plate supplemented with carbenicillin (for pEX18AP plasmid) or gentamicin (for pEXG2 plasmid). Genome modification of antibiotic sensitive strains was confirmed by PCR and/or DNA sequencing. Figure 2-4 illustrates a schematic representation of gene-deletion by a two-step allelic exchange method.

2.4 Epifluorescence microscopy

Epifluorescence illumination is a technique where a single lens system is used to both excite and collect fluorescence from a fluorophore. Cells harboring fluorescent proteins were excited by transmitting light through an optical filter and emitted light was collected back through the same objective and passed through the dichroic mirror to a second filter and finally reaching a CCD camera.

2.4. A. Live cell imaging

Live cell imaging is best suited to visualize fluorescently tagged proteins under their native biological conditions. To visualize chromosomal regions inside live cells, *P. aeruginosa* strains containing *tetO* tagged chromosomal segments and the pPSV35Ap-TetR-CFP plasmid, were grown overnight in M9 minimal media (pH 7.5) supplemented with 0.25% w/v sodium citrate, gentamicin (30 µg/mL) and carbenicillin (200 µg/mL). Cells were then diluted to an OD_{600} of 0.01 and re-grown in M9 minimal media (pH 7.5) supplemented with 0.25% sodium citrate, gentamicin (30 µg/mL) and carbenicillin (200 µg/mL) at 30 °C. At an OD_{600} of 0.05, Isopropyl β-D-1-thiogalactopyranoside (IPTG) was added to the medium at a final concentration of 0.05 mM. IPTG induces expression of TetR-CFP chimera, which binds to *tetO* repeats located on chromosome. Cells were grown until an OD_{600} of 0.1 and then spread onto a thin agarose pad (1% agarose in M9 medium (pH 7.5) supplemented with 0.25% sodium citrate), and observed immediately using an Olympus BX-50 microscope; equipped with a BX-FLA mercury light source, a 100X, 1.43 NA oil-immersion objective and a SPOT Insight QE Camera. Images acquired by phase-contrast and fluorescent channels were analyzed by the spot-sizing software Nucleus [152].

2.4.B. Time-lapse imaging

For time-lapse imaging, strains were grown overnight at 37 °C in M9 minimal media (pH 7.5) supplemented with 0.25% sodium citrate. Cells were then diluted to an OD_{600} of 0.01 and re-grown in M9 minimal media (pH 7.5) supplemented with gentamicin (30 µg/mL) and carbenicillin (200 µg/mL) at 30 °C.

Cells were grown until an OD_{600} of 0.1 and then spread onto a thin agarose pad (1% in M9 minimal medium (pH 7.5) supplemented with 0.25% sodium citrate), and observed using an Olympus IX81 inverted microscope equipped with a X-Cite 120 LED light source (Lumen Dynamics), a 100X UPlanSApo 1.40 NA oil-immersion objective (Olympus) and an iXon3 EMCCD camera (ANDOR technology). To compensate for vertical focal drift during image acquisition, an automated Z-drift compensation module (IX2-ZDC2), was used. Images were captured automatically every 60 seconds using the Micro-Manager plugin controlled by the Image J software package [153, 154]. An exposure time of 400 ms and electron-multiplying (EM) gain of 40 e^-/count was chosen to capture images for the GFP and mCherry tagged proteins.

2.5 Image Processing

The number and position of fluorescent foci were analyzed using the spot sizing software Nucleus [152]. This program detects bright signals from fluorescent images while cell contour is detected from phase-contrast images. Spots are defined based on the intensity of its pixels compared to the intensity of neighboring background pixels. Cell size is measured in pixels from phase-contrast images. The positions of fluorescent spots are measured as a distance in pixels from the mid-cell region, as determined from phase-contrast images. A 3X3 median filter was also applied to every image to reduce background noise. Manual inspection of each detected spot was performed before statistical analysis. To analyze the localization of fluorescent proteins over a longer period of time, the image processing software package FIJI was used.

2.6 Flow cytometry analysis

To analyze DNA content and the number of chromosomes inside a cell, flow cytometry was used. PAO1 cells were grown in M9 minimal medium (pH 7.5) overnight, diluted to an OD_{600} of 0.01 and further grown to an OD_{600} of 0.1 at 30 °C. Cells were then harvested and fixed overnight with 70% ethanol in a buffer containing 20 mM Tris-Cl (pH 7.5) and 120 mM NaCl. Cells were then washed 3 times at 4 °C and incubated with 30 units/mL DNase free RNaseA (New England Biolabs) for 30 mins at 37 °C, followed by further incubation with 50 µg/mL propidium iodide for 15 min at room temperature in the dark. Cells were then passed through a 40 µm cell strainer (Corning) and analyzed directly using a BD Acuri C6 flow cytometer. Flow cytometry data were then analyzed using the FlowJo software (FLOWJO, LLC). A representative analysis of one such experiment is shown in Figure 2-5. In this image, the left panel demonstrates the plot between the forward scatter vs. the side scatter data. Cells were binned into four boxes according to increasing cell size. Florescent intensity of cells in each bin was then plotted on the right.

2.7 Marker frequency analysis

To determine the replication profile of the PAO1 chromosome, high throughput sequencing based marker frequency analysis was used. For this analysis, *P. aeruginosa* cells were grown in M9 minimal medium (pH 7.5) supplemented with 0.25% sodium citrate or LB medium at 30 °C. Cells were harvested at an OD_{600} of 0.1 and their genomic DNA was isolated using the

GenElute™ Bacterial Genomic DNA Kit (Sigma), following manufacturers protocol. The concentration and purity of isolated product were determined by NanoDrop™ 2000c Spectrophotometer (Thermo Scientific). Genomic DNA with A260/280 and A260/230 values greater than 1.8 was achieved following the purification protocol. High throughput sequencing of *P. aeruginosa* PAO1 genome was performed using the sequencing facility at Oklahoma Medical Research Foundation. The binary version of sequence alignment/map (bam) files were obtained from the facility and analyzed in house using MATLAB to determine copy numbers of each gene. By analyzing the copy number of each gene, we can determine the positions of the replication origin and terminus. Depending on the growth conditions, genes located close to *oriC* will have two or four copies as they are first to replicate. As replication proceeds along the arms, the copy number of genes decreases. Finally, genes located close to replication terminus will have a single copy.

2.8 Degron mediated controlled degradation of proteins

For the controlled degradation of desired gene products, the DAS4 mediated degradation system was adopted. This system is modified from the *E. coli* degron system where, an SspB adapter protein enhances the degradation of ssrA-tagged protein *via* ClpXP protease [155, 156]. We used a DAS4 tag (modified from the native ssrA tag), appended at the C-terminus of the desired protein to direct it for ClpXP mediated degradation (Figure 2-6). For this purpose, a DAS4 tag (AANDENYSENYADAS) was cloned at the 3` end of the gene of interest followed by its native stop codon. This tag is a poor substrate for ClpXP

unless the adaptor protein SspB is present [157]. For controlled degradation of MksB and SMC, the endogenous *sspB* gene was first excised from PAO1 by recombination using the deletion plasmid pEXG2-*sspB.* Endogenous copies of *mksB* and *smc* were then replaced by DAS4 tagged versions. Finally, the SspB expression plasmid, pPSPK-*sspB* was introduced into these strains *via* electroporation. Expression of SspB was controlled by adding IPTG to a final concentration of 0.1 mM. Degradation of the proteins was verified by western blot.

Strains and primers used are described in Tables 1 and 2.

2.9 Growth and maintenance of *Sf9* insect cell line

Sf9 Insect cells (Invitrogen, Catalog no. B825-01) were cultured and maintained as per the manufacturer's guideline. In short, frozen cells were thawed rapidly in a 37 °C incubator. Cells were seeded in pre-warmed *Trichoplusia ni* Medium-Formulation Hink (TNM-FH) complete medium (Invitrogen, Catalog no. 11605-094) at a density of 2-5 $\times 10^4$ viable cells/mL inside a sterile T25 flask (ThermoFisher Scientific). Adherence of cells was monitored using an inverted microscope. Once most of the cells were adhered to the flask, spent medium was carefully removed and replaced with fresh TNM-FH medium supplemented with gentamicin (10 µg/mL) (Invitrogen, Catalog no. 15710-064), amphotericin B (0.25 µg/mL) (Invitrogen Catalog no. 15290-018), Penicillin-Streptomycin (100 µg/mL) (Invitrogen, Catalog no. 15140-122) and incubated at 27 °C. Once cells reach ~90% confluency, that is when the cells have formed a single layer over the entire surface area available for growth, they were dislodged

from the flask using sloughing and reseeded into a sterile T25 flask containing fresh culture medium, at a density of 2-5 $\times 10^4$ viable cells/mL (Figure 2-7). Cell viability was assessed by trypan blue dye exclusion test. This die can penetrate dead cells only thereby, we can differentiate between live and dead cells under light microscope. For scaling-up purposes, 5×10^4 viable cells/mL were seeded in a 125-mL shaker flask, containing 30-50 mL of Sf-900™ II Serum Free Medium (SFM) (Invitrogen, Catalog no.10902-096), and incubated at 27 °C with a shaking speed of 130 rpm (C76 water bath shaker, New Brunswick Scientific). Once cells in suspension cultures reach a density of 2-4 $\times 10^6$ cells/mL, they were reseeded into a sterile shaker flask at a final density of $3\text{-}5 \times 10^5$ viable cells/mL.

2.10 Transfecting insect cells with recombinant bacmids

Transfection of recombinant bacmids into *Sf9* cells was performed following manufacturers protocol. In brief, 1 µL of purified bacmid DNA (500 ng/µL in TE Buffer, pH 8.0) and 8 µL of Cellfectin® II reagent (Invitrogen, Catalog no. 10362-100) was diluted into 200 µL of un-supplemented Grace's Medium. After incubation for 30 minutes at room temperature, this transfection mixture were added to 8×10^5 *Sf9* cells adhered to a single well of a six well plate. After incubating for 5 hours at 27 °C in the dark, the transfection mixture were replaced with 2 mL of pre-warmed Grace's Insect Medium (Invitrogen, Catalog no. 11595-030), supplemented with 10% Fetal Bovine Serum (FBS, Invitrogen, 10082-139). Cells were then incubated at 27 °C for 72 hours while monitoring for signs of infection every 24 hours (Figure 2-8).

2.11 Isolation and amplification of viral stocks

Viral amplification was performed following the manufacturer's protocol. At first, the medium from a single well containing P1 viral stock was collected and centrifuged at 500 rpm for 15 minutes (Eppendorf 5810 R) to remove uninfected cells and large cell debris. 2×10^6 *Sf9* cells in 2 mL of pre-warmed Grace's Insect Medium, supplemented with 10% FBS, were added into each well of a 6 well plate. Once the cells were attached after 30 min, 100 µL of P1 stock was added to each well and was incubated at 27 °C. Medium containing P2 viral stock was collected 72 hours post-infection, and centrifuged at 500 × g for 15 minutes (Eppendorf 5810 R). Clear supernatant containing virus particle was then collected and stored at 4 °C.

2.12 Protein expression and purification

To express proteins in *Sf*9 cells, cells in mid-log phase were infected with 100 µL of P2 viral stock. *Sf*9 cells were collected 72 hours post-infection and resuspended in lysis buffer (1×10^7 cells/mL) at 4 °C. After an incubation of 45 min in lysis buffer, cells were lysed by sonication (3×15 seconds at 50% output) (Branson Sonifier 450). Triton was added at a final concentration of 1% after sonication. Clarified lysates were incubated with MagneHis Ni particles (Promega, Catalog no. V8500), and washed with 5 particle volumes of wash buffer. Finally, proteins were eluted from the Ni particles using an increasing concentration of imidazole added to the wash buffer. Buffer compositions are

listed below. Eluted fractions were analyzed using SDS-PAGE followed by silver staining.

Lysis buffer: 20 mM Tris-HCl (pH 7.9), 150 mM sodium chloride, 1 mM EDTA, 1 mM EGTA, 1 mM DTT, 1 mM sodium orthovanadate, 1 mM PMSF, 10 µg /mL aprotinin, 10 µg/mL leupeptin, 10 µg/mL pepstatin and 5 mM sodium fluoride.

Wash buffer: 20 mM Tris-HCl (pH 7.9), 150 mM sodium chloride, 20 mM Imidazole (pH 7.9).

Elution buffer: 20 mM Tris-HCl (pH 7.9), 150 mM sodium chloride, 40-500 mM Imidazole (pH 7.9).

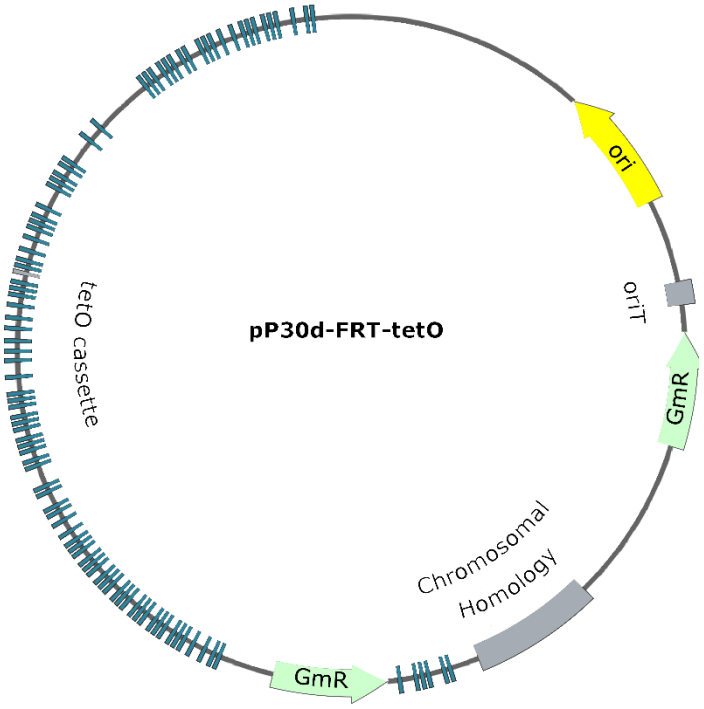

Figure 2-1: Plasmid map of pP30D-FRT-tetO integration vector. This plasmid was used to integrate *tetO* repeats in the *P. aeruginosa* chromosome. Approximately 500 base pairs of chromosomal segments were amplified and inserted between KpnI/HindIII restriction sites. Plasmid map created by SnapGene®Viewer software.

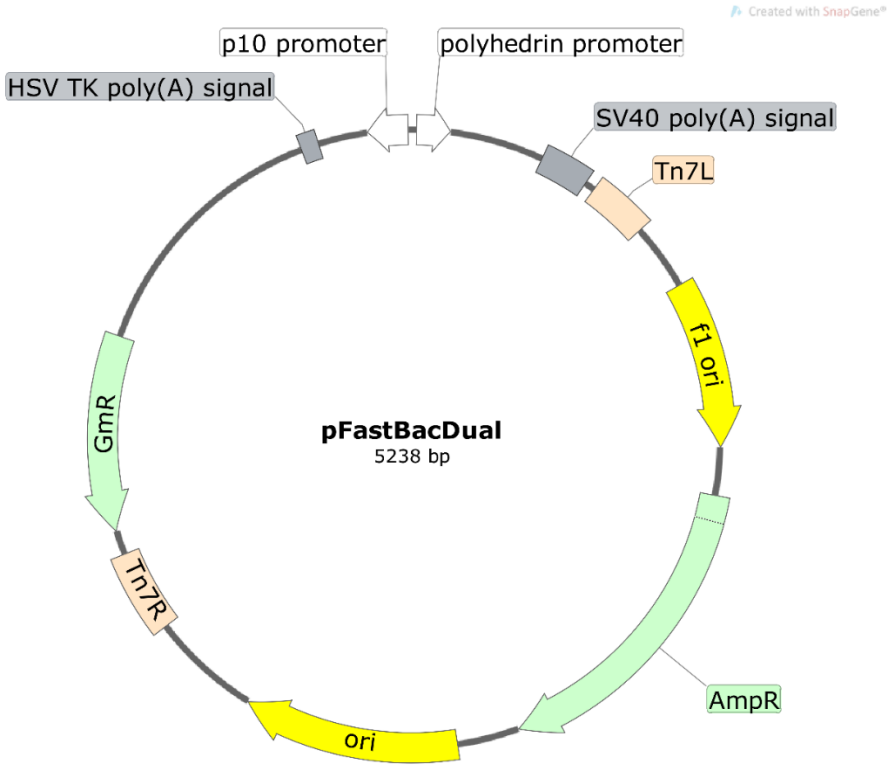

Figure 2-2: Map of the pFastBac™Dual expression vector

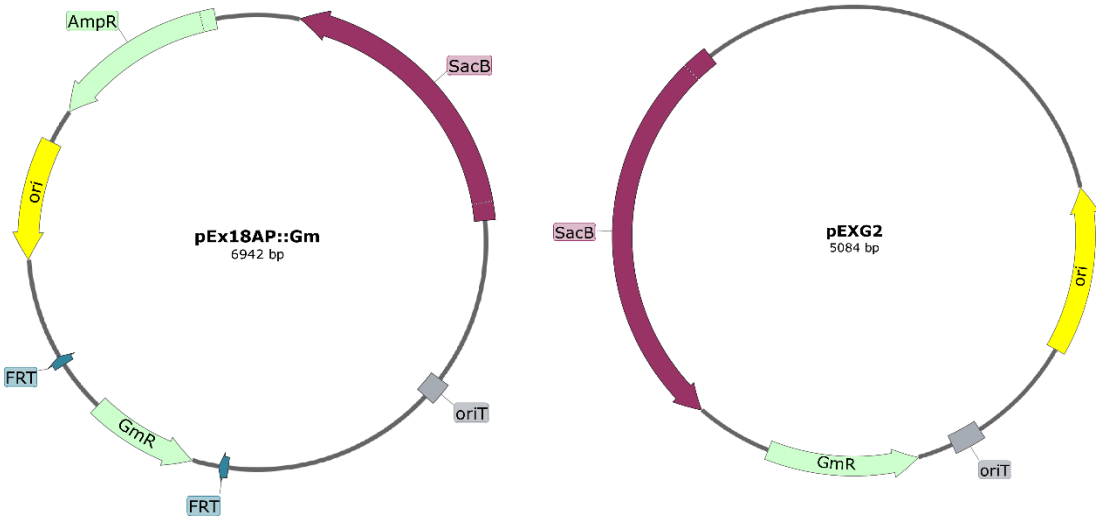

Figure 2-3: Plasmid maps of suicide vectors pEX18Ap::Gm and pEXG2.

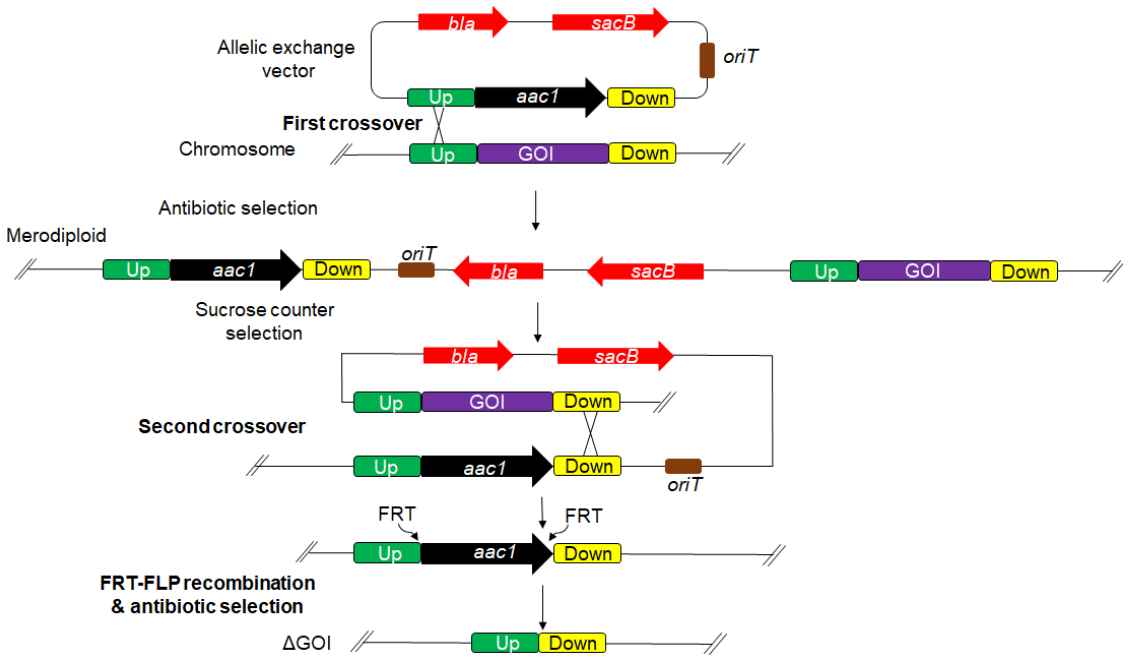

Figure 2-4: Diagram of gene-deletion by two-step allelic exchange method.

The map is adopted from [151].

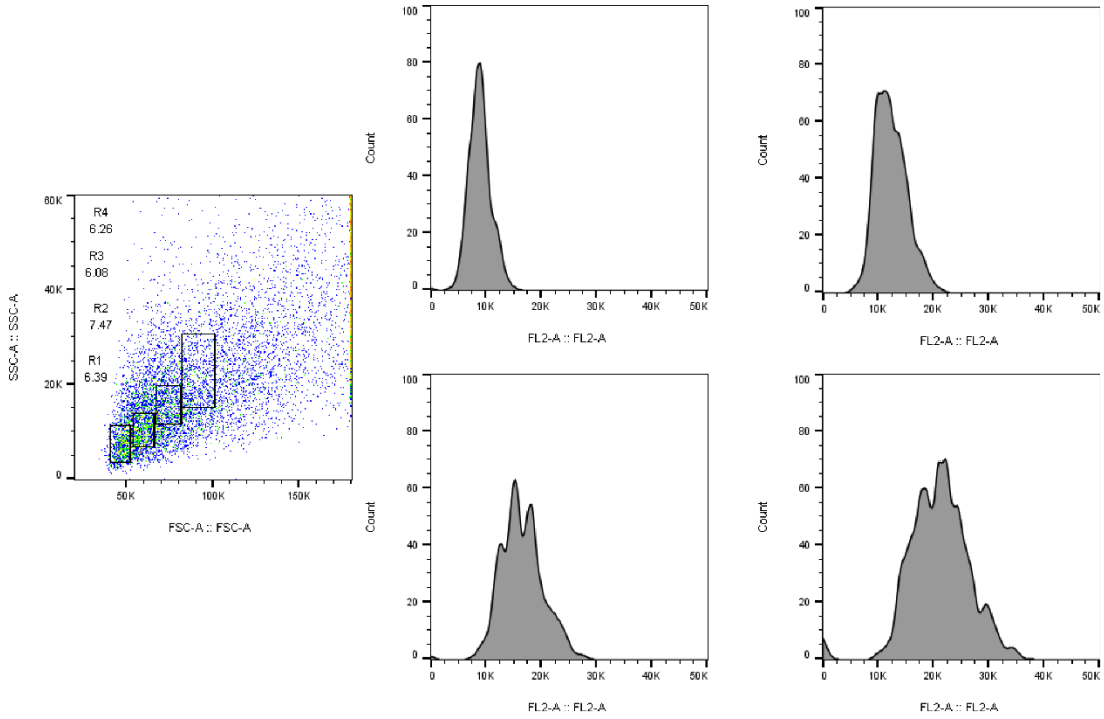

Figure 2-5: Flow cytometric analysis of DNA content in *P. aeruginosa*.

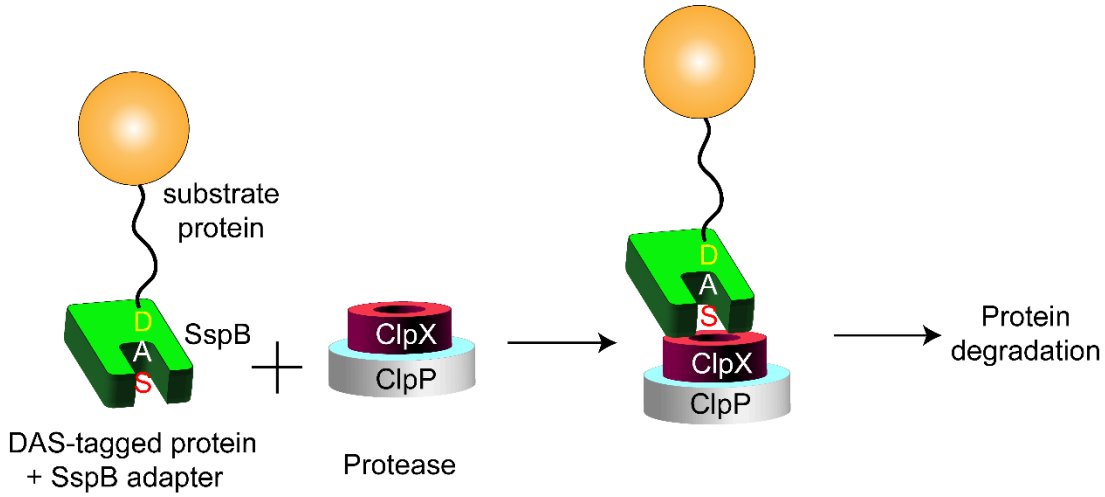

Figure 2-6: DAS4 mediated controlled protein degradation system.

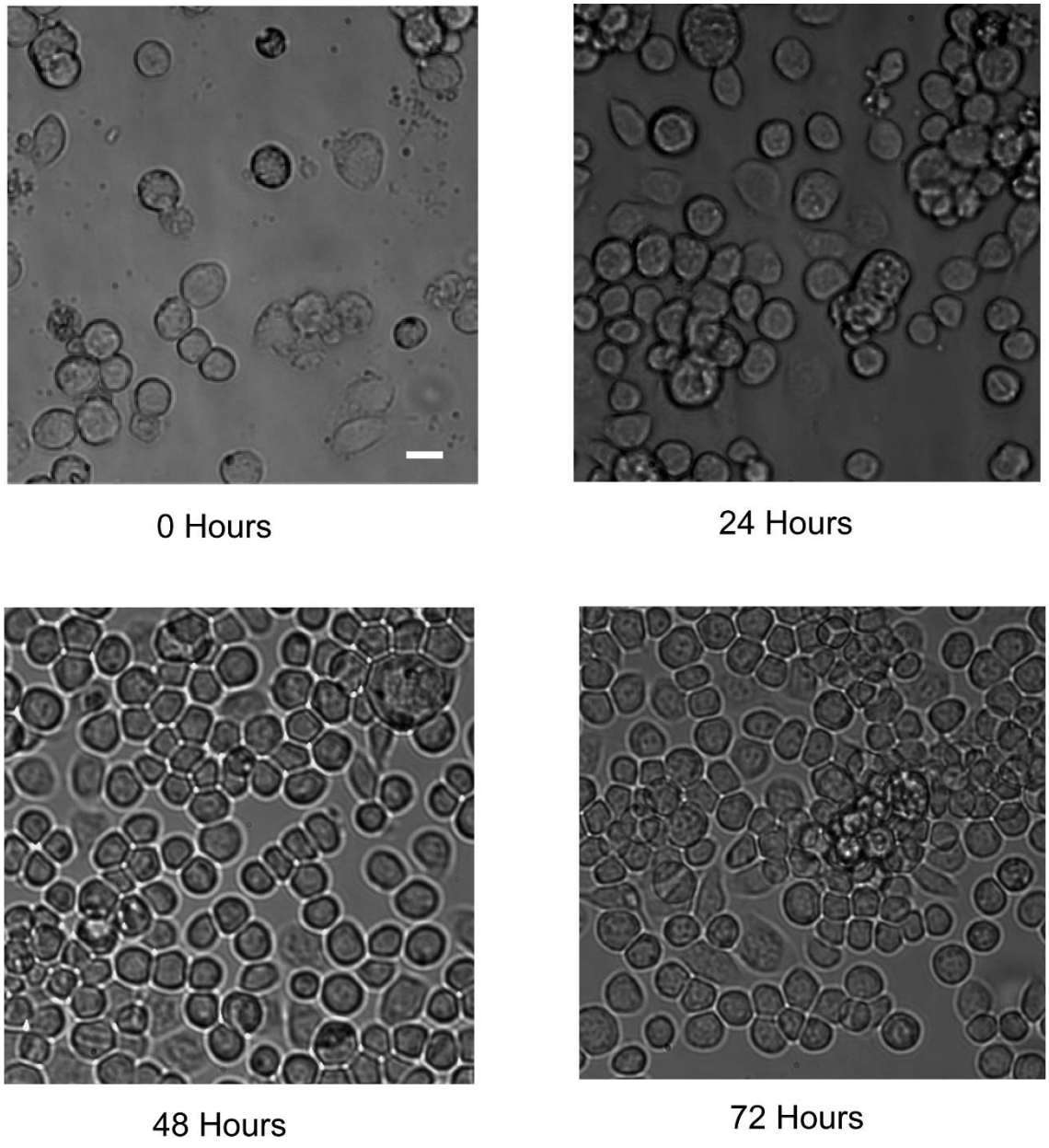

Figure 2-7: Growth and maintenance of *Sf*9 cells. Representative images of *Sf9* cells grown in adherent culture. Images were taken every 24 hours after initiating cell culture. Initially, cell debris can be seen (0 hours) and cells have a much lower density. After 48 hours, cells reach more than 80% confluency and remain as a monolayer. After 72 hours, cells start to form clumps and some cells begins to differentiate. Scale bar 20 μm.

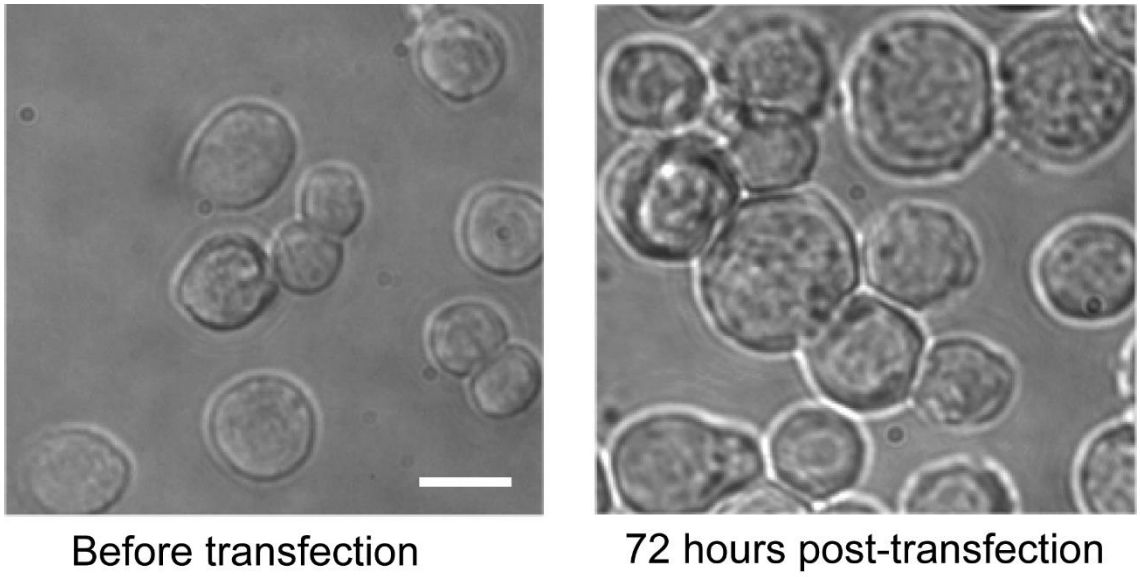

Figure 2-8: Morphological changes following transfection of *Sf*9 cells with recombinant bacmid. Representative images of *Sf*9 cells following transfection with recombinant bacmid. Characteristic morphological changes can be seen 72 hours post transection. Increased cell size, granular appearances inside cell, and uneven cell membranes can be seen after successful transfection. Scale bar 20 µm.

Chapter 3: Chromosome segregation but not replication terminates at *dif* in *Pseudomonas aeruginosa*

3.1 Introduction

In this chapter we tested the hypothesis that chromosome segregation starts from the *oriC* locus and ends at *dif*. In doing so, we determined whether or not a strict coordination exists, between chromosome replication and segregation. For this purpose, we first determined chromosome segregation in the opportunistic human pathogen *P. aeruginosa*. The single chromosome of *P. aeruginosa* strain PAO1 is 6.3 Mbp long and contains 5,570 predicted ORFs. An interesting feature of PAO1 chromosome is the presence of an inversion between two ribosomal RNA operons (*rrnA* and *rrnB*) located in opposite chromosomal arms and separated by 2.2 Mbp [18]. As a consequence of this inversion, the origin of replication (*oriC*) and sister-chromosome resolution site (*dif*) are asymmetrically located (Figure 3-1).

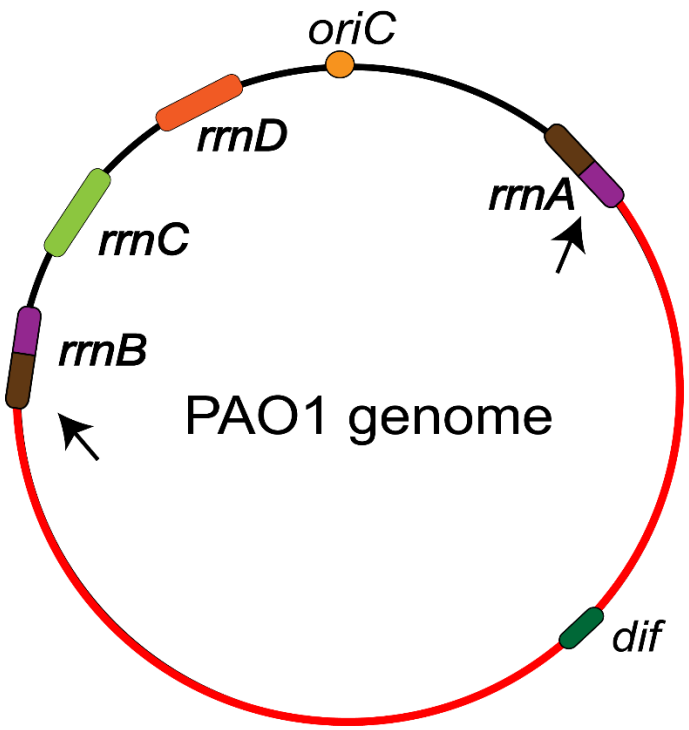

Figure 3-1: Asymmetric orientation od PAO1 chromosome. The arrows indicate the recombination sites. As a consequence of this inversion, the *dif* site is located at an asymmetric position compared to the *oriC*.

To visualize different segments of the chromosome in live cells, we used the Fluorescence Repressor Operator System (FROS). In short, a cassette of 140 *tetO* sequences was inserted at twelve different locations on PAO1 chromosome (Figure 3-2 A). To visualize tagged segments of the chromosome, the pPSV35Ap-TetR-CFP plasmid was introduced into those cells. Induction with 0.05 mM IPTG led to the production of TetR-CFP chimera, which then binds to the *tetO* cassette. The location of the fluorescent focus was determined by observing live cells using a fluorescent microscope (Figure 3-2 B). These results were contrasted with the analysis of replication fork progression using marker frequency analysis of purified PAO1 genome.

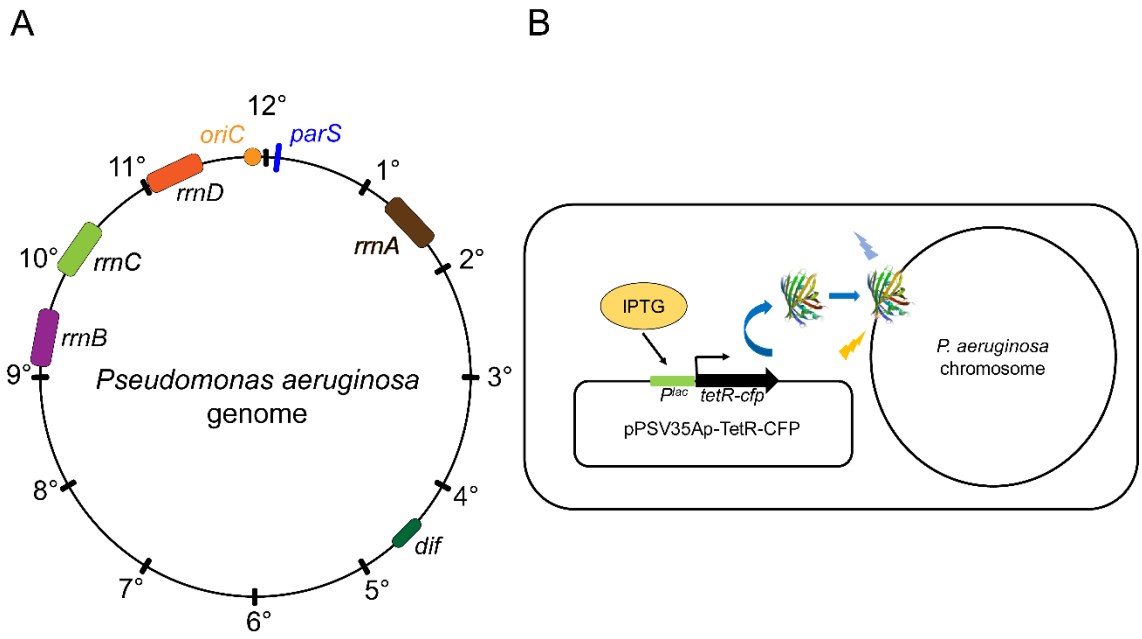

Figure 3-2: Visualization of PAO1 chromosome. (A) A map of PAO1 genome with major chromosomal elements marked; *tetO* cassettes were inserted at the indicated locations on the chromosome indicated by numbers 1-12. (B) Schematic representation of the FROS system used in this study.

3.2 *Pseudomonas aeruginosa* PAO1 chromosome is longitudinally oriented

For the analysis of chromosome segregation, *tetO* tags were inserted at twelve locations of the chromosome. To minimize multiple rounds of replication, cells were grown in M9 minimal medium (pH 7.5) supplemented with 0.25% sodium citrate at 30 °C, and TetR-CFP expression was induced by the addition of 0.05 mM IPTG. At these conditions, the doubling time was 55 min, and at most one new round of replication was initiated (but did not progress far) prior to cell division. The cells were then deposited on a thin agarose pad and observed using

a fluorescent microscope. The subcellular localization of TetR foci was quantified using the spot finding software Nucleus, and the results were binned according to the cell length.

We first determined the average location of each tagged locus in the newly born cells, i.e. those shorter than 2.1 μm. Such cells contain only one chromosome and, accordingly, most of them contained only one TetR-CFP cluster (Figure 3-3 C). The average location of each cluster within cell correlated with its genomic position. The *oriC* proximal cluster was found at the mid-cell, the *dif*-proximal cluster was found close to the cell pole, and the rest of the tagged loci were found in between. Notably, most of loci in the left arm are located in the mid-cell region (Figure 3-3 A, B). Thus, the PAO1 chromosome is longitudinally arranged within the cell with *oriC* and *dif* located at two extremes. This arrangement is similar to that found for PAO cells, which carry *oriC* and *dif* at diametrically opposite positions[149].

We then determined the location of *oriC* and *dif* throughout the cell cycle by monitoring their locations inside cells of different lengths. In short cells, corresponding to early in the cell cycle, *oriC* was located in the mid-cell region and *dif* was located at the cell pole. As cells grew, and progressed through the cell cycle newly generated copies of *oriC* migrated to the quarter position and remained there until a second round of segregation took place. The *dif* loci migrated to the mid-cell and remained there until they segregate (Figure 3-3 C). While the majority of the cells had a single copy of *dif*, two copies of *oriC* were found. This suggest that *oriC* is the first locus to segregate and that *dif* segregates

last (Figure 3-3 D, E). In larger cells, the presence of four *oriC* loci but a single *dif* locus suggests that *oriC* undergoes a second round of segregation before the segregation of the entire chromosome is complete.

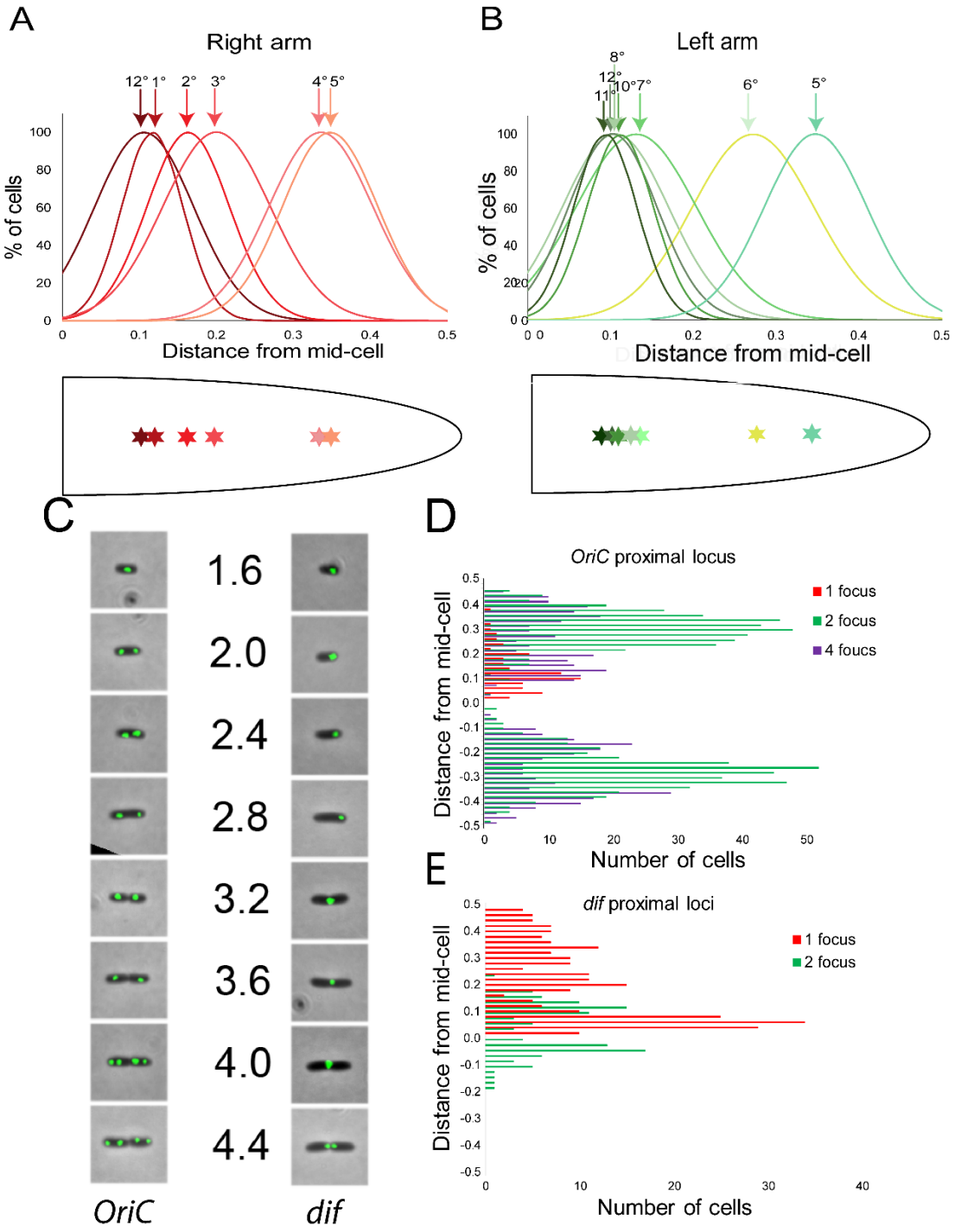

Figure 3-3. Sequential segregation of PAO1 chromosome. (A) Intracellular locations of chromosomal loci on the right arm. Bottom panel schematically

depicts these locations in a half-cell. (B) Intracellular locations of the chromosomal loci on the left arm. Bottom panel represents these locations in a half-cell. (C) Representative images of cells with tagged *oriC*- and dif- proximal loci. Scale bar is 1μm. (D) Distribution of *oriC* and (E) *dif* locations within a cell. For both panels, cells having one, two and four foci were binned according to the subcellular location of each locus.

3.3 *P. aeruginosa* chromosome segregates from *oriC* to *dif*

We next analyzed the localization of the tagged chromosomal loci located within cells of varying cell length. Figure 3-4 A, B illustrates the percentage of two and where appropriate, four focus cells for a given length. In short cells, each chromosomal locus exists as a single focus. As the cells grow, they segregate, generating cells with two foci. A significantly high number of short cells contained two *oriC* foci, suggesting that in these cells, *oriC* has already segregated before the last cell division was complete. This idea is corroborated by the observation that the majority of large cells had four *oriC* foci.

The next locus to segregate after *oriC* were located at the 1 o'clock and 11 o'clock positions on the chromosome. This is expected if chromosome segregation is bidirectional. The rest of the chromosomal loci segregated sequentially depending on their distance from *oriC*. Interestingly, the *dif*- proximal locus segregates only in long cells (>4 μm), after segregation of all the other loci. This implies that, in PAO1, segregation finishes at the *dif* site. Notably, in more than 20% of cells, *dif* remains as a single locus, even in long cells. This indicates that, in these cells, *dif* segregates simultaneously with cell division. To determine

if this defect was due to guillotinization of the chromosome at the *dif* site, we tested for the presence of this locus in several individual colonies by PCR. Our results indicate that all of them had a complete *dif* locus (data not shown).

Figure 3-4 C, D illustrates the average location and timing of segregation of the 12 tagged loci as binned according to the cell size. illustrates the average location and timing of segregation of all the 12 loci according to the cell size. *oriC* proximal locus is first to segregate. As the cells grew, each locus sequentially relocated towards the mid-cell, duplicated, and then the two sister loci migrated towards their new positions in the emerging daughter cells. This pattern is consistent with the observation that the replication machinery of *P. aeruginosa* is located at the mid-cell [149], The locus closest to *dif* is the last one to segregate. After the analysis of the segregation pattern of the entire chromosome, it is clear that in PAO1 the chromosome segregates from *oriC* to *dif*.

This surprising finding is in direct contradiction with the segregation pattern reported for several model laboratory bacteria, where chromosome segregation ends at the terminus region, which was always found opposite to *oriC*. However, in these bacteria, the *dif* site is also located in the terminus region, flanked by *Ter* sites. Taken together, our results indicate that irrespective of its location, *dif* site is where chromosome segregation ends, and the pattern found in other bacteria may be a result of *dif* being present in the terminus region.

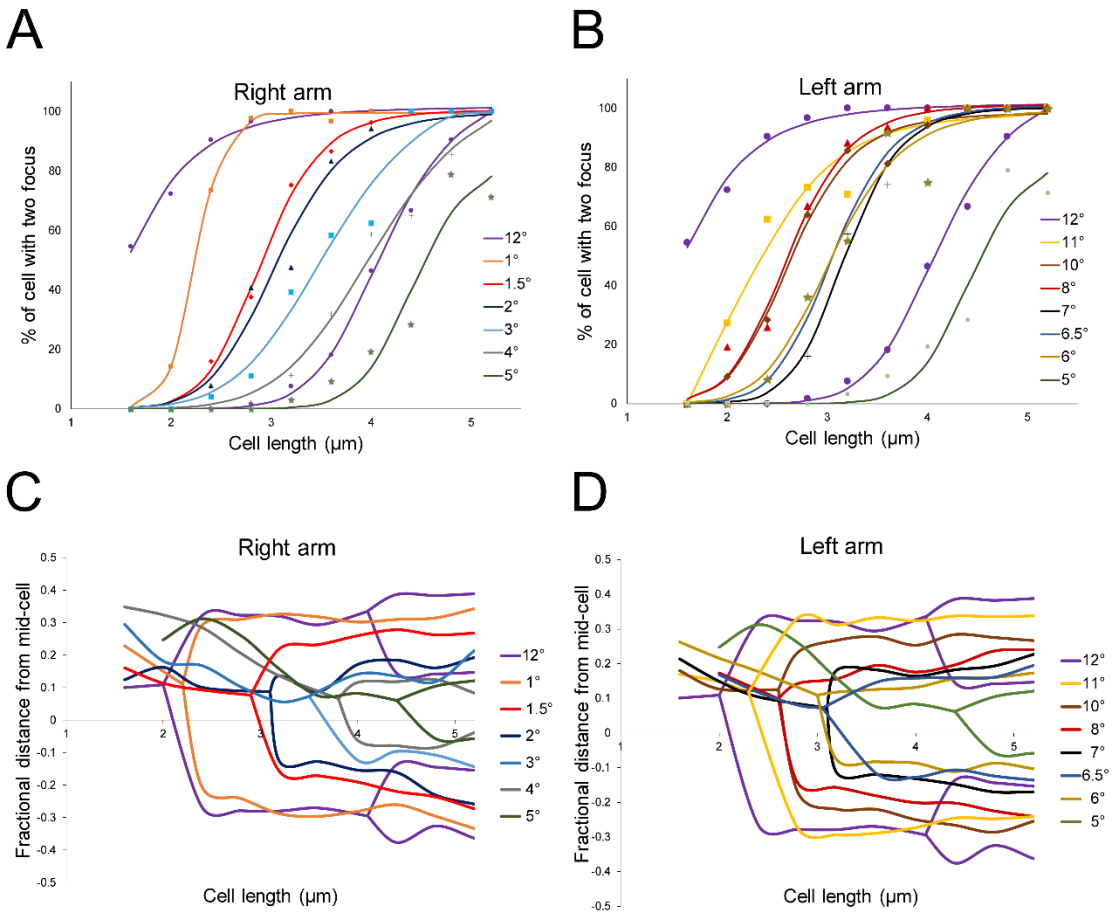

Figure 3-4: PAO1 chromosome segregates sequentially from *oriC* to *dif*. (A, B) Percentage of two- and four- focus cells in a given population of PAO1 cells. Proportions of cells were calculated for given cell length. The best fit line for each locus was derived by fitting the data in a sigmoid function and was plotted against corresponding cell length. (C, D) Average distance from mid-cell was calculated for each chromosomal locus and was plotted against corresponding cell length. Each line represents sub-cellular location of an indicated locus. Split point for

each locus was determined for the cell length, when 50% cells had two or when appropriate, four foci.

3.4 PAO1 chromosome segregates discontinuously along the chromosomal arms

Because of the asymmetric location of *oriC* and *dif*, the left arm of the PAO1 chromosome is 56% longer than the right arm. In spite of this size difference, segregation along both arms finishes at the same time. To gain insight into the coordination of segregation between the arms, we determined at what cell length, 50% of the population have two visible foci for each tagged locus. Comparing this information with respect to the genomic location of the corresponding locus provides a timeline at which each locus segregates. Figure 3-5 A illustrates this difference in segregation pattern of the two chromosomal arms. While the shorter right arm maintains a continuous mode of segregation, the left arm segregates in discrete steps.

Figure 3-5 B summarizes the synchronicity in segregation between the two chromosomal arms of *P. aeruginosa*. An interesting feature of the longer left arm is the presence of two distinct domains. Two large segments of the chromosome the first located between the 8 o'clock and 10 o'clock, and the second between the 6 o'clock and 7 o'clock, appear to segregate as two separate domains. These two chromosomal segments span 1 Mb and 0.5 Mb respectively, and resemble the macrodomains present in the *E. coli* chromosome. No such domains were previously described for the *P. aeruginosa* chromosome.

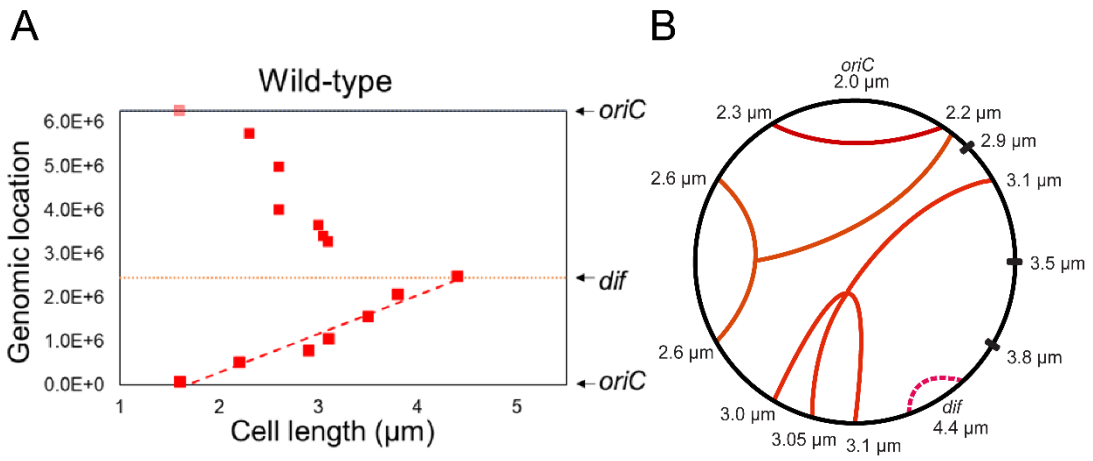

Figure 3-5: Chromosome segregates discontinuously along the arms. (A) Cell length at which 50% of cells had two visible foci was calculated for each chromosomal locus and then plotted against their genomic locations. Locations of *oriC* and *dif* were also indicated. (B) Synchronicity between two chromosomal arms. For each locus on the left arm, the cell length at with a single focus splits into two was calculated and their corresponding locus on the right arm was interpolated. The timing of the segregation of loci on the right arm are also indicated.

3.5 Chromosome replication proceeds from origin to terminus

Having found the asymmetric segregation pattern of the PAO1 chromosome, we decided to elucidate the coordination between chromosome segregation and replication. To this end, we performed a high-throughput sequencing based marker frequency analysis of purified PAO1 genomes. This technique provides the copy number of each gene on the chromosome. Figure 3-6 illustrates the replication fork progression in the PAO1 genome extracted from cells grown under slow growth condition (M9 minimal medium) as well as faster

growth condition (LB). Since replication starts at *oriC*, genes located close to this locus will have a higher copy number. As the replication fork proceeds, the copy number of genes decreases gradually, implying that replication proceeds consistently along the arms. Judging by the copy number of genes, in PAO1, replication ends at a location opposite to *oriC*. When grown in the faster growth condition, a second round of replication initiation takes place before the first-round ends, thus producing four copies of the genes located close to *oriC*. Our results suggest that in PAO1, replication ends opposite to *oriC* when two opposing replication forks collide. Comparison of replication and segregation also indicates that there is no obvious coordination between these two processes. Replication terminates at a location opposite to *oriC,* segregation ends at *dif* and these two locations are separated by 1Mbp.

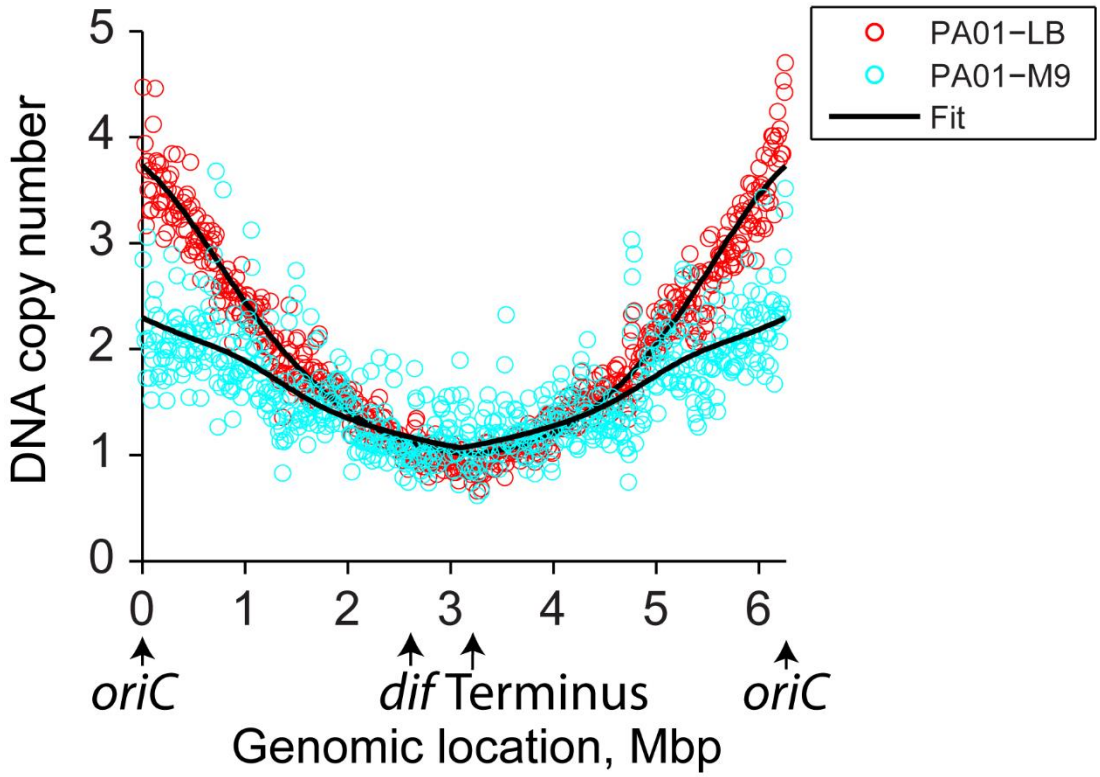

Figure 3-6. Replication proceeds from *oriC* to terminus. Genomic DNA was isolated from cells grown in LB and M9 minimal medium. Copy number of each gene was determined after sequencing the entire genome. We modelled replication fork movement based on the assumption that genes behind replication fork will have two copies, whereas genes in front of the fork will have a single copy. Based on the cell size distribution we then postulated the velocity of fork movement and used it as a fit parameter.

3.6 Chromosome segregation coincides with cell cycle

To maintain genomic integrity during the cell cycle, proper coordination between chromosome dynamics and cell division is necessary. We explored the correlation between chromosome segregation and septum formation. The timing of septum formation was determined by the presence of cell-wall constriction in phase-contrast images of cells. Figure 3-7 indicates that segregation of the *dif* proximal loci coincides with septum formation. Segregation of the *dif* locus was monitored in cells grown in M9 minimal medium. At these conditions, the *dif* locus is relocated from the cell pole to the mid-cell region during septum formation and the segregation of *dif* happens only after the septum was formed. This result suggests that there is a coordination between the dynamics of the *dif* locus and cell division. However, how these two processes communicate with each other is unclear.

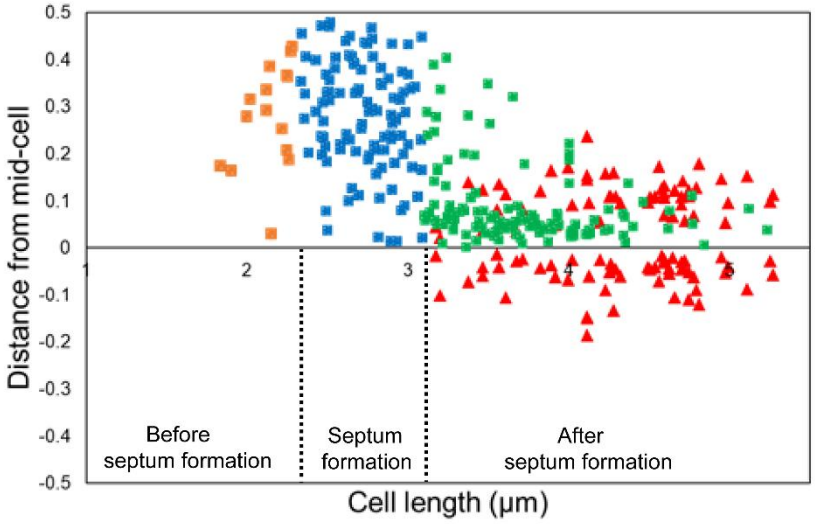

Figure 3-7: *dif* segregation coincides with septum formation in PAO1. Location of *dif* was determined by using spot sizing software nucleus. Septum formation was determined from phase contrast images by monitoring constriction in cell wall. Cells with visible *dif* locus was differentiated based on timing of septum formation.

Chapter 4: Elucidating contributions of the two condensins and ParAB*S* to organization and segregation of the *P. aeruginosa* chromosome

4.1 Introduction

In this chapter we tested our second hypothesis, that condensins mediate global chromosome organization and facilitate proper chromosome segregation. Notably, in *P. aeruginosa*, two condensins from two different families are found: SMC-ScpAB and MksBEF. SMC and MksB also have opposite effects on cell physiology. SMC is required for planktonic growth, whereas MksB facilitates sessile growth. Interestingly, both these proteins are required for virulence in *P. aeruginosa* [17]. Recently Dr. Zhao found that both of these proteins form dynamic clusters within the cell (Figure 4-1) [158]. Their differential segregation pattern suggests that they have different modes of action in chromosome organization. However, their role in chromosome segregation is unclear. To determine the roles of each condensin in PAO1 chromosome segregation, we used a similar FROS based approach in strains deficient in condensins. We also elucidated the interaction between condensins and the chromosomal partitioning system (ParAB*S*)

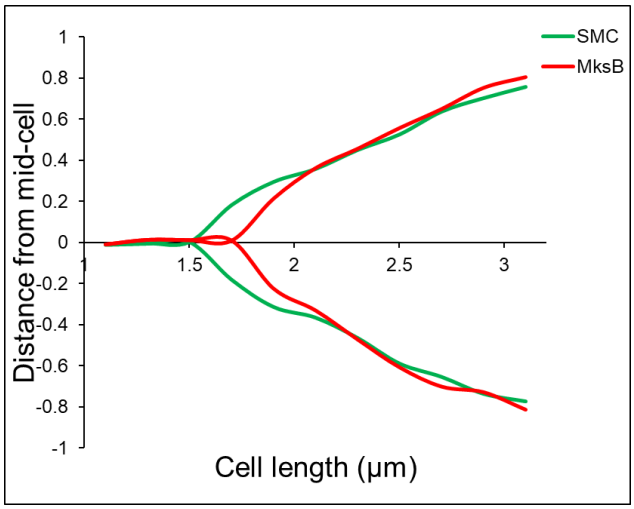

Figure 4-1: Segregation of SMC and MksB. Localization of fluorescently tagged SMC and MksB was determined and plotted against cell length in poly-lysine fixed *P. aeruginosa* cells. Figure was reproduced with permission from Dr. Zhao.

4.2 Deletion of *smc* disperses genomic domains and accelerates chromosome segregation

We first analyzed the segregation patterns of the chromosome in the Δ*smc* strain of PAO1. Figure 4-2B suggests that the chromosome in a Δ*smc* strain retains the longitudinal organization. Both chromosomal domains are dispersed in this mutant. Interestingly, segregation of *dif* proximal region is accelerated in Δ*smc* strain. In this mutant, a chromosomal locus located opposite to *oriC* segregated at the end of the segregation cycle. Similar to the *dif* site, bulk of the chromosome was also segregated sooner in Δ*smc* strain.

To help interpret this data we need to recall that the biochemical activity of SMC is to bridge distant segments of DNA. In this light, deletion of SMC should

decrease the overall compactness of DNA at locations where it is recruited to. The finding that in Δ*smc* cells chromosomal domains are dispersed is consistent with this activity and suggests that SMC was indeed recruited on those sites. The early segregation of *dif,* however, is not consistent with this straight-forward view. We propose, that SMC maintains delayed segregation of *dif* by tethering this locus.

4.3 Deletion of *mksB* delays chromosome segregation and also disperses genomic domains

To determine the segregation pattern of chromosomes within the Δ*mksB* mutant, we analyzed the localization of twelve chromosomal loci distributed on both arms. Similar to the parental strain, the chromosome of Δ*mksB* segregated sequentially from *oriC* to *dif* (Figure 4-2 F), suggesting that the longitudinal chromosome arrangement is maintained in Δ*mksB* cells. Comparison of chromosome segregation between the parental strain and Δ*mksB* cells revealed a delay in segregation of the entire chromosome with the exception of *oriC*, which segregated earlier. Both chromosomal domains were also dispersed in Δ*mksB* cells (Figure 4-2E). Surprisingly, deletion of MksB resulted in a major segregation defect at the *dif.* In Δ*mksB* cells the *dif* site was always observed as a single focus, even in longer cells. No cells without a *dif* focus was observed either. This suggest, in Δ*mksB* cells, segregation of the *dif* site happens simultaneously with cell division. These data suggest that MksB is also required for compaction of the entire chromosome.

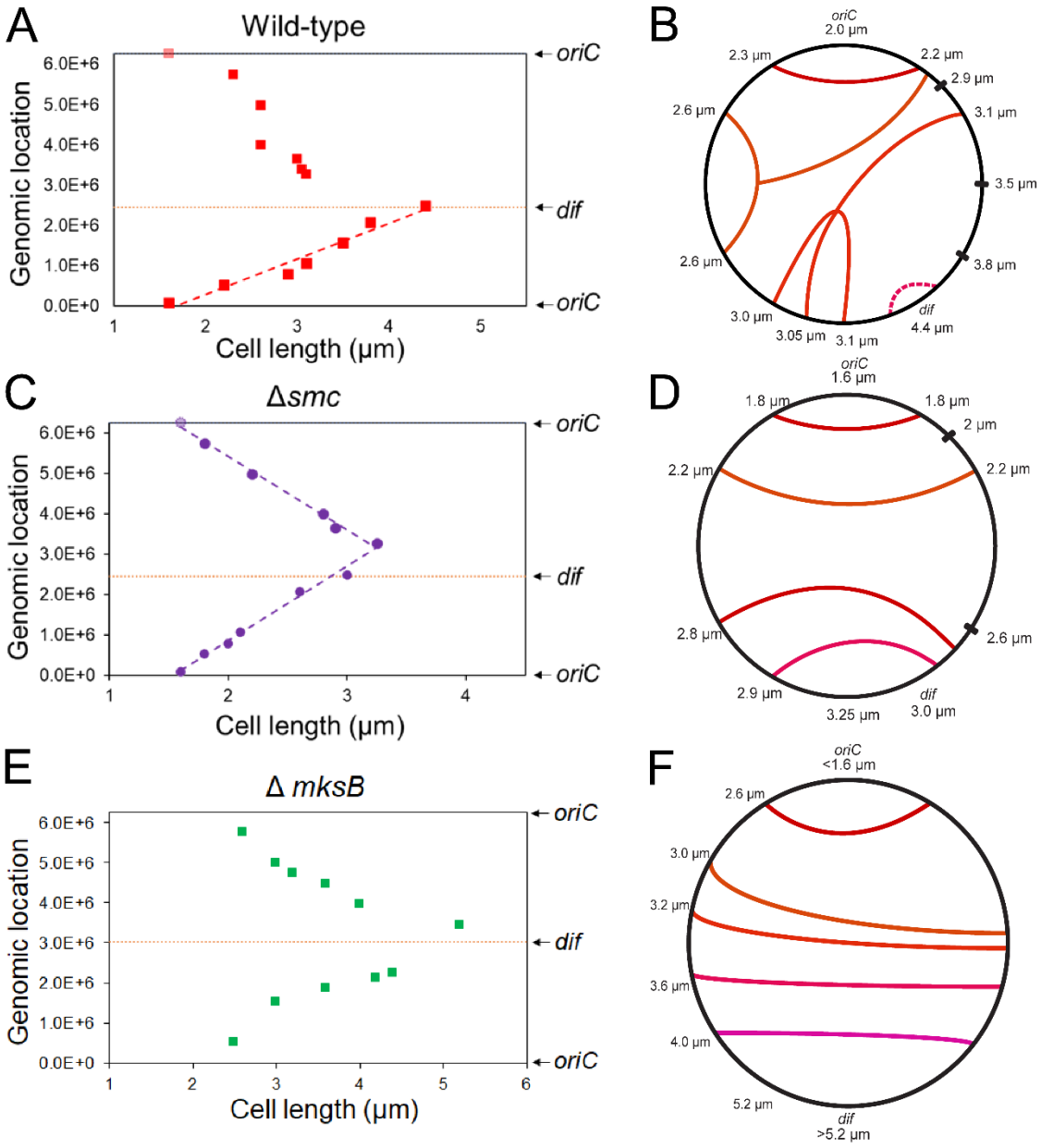

Figure 4-2: Condensins are required for proper chromosome segregation pattern. (A, C and E) shows the cell length at which a particular chromosomal locus split into two daughter loci. (B, D and F) shows the synchronized segregation between the two chromosomal arms in wild type, Δ*mksB* and Δ*SMC* mutants respectively.

4.4 Deletion of *mksB,* but not *smc,* promotes recombination between ribosomal RNA (*rrn*) sites located on opposite arms

Next, we determined the replication fork movement in the Δ*mksB* and Δ*smc* mutants. Unexpectedly, we found an inversion between two ribosomal RNA operons *rrnA* and *rrnB* in the chromosome of the Δ*mksB* mutant. In the parental strain, these two operons are located on opposite chromosomal arms, oriented in opposite direction, and separated by 2.2 Mbp. To confirm this inversion, in the Δ*mksB* mutant, we designed two sets of primers (BB321/BB510 flanking *rrnA* and BB323/BB324 flanking *rrnB*) (Figure 4-3 A). Successful PCR amplification using these sets of primers is possible only if there is no inversion on the chromosome. To check for inversion between *rrnA* and *rrnB,* we used primer sets BB321/ BB323 and BB510/BB324 (Figure 4-3 B). These primer sets will generate product only if the chromosome acquires an inversion between *rrnA* and *rrnB*. Purified genomic DNA from four independent clones of wild type, Δ*mksB* and Δ*smc* were tested by PCR. Figure 4-3 C, D illustrates the PCR products obtained, from each strain, by using the primer sets mentioned above. All four Δ*mksB* strains tested positive for inversion between *rrnA* and *rrnB*, whereas, both wild type and Δ*smc* strains tested negative. This result indicates that MksB is required to prevent this inversion. How MksB prevents this re-organization is unclear. One possibility is that MksB organizes both chromosomal arms, thus preventing random collision between them. As a consequence of this inversion, the chromosome of Δ*mksB,* cells is symmetric, with *dif* site located diametrically opposite from *oriC*.

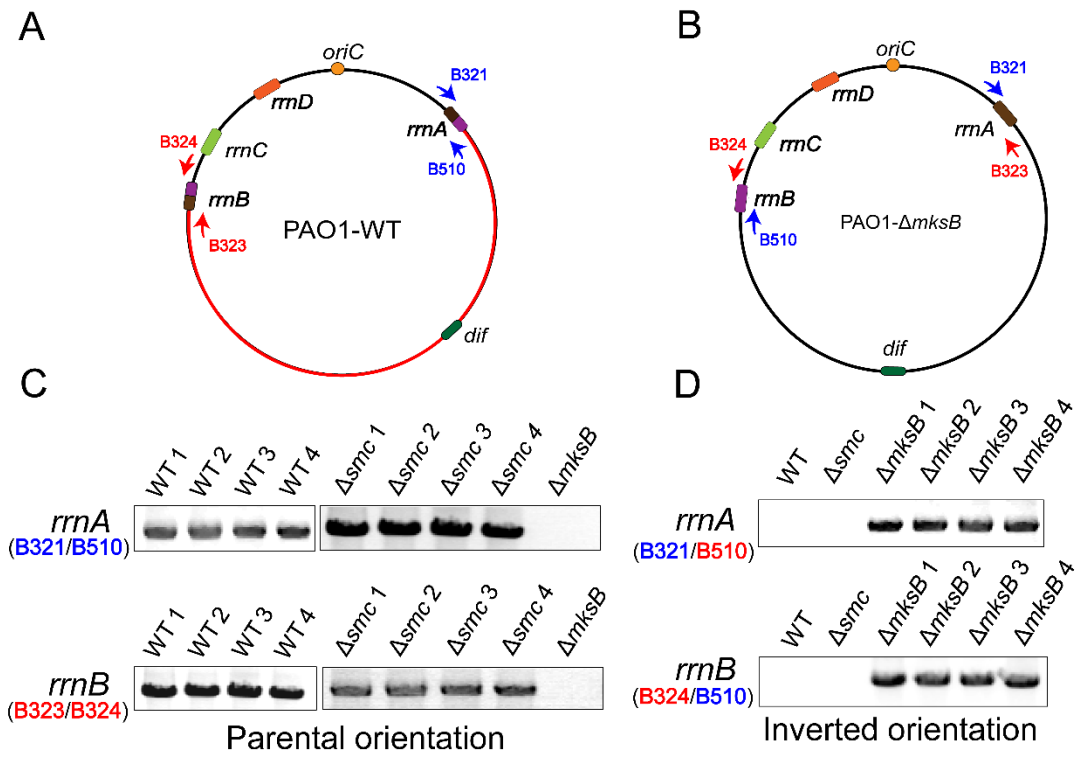

Figure 4-3: MksB prevents recombination between opposite arms. (A) shows the chromosomal map of PAO1 wild type stran and (B) Δ*mksB* strain, the primer used to determine inversion are also mentioned. (C, D) Agarose gel showing amplified PCR products in wild type, Δ*mksB* and Δ*smc* strains. Primers used to determine inversion between *rrnA* and *rrnB* are also indicated.

4.5 SMC but not MksB colocalizes with *oriC*

The results from previous sections suggest that MksB and SMC control different aspects of chromosome segregation. This can be achieved by interacting with different regions on the chromosome. To test this idea, we determined the localization of MksB and SMC on the chromosome. To observe the location of these proteins with respect to *oriC*, we replaced the endogenous

copy of SMC and MksB with their GFP tagged versions. *oriC* locus was observed by inserting *tetO* repeats in this locus and expressing the TetR-mCherry chimera from an IPTG inducible promoter. Finally, both these fluorophores were observed consecutively inside a single cell using fluorescent microscopy.

Figure 4-4 A, B shows that SMC but not MksB, colocalizes with the *oriC* locus. To confirm that this localization pattern is representative for the entire population of cells, we observed localization of MksB and SMC in many cells (n>100). Quantification of their average location and intensity was performed by Dr. Rybenkov using MATLAB. Figure 4-4 C shows the distance between the MksB-GFP focus and *oriC.* Distance of these proteins from mid-cell was also calculated. *oriC* proximal locus was located at the cell quarters whereas MksB occupied the mid-cell positions. No overlap between these two fluorophores were found. Figure 4-4 E shows the location of peak intensities of both fluorophores inside cell. Majority of the MKsB protein did not overlap with *oriC* locus. These results suggest that MksB does not bind to the *oriC* locus. Similar analysis involving SMC-GFP and *oriC* shows that SMC proteins co-localize with *oriC* at the quarter positions. (Figure 4-4 D, F). These results indicate that MksB and

SMC proteins bind to different regions on the chromosome.

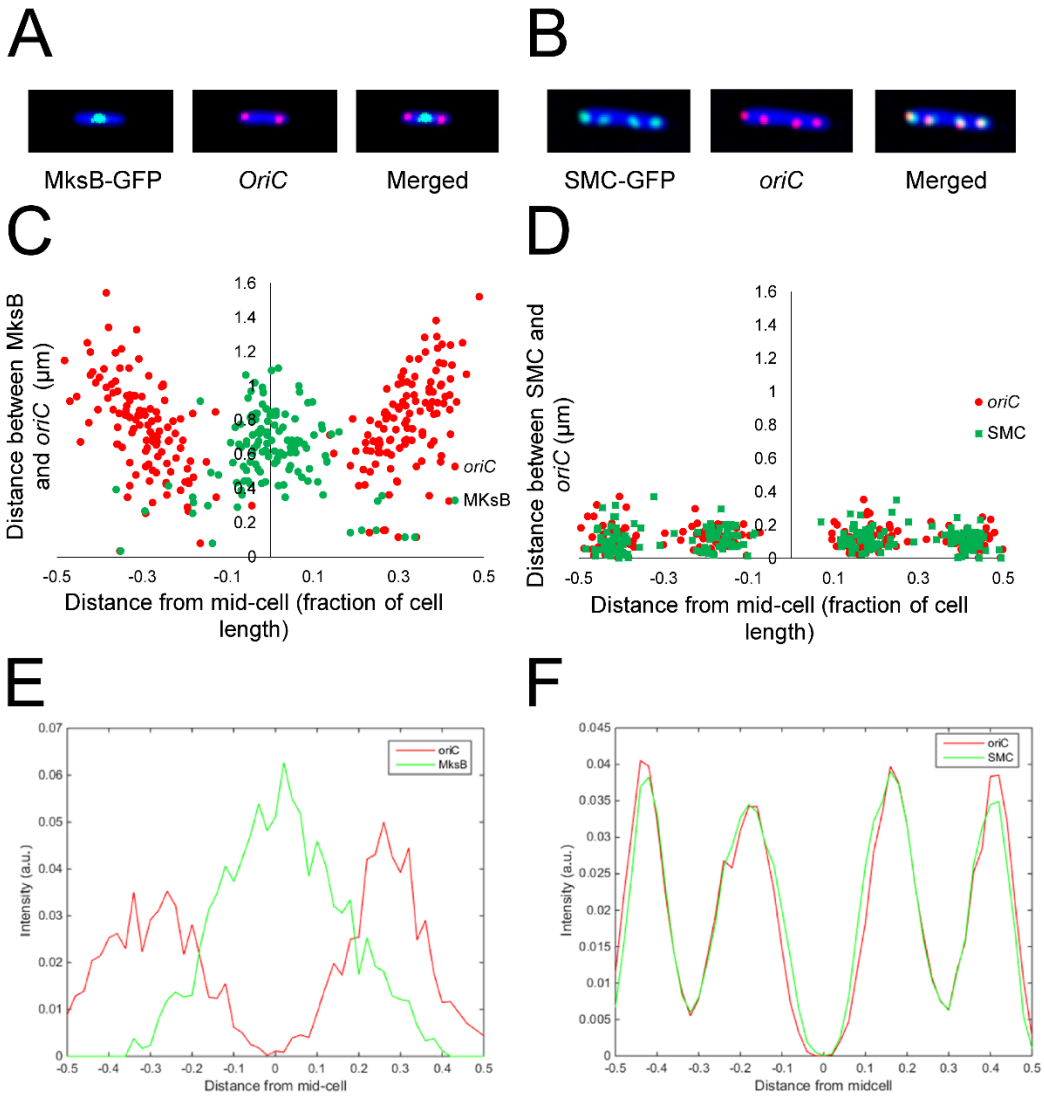

Figure 4-4: SMC but not MksB colocalizes with *oriC.* (A) Representative images of MksB-GFP, and SMC-GFP (B). *oriC* locus was tagged with *tetO* repeats and visualized by observing TetR-mCherry, expressed from pPSV35Ap-TetR-mCherry plasmid. (C) Distance between MksB foci and *oriC* foci and their subcellular location was determined using MATLAB. Similar analysis was performed for SMC (C). (E, F) Relative intensity of MksB-GFP, SMC-GFP and

mCherry tagged *oriC* was determined and their location inside cell was determined using MATLAB.

4.6 SMC and MksB cumulatively delay segregation of *oriC* but do not impair its positioning

To determine the role of condensins in the origin segregation, we analyzed the intracellular localization of *oriC* in wild type, Δ*mksB*, Δ*smc*, and Δ*mksB* Δ*smc* cells. Figure 4-5 indicates that neither SMC nor MksB have any significant influence on the proper positioning of the newly replicated *oriC* loci because in all cases, newly replicated *oriC*s were migrated towards the quarter positions. Interestingly, no obvious defects in *oriC* positioning were observed in Δ*mksB* Δ*smc* mutant either. Similar to the parental strain, the newly replicated copies of *oriC* migrated to the quarter positions in all three mutants. Interestingly, deletion of condensins accelerated the timing of *oriC* segregation. While *oriC* in the Δ*mksB* mutant segregates earlier than the wild type strain, segregation in the Δ*smc* mutant happened even earlier. *oriC* in Δ*mksB* Δ*smc* was the earliest one to segregate among all four tested strains.

These results reveal that condensins play a major role in proper timing of *oriC* segregation. It supports our earlier conclusion that both SMC and MksB participate in chromosome compaction. Condensed chromosomes are expected to move as a whole. Therefore, pulling condensed chromosomes will engage bigger mass than for decondensed chromosomes. This supports our previous

conclusion that condensins are required for the compaction of bulk of the chromosome.

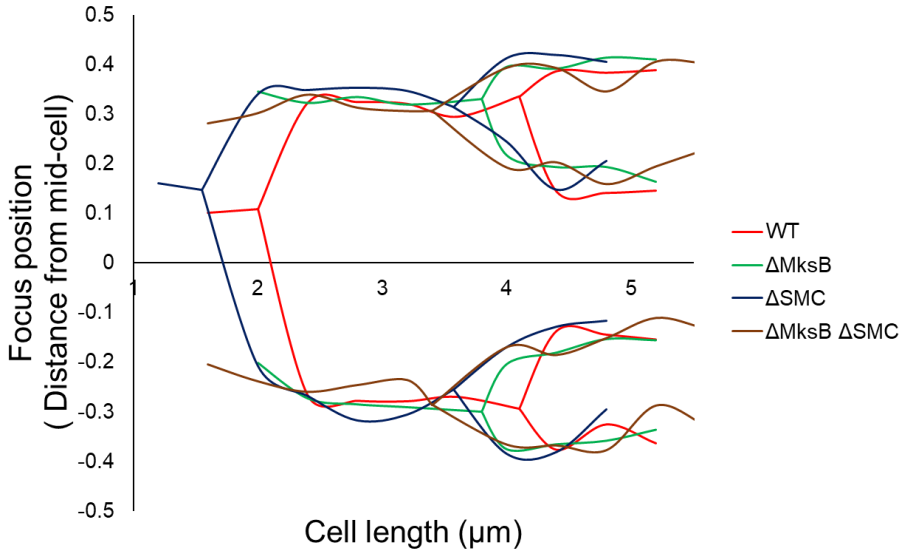

Figure 4-5: Condensins are required for proper timing of *oriC* segregation. Average location of *oriC* was plotted against cell-length for wild type (red), Δ*mksB* (green), Δ*smc* (magenta) and Δ*mksb* Δ*smc* (maroon) mutants.

4.7 Deletion of *parB* impairs proper *oriC* positioning

In bacteria, three major forces are postulated to drive chromosome segregation. The first one is condensins. Surprisingly, we found that in *P. aeruginosa*, condensins are not required for chromosome segregation. The second force that plays a vital role in chromosome segregation is the ParABS system. To determine the influence of ParABS system in *oriC* segregation, we analyzed localization of *oriC* locus in Δ*parB* mutants.

Figure 4-6 A, left panel summarizes the segregation pattern of *oriC* locus in *praB* mutant cells. Interestingly, *oriC* was able to segregate without the help of

the *parB* partitioning system, although positioning of newly replicated *oriC* was greatly affected. After segregation, one of the two newly replicated foci remained in a fixed position close to mid-cell, whereas the other focus occupied the quarter position. An abnormally higher proportion of cells carrying three *oriC* loci has also been observed Figure 4-6 A, right panel.

To understand the dynamics of *oriC* segregation in Δ*parB* cells, we monitored the movements of the *oriC* locus inside a single cell for an extended period of time. Figure 4-6 B - D displays the movement of the *oriC* locus in two representative cell types. The results from this time-lapse experiment are summarized in Figure 4-7. We found that depending on the location at the beginning of the segregation cycle, *oriC* takes one of the two possible paths of segregation.

In the first population of cells, *oriC* occupies the mid-cell region and undergoes replication in that region (Figure 4-6 B, D). One of the two newly replicated copies of *oriC* then migrates towards the old-pole and remains close to this pole, whereas the second copy occupies the quarte position. At this point in time, a second round of segregation takes place. Interestingly, *oriC* located close to the old cell-pole is always first to segregate, generating cells with three *oriC* loci. In these cells, one *oriC* copy remains close to the old pole, the second one moves towards the mid-cell and the third copy occupies the quarter position in the other cell-half. Finally, *oriC* located at the quarter position segregates, generating cells carrying four copies of *oriC*.

In the second population of cells, a single *oriC* focus can be found at the old-cell pole (Figure 4-6 C). As cells grow, this locus gets duplicated generating two copies of *oriC*. Notably, this duplication happens close to the cell quarters instead of mid-cell. Following duplication, one of the two *oriC* copies remains close to the cell-pole whereas the other copy migrates towards the quarter position of the opposite cell-half.

As a consequence of this asymmetric segregation of *oriC* a positioning defect can also be observed in cells with four copies of *oriC*. In these cells, two copies of *oriC* remain close to the opposite cell poles and the other two copies remain close to the mid-cell. Cell division can take place during an intermediate time in this segregation cycle, generating cells with either one or two *oriC* copies. Altogether, our results suggest that ParAB*S* system is also not required for chromosome segregation. However, this system is required for proper positioning of chromosome.

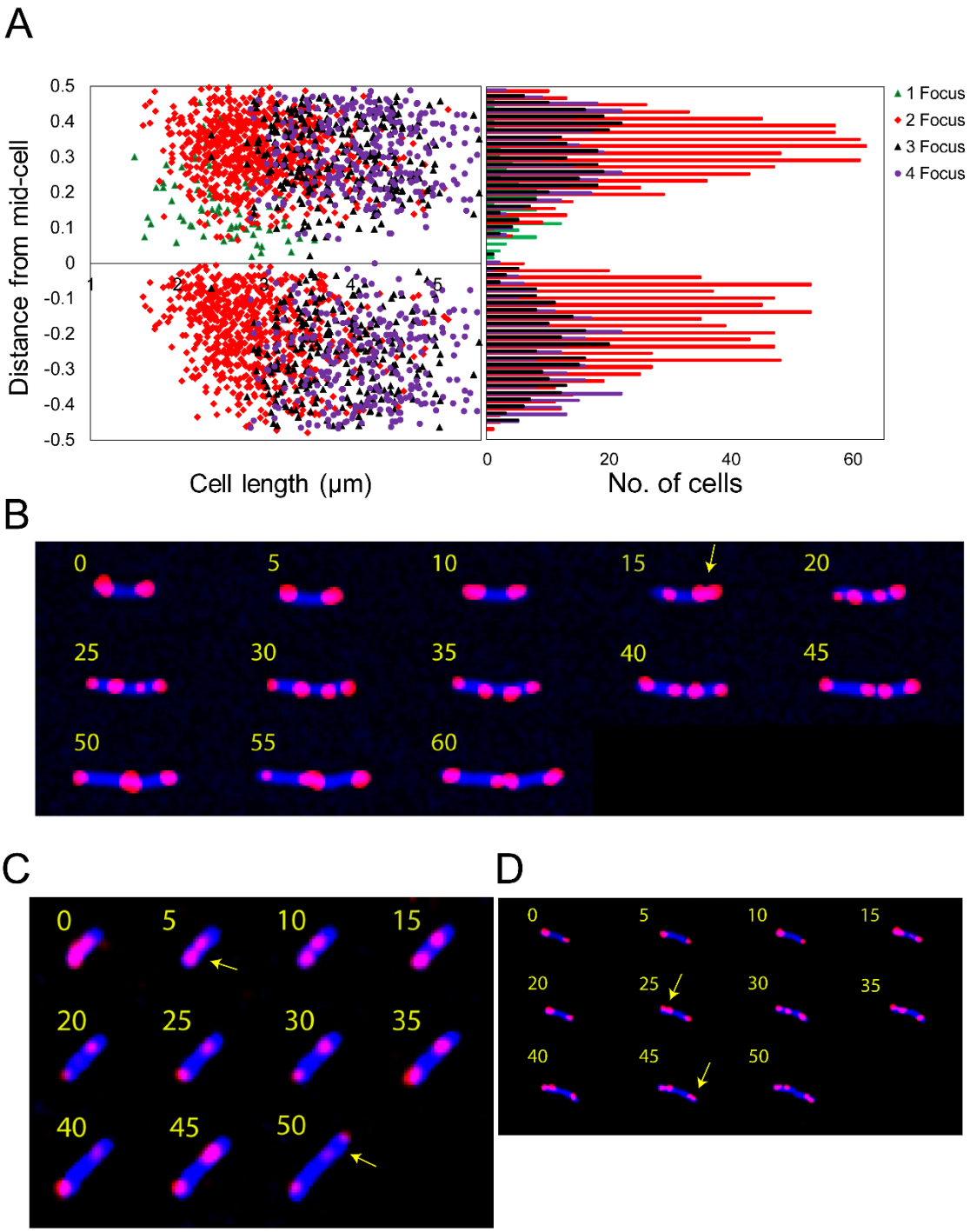

Figure 4-6: ParB is required for proper positioning of *oriC.* (A) Left panel presents the relative location of each focus in one- (green), two- (red), three-

(black) and four- (magenta) focus cells. Position of each locus was determined from mid-cell. Right panel presents the number of cells and their relative positions. (B) *oriC* segregation in Δ*parB* mutant. Images represent location of *oriC* in every five-minute interval. Arrow indicates earlier segregation of pole proximal *oriC.* (C) *oriC* also separates at the cell pole in Δ*parB* cells. After separation one of the two copies migrate to the opposite cell pole. Arrows indicate separation of *oriC* locus at the cell pole (5 min) and at the cell quarter (50 min). (D) in two focus cells, *oriC* located close to the cell-pole segregates earlier (25 min) than the other located at the cell quarter (45 min). Arrows indicate separation of *oriC* locus.

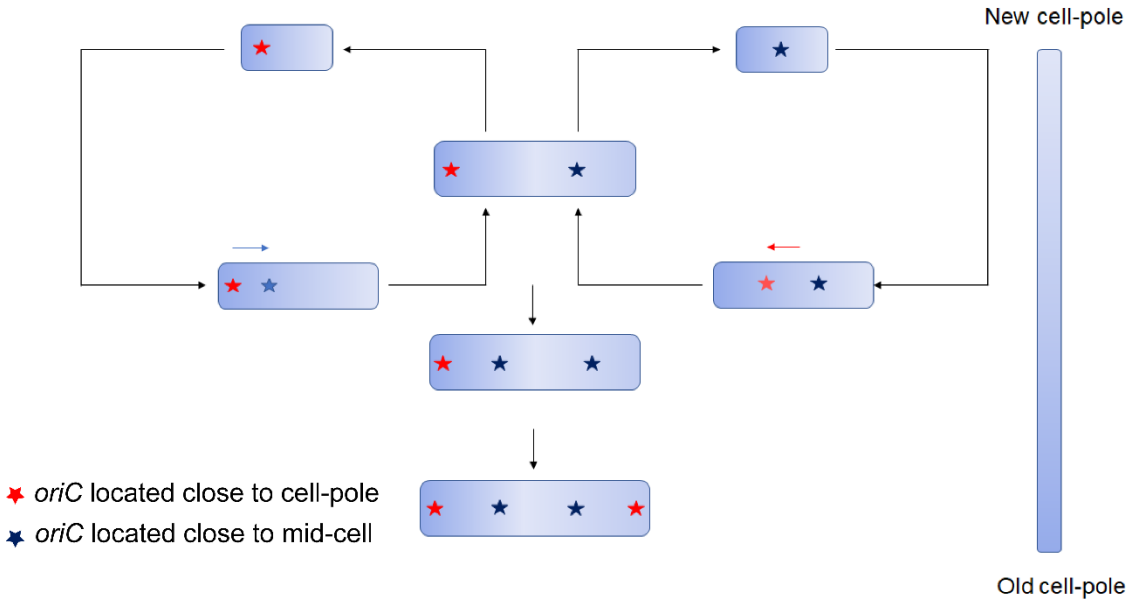

Figure 4-7: Schematic representation of *oriC* segregation in ΔparB mutant.

4.8 Condensins are synthetically lethal with ParB

Having found that neither condensins nor ParB is required for *oriC* segregation, we tried to determine the possibility of any other force behind chromosome segregation. To test this idea, we tried to knock out all three genes using the conventional allele replacement method. Interestingly, cells lacking all three genes were not viable. This mortality can arise due to lethality caused by deletion of both condensin and ParB together, or due to inefficient recombination while creating the mutant. To test this, we used a modified knock out approach.

To this end, we first deleted *smc* and *parB* from PAO1 and then went on to delete *mksB* using pEX-Δ*mksB* suicide vector. We first constructed a merodiploid mutant where a functional *mksB* gene is present. A second round of recombination would result in the deletion of *mksB,* and at the same time would confer a resistance to gentamicin. During this recombination, this merodeploid mutant can also undergo a reversion bringing back the wild type *mksB* gene. Four different *mksB* merodiploids were spotted on a LB plate supplemented with sucrose and gentamicin. All four merodiploids were also plated on a LB plate supplemented with sucrose without gentamicin. If forward recombination take place cells will retain gentamicin resistance and will grow on gentamicin plate. On the other hand, cells from both forward and reverse recombination will grow on plates lacking gentamicin. Figure 4-8A illustrates that colony formation was only possible when reversion happened. The same result was found when we repeated this experiment in a different order, when we tried to remove *smc* from Δ*parB* Δ*mksB* strain (Figure 4-8B). As a control, we removed an unrelated operon

MexGHID from both Δ*parB* Δ*smc* and Δ*parB* Δ*mksB* mutants, in both controls cells were viable suggesting the lethality is caused by the deletion of all three proteins.

To confirm our result, we determined cell viability using a second viability assay. In this assay, we used the bacterial degron system to degrade SMC and MksB proteins in Δ*parB* cells. The degron system recognizes proteins with a DAS4 tag attached to their C-terminus and degrades them *via* a ClpXP mediated degradation system.

For the controlled degradation of MksB, the endogenous *sspB* gene was first removed from Δ*parB* mutant cells. The endogenous copy of *mksB* gene was then replaced with its DAS4 tagged version in Δ*parB* Δ*sspB* cells. Figure 4-8 C, top panel illustrates that the expression level of this DAS4 tagged MksB was similar to the parental strain. Upon the introduction of an SspB expression plasmid, the DAS4 tagged MksB was completely degraded (Figure 4-8 C, top panel). But, no degradation was observed when an empty plasmid was introduced in this strain. The same result was obtained when we replaced SMC with its DAS4 tagged copy in Δ*parB* Δ*sspB* cells, where, introduction of SspB expression plasmid led to the complete degradation of DAS4 tagged SMC (Figure 4-8 C, bottom panel). Finally, we replaced both MksB and SMC with their DAS4 tagged copy in Δ*parB* Δ*sspB* cells. Both SspB expression plasmid and an empty plasmid were introduced in this strain via electroporation. After an incubation of 60 minutes at 37 °C, electroporated cells were spotted on an LB-agar plate supplemented with 30 µg/mL gentamicin. Figure 4-7 D, indicates that cells

carrying SspB expression plasmid did not survive whereas, cells harboring the empty plasmid grew normally. Taken together, these results suggest that, although SMC, MksB and ParB play different roles in chromosome biology, at least one of them is necessary for cell survival.

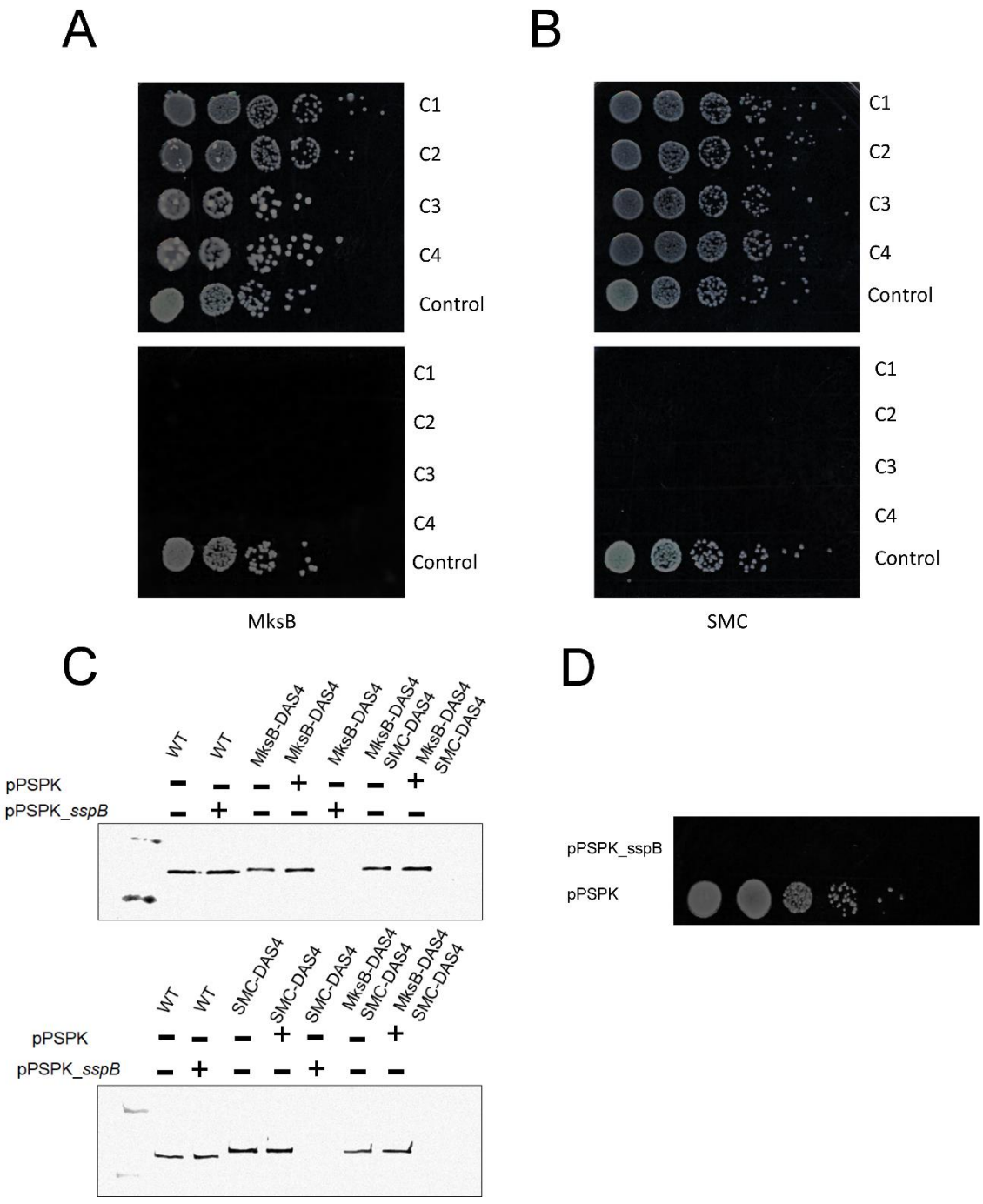

Figure 4-8: Condensins are synthetically lethal with ParB. (A) Top panel, four *mksB* merodiploid mutants were spotted on LB plate supplemented with 15% sucrose. Bottom panel, same four mutants were spotted on LB plate supplemented with 15% sucrose and gentamicin (15 µg/mL). (B) Top panel, four *smc* merodiploid mutants were spotted on LB plate supplemented with 15% sucrose. Bottom panel, same four mutants were spotted on LB plate supplemented with 15% sucrose and gentamicin (15 µg/mL). (C) Controlled degradation of MksB-DAS4 proteins and SMC-DAS4 proteins upon introduction of SspB expression plasmid. (D) SspB expression plasmid was introduced into Δ*parB* Δ*sspB* mutants carrying DAS4 tagged MksB and SMC. Cells were then spotted on LB plates supplemented with gentamicin (30 µg/mL) and IPTG (0.1%). As a control cells carrying an empty vector was also spotted on the same plate.

Chapter 5: Expression of recombinant human SMC2/4 protein using Baculovirus expression system

5.1 Introduction

Our investigation of bacterial condensins revealed that these proteins play a vital role in chromosome segregation. To understand how condensins influence chromosome segregation in eukaryotes, we decided to study the human condensins. A gap in our current understanding about condensin activity in eukaryotes is that it is still unclear whether they physically bind DNA or topologically entrap them. To determine the activity and mechanism of a human condensin, we started by expressing and purifying one of them. Much like bacteria, the activity of eukaryotic condensins is expected to be dictated by their SMC subunits. Therefore, we first started out to express the SMC subunits of human condensins: SMC2 and SMC4.

To express these proteins, we choose the Baculovirus expression system. Baculovirus expression system is one of the most widely used systems for expressing heterologous genes. This system works by infecting cultured insect cell lines with recombinant Baculovirus particles. In the late phase of infection, heterologous genes are expressed from a strong late-phase promoter. Using this system, a high level of recombinant gene expression can be achieved at the expense of host protein synthesis, which is diminished following infection. Being nonpathogenic to mammals and plants and having a restricted host range, Baculovirus can be used under a BSL-2 environment. In this chapter, we describe

the use of pFast Bac-to-Bac™ Baculovirus expression system to express human SMC subunits.

The Backbone of this system is the pFastBac™Dual plasmid (ThermoFisher Scientific). This bi-cistronic plasmid, can express two different genes simultaneously. Expression of the genes are controlled by two strong, late-stage promoters: a polyhedrin promoter (P_{PH}) and a p10 protein promoter (P_{P10}).

5.2 Expression and purification of SMC2 subunit

To express SMC2 protein, pFastBacDual_SMC2_His_pH plasmid was used. To check promoter efficiency of both PH and P10 promoters, this tagged SMC2 protein was expressed under the control of the P10 promoter as well. *Sf*9 cells in mid-log phase were infected with recombinant bacmids and 72 hours post infection cells were collected and lysed. Proteins were purified by binding with MagneHis NI particle (Promega) and eluted with imidazole. The concentration of purified proteins were measured using a Bradford assay comparing against standard BSA concentrations. Approximately 8 µg of purified protein were isolated from $8X10^6$ cells. Figure 5-1 shows the plasmid maps used and corresponding SDS-PAGE analysis illustrates that both promoters behaves in a similar manner and SMC2 proteins are expressed in similar quantity.

5.3 DNA binding activity of SMC2 protein

To determine the DNA binding activity of purified SMC2 proteins, electrophoretic mobility shift assay was performed. In short, 10 ng of pBR322 plasmid DNA was mixed with an indicated amount of SMC2 proteins. the mixture

was incubated at 37 °C for 30 minutes, and the reaction was quenched by placing the tube on ice. The resulting mixture was then analyzed by gel electrophoresis through a 0.7% agarose gel in 89 mM Tris borate, pH 8.3, for 12 hours at 4 V/cm at 4 °C. To visualize DNA, the gel was stained with SYBR Gold Nucleic Acid Gel Stain (Invitrogen). Figure 5-2 illustrates DNA binding activity of SMC2 proteins. the protein-DNA complex migrated slowly through the gel, owing to its high molecular weight. As the protein concentration was increased, the mobility of the complex decreased. Discrete DNA bands observed at lower protein concentrations indicate that several proteins were bound to the same DNA molecule thus generating a complex with a different mobility. A similar gel shift pattern was previously reported for bacterial condensins [12, 159]. This result indicates that SMC2 protein, by itself, can bind to DNA. A sigmoidal pattern in gel-shift suggests that SMC2 binds DNA in a co-operative manner.

5.4 Expression and purification of SMC4 subunit

Several attempts were made to express SMC4 using the Baculovirus system. Recombinant bacmid generated from plasmid pFastBacDual- SMC4-C-His-pH was used to infect *Sf*9 cells and cells were collected every 24 hours and lysed. Clarified lysate was purified using MagneHis Ni particles. Protein expression was analyzed by SDS-PAGE followed by silver staining. No protein expression was detected (Figure 5-3).

To test if simultaneous expression of both SMC subunits stabilizes the SMC4 protein, we used the recombinant bacmid generated from the plasmid pFastBacDual-SMC2-His(pH)-SMC4 (p10) to infect *Sf*9 cells. This plasmid

should express His tagged SMC2 from PH promoter and SMC4 from p10 promoter. Infected *Sf*9 cells were collected after 72 hours and lysed. Clarified lysate was purified using MagneHis Ni particles. protein expression was analyzed by SDS-PAGE followed by silver staining. SMC2_His protein was expressed and eluted at 300 mM imidazole concentration. No SMC4 was co-purified with SMC2 (Figure 5-4).

Expression of SMC2 from pH promoter was successful. Therefore, we tested whether or not this promoter will help expressing SMC4. For this purpose, recombinant bacmid was generated from pFastBacDual-SMC2(p10)-SMC4-HIS(pH) plasmid. This plasmid should express SMC2 from p10 promoter and His tagged SMC4 from PH promoter. Infected *Sf*9 cells were collected after 72 hours and lysed. Clarified lysate was purified using MagneHis Ni particles. Protein expression was analyzed by SDS-PAGE followed by silver staining. As the tag was on SMC4 protein, no protein was detected after staining (Figure 5-5).

To test if co-infection of two different virus particles, each harboring a single *smc* gene, will help to express these proteins, we transfected *Sf*9 with recombinant bacmid generated from pFastBacDual-SMC4-C-His-pH plasmid and pFastBacDual-SMC2-pH plasmid or pFastBacDual-SMC2-C-His-pH and pFastBacDual-SMC4-pH was attempted. SMC2 was expressed in both cases, but SMC4 was never been detected (Figure 5-6).

Finally, we wanted to express SMC4 by replacing His-tag with either Strep tag or Maltose binding protein (MBP) tag. MBP tag often help to solubilize insoluble proteins. pFastBacDual-SMC4-TEV-STREP-pH plasmid was used to

infect *Sf*9 cells and 72 hours post-infection cells were lysed and loaded on StrepTactin™ resin (GE Healthcare Cat # 28-9355-99). The protein was eluted with 2.5 mM desthiobiotin. To purify the protein using an MBP tag, pFastBacDual-SMC4-His-MBP-pH plasmid was used to generate a bacmid. Virus particles were then used to infect S9 cells. 73 hours post-infection, cells were harvested, lysed and loaded on amylose resin (New England Biolabs, Cat# E8021S). Bound proteins were eluted using 10 mM maltose. Judging from the SDS_PAGE gels, no proteins were expressed using either construct (Figure 5-7).

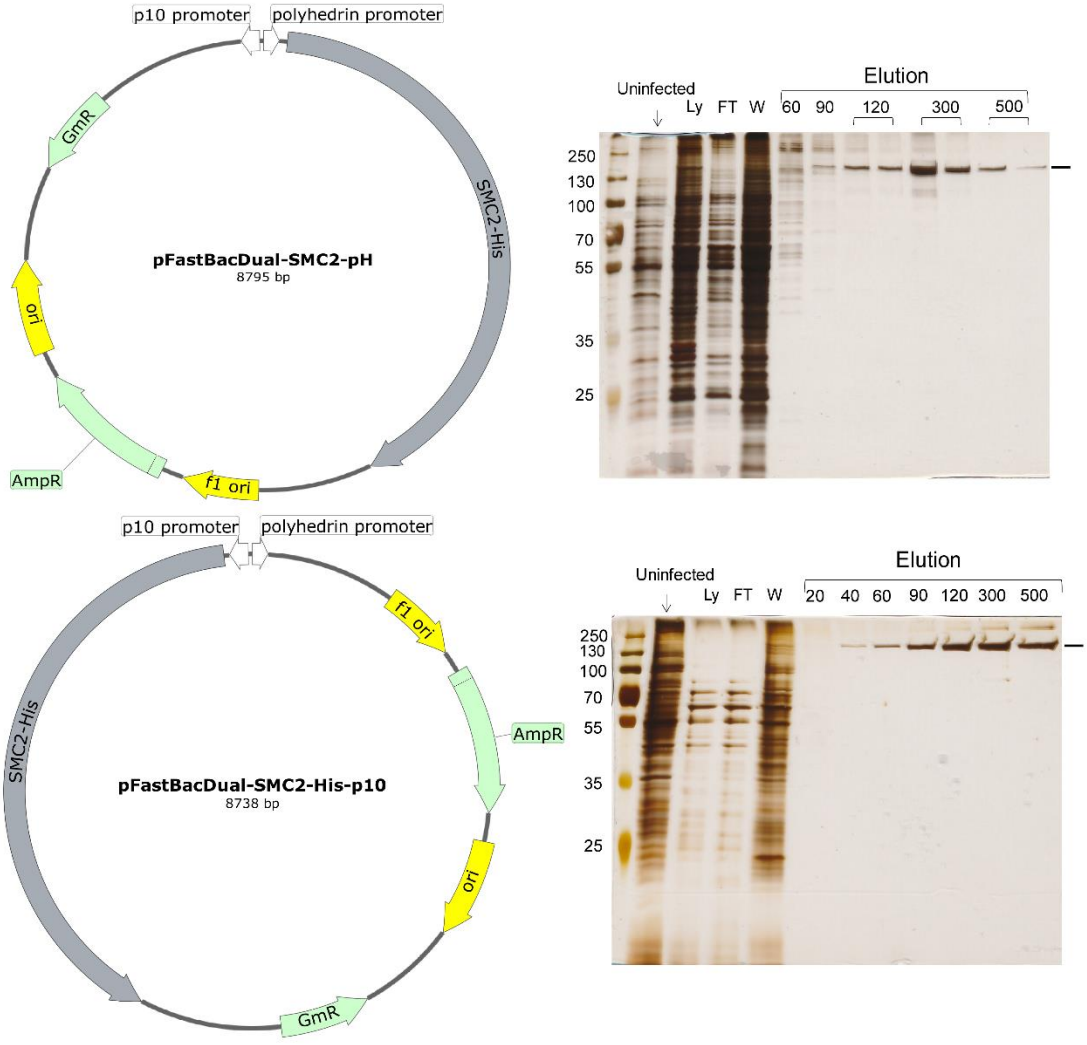

Figure 5-1: Plasmid maps and purification of SMC2 protein. SMC2 proteins can be expressed from either PH or P10 promoter. Similar amount of protein (~ 8µg from 8X10^6 cells) was eluted from both experiments.

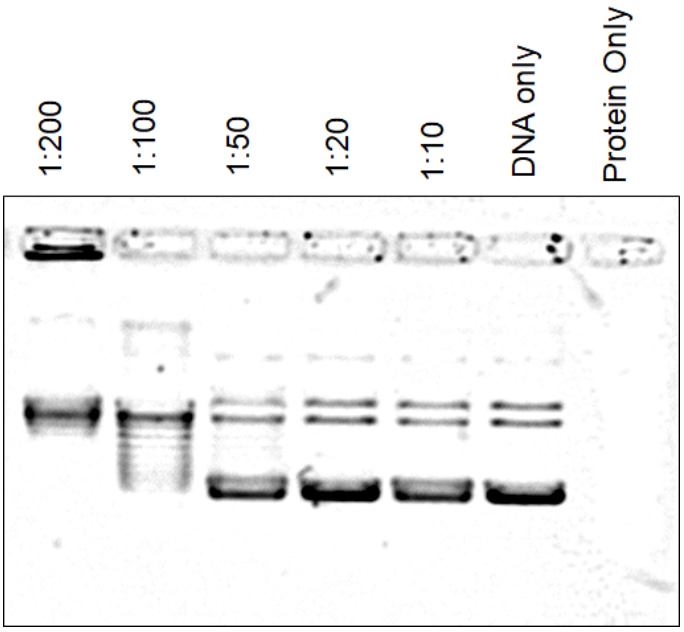

Figure 5-2: Electrophoretic Mobility Shift Assay of purified SMC2 protein. Increasing amount of SMC2 was incubated with 10 ng of pBR322 plasmid for 30 minutes at 37 °C, reaction was quenched and mixture was resolved by agarose gel electrophoresis. DNA was visualized by SYBR™ Gold Nucleic Acid Gel Stain. Amount of SMC2 used in this assay is shown for each lane as DNA: protein molar ratio. Reaction was performed in reaction buffer containing 20 mM Tris-Cl (pH-7.9), 200 mM sodium chloride, 1 mM DTT and 2 mM magnesium chloride.

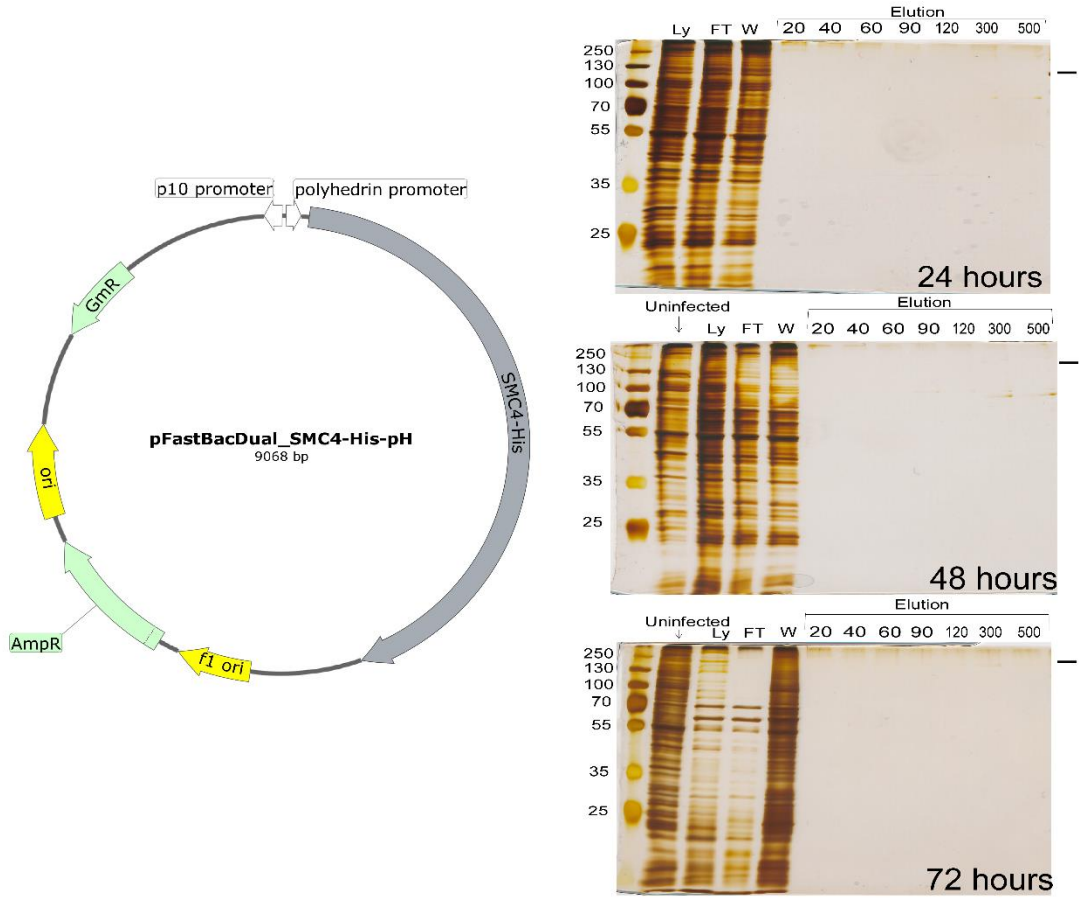

Figure 5-3: Expression of SMC4 at different interval post-transfection. Infected cells were collected after 24, 48 and 72 hours post-transfection and loaded on MagneHis Ni particles. Imidazole concentration in elution buffer is mentioned over each lane. predicted location of SMC4 are indicated.

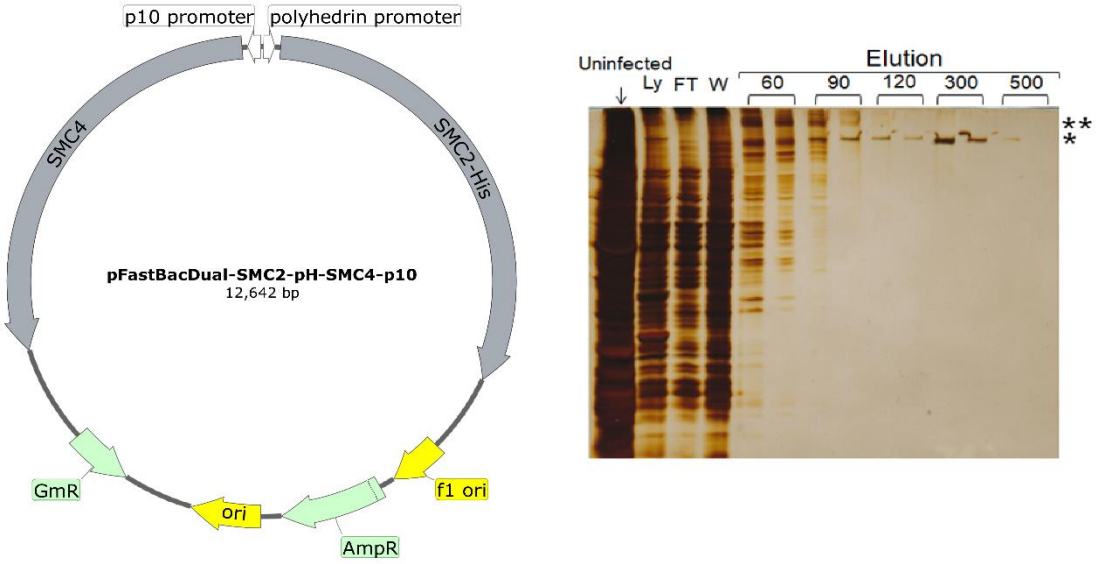

Figure 5-4: Co-expression of SMC2-His and SMC4 Cells were infected with virus particle carrying SMC2-His(pH) and SMC4 (p10) together. Purification was performed as described earlier. * indicates purified SMC2-His and ** indicates predicted location of purified SMC4.

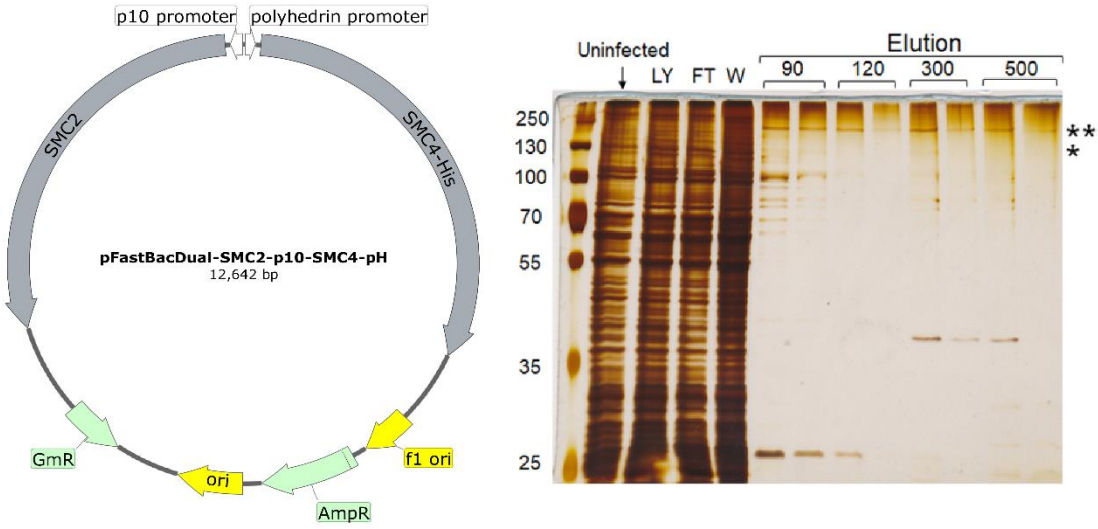

Figure 5-5: Co-expression of SMC2 and SMC4-His. Cells were infected with virus particle carrying SMC4-His(pH) and SMC2 (10) together. Purification was

performed as described earlier. * indicates purified SMC2-His and ** indicates predicted location of purified SMC4.

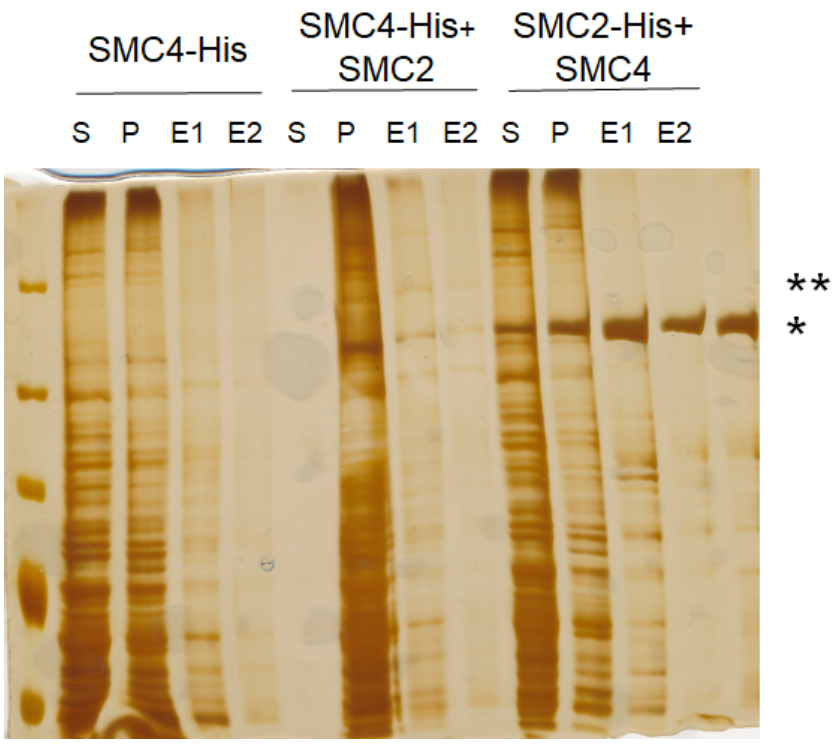

Figure 5-6: Expression of SMC2 and SMC4 followed by co-infection. Single *Sf*9 culture was co-infected by different viral particles carrying SMC2 and SMC4 gene. Purification was performed as described earlier. * indicates purified SMC2 protein and ** indicates predicted location of SMC4.

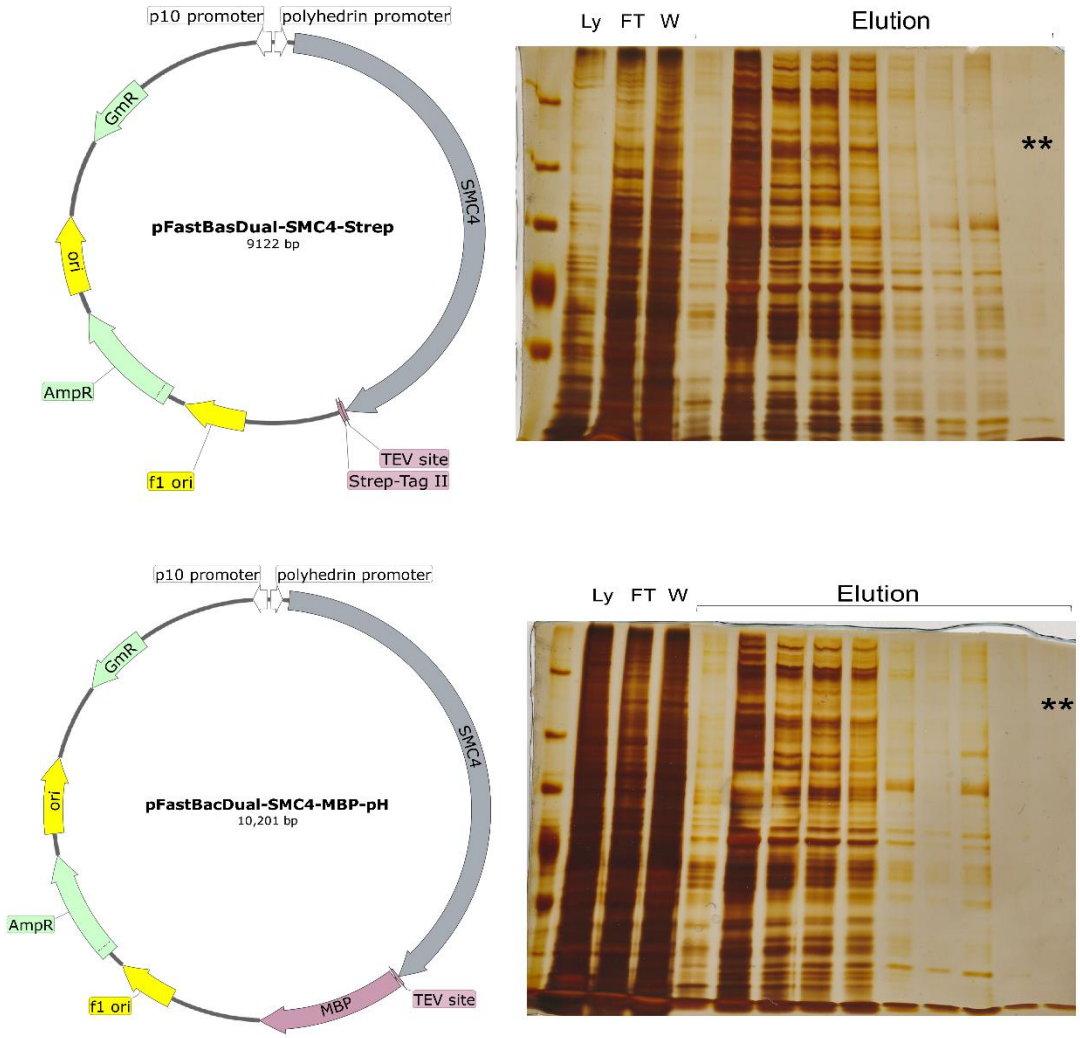

SMC4-Strep SMC4-MBP

Figure 5-7: Expression of SMC4-STREP and SMC4-MBP. *Sf*9 cells were infected with virus carrying Strep or MBP tagged *smc4* genes and purified by using Sterp-Tactin resin or amylose resin respectively. ** indicates predicted location of SMC4 protein.

Chapter 6: Discussion

Proper chromosome organization and faithful segregation are one of life's most fundamental biological processes. In bacteria, several systems are dedicated to these particular processes. Small Nucleoid Associated Proteins provide local structure to DNA by binding, bending and wrapping the long DNA strands. For global organization of the chromosome, condensins play a vital role. The ability of these proteins to bridge distant segments of DNA, allows them to form and stabilize giant DNA loops. Although, these proteins bind DNA in a non-specific manner, they are often visible as clusters, localized close to origin.

The second major system, directly involved in chromosome segregation is the ParAB*S* system. ParB proteins binds to a centromere-like *parS* sequence located close to the origin. The motor protein ParA then actively separates the ParB-*parS* nucleoprotein complex, thus generating the force behind segregation of the origins. Interestingly, in several bacteria including *B. subtilis*, ParB is required to load SMC onto the chromosome suggesting that chromosome organization is linked to segregation. Although quite widespread, several bacterial species including *E. coli* lack a functional ParAB*S* system or its homologue. This suggest that in *E. coli*, condensins mediated chromosome organization and its interaction with ParC play a vital role in chromosome segregation.

In this study, we determined the role of condensins and ParB in maintaining proper chromosome structure and segregation in *P. aeruginosa*. Notably, in *P. aeruginosa*, two different families of condensins can be found:

MksBEF and SMC-ScpAB. To determine their role in chromosome segregation, we first determined the chromosomal segregation pattern in wild type PAO1. Our results suggest that the PAO1 chromosome is longitudinally organized between *oriC* and *dif*. Both chromosomal arms run in parallel between *oriC* and *dif*. Notably, each locus on the chromosome occupies a specific position inside the cell and this pattern is recuperated after segregation. How this pattern is maintained is still unclear. Surprisingly, condensins are not required to maintain this orientation.

In newly born PAO1 cells, *oriC* occupies a position close to mid-cell. After segregation, newly formed *oriC* loci migrate readily towards the quarter positions and remain there for the rest of the cell cycle. Following cell division, these quarter positions form the middle of the daughter cells. This might suggest that *oriC* locus is tethered to the mid-cell region. In *Corynebacterium glutamicum,* the ParB-*parS* complex tethers *oriC* to cell poles [160]. Interestingly, in PAO1, deletion of *parB* affects positioning of one of the two newly replicated *oriC*s. In this mutant, *oriC* is located close to the old cell-pole and occupies the quarter position, whereas the other *oriC* remained stuck to the mid-cell. Interestingly, condensins are not required for the proper positioning of *oriC*. Deletion of condensins leads to an earlier segregation of *oriC*. This may indicate that after replication, condensins may hold newly replicated *oriC* together.

In PAO1, *dif* is the last to segregate. This locus occupies the new cell-pole in short cells and migrates to mid-cell before segregation. A fixed location of *dif* at the cell pole suggests the presence of another tethering in this locus.

Interestingly, *dif* in Δ*smc* mutant lacks its characteristic segregation pattern. This indicates that SMC tether the *dif* locus and allows it to segregate last. This role of SMC in organizing *dif* is unique and has not been observed before in any other organism.

An interesting feature of the PAO1 chromosome is its asymmetric organization as related to *oriC* and *dif*. As a result of this, the chromosomal left arm is 56% longer than the right arm. In spite of this discrepancy, segregation along both arms finishes at the same time. The presence of domains in the longer arm may help in maintaining a co-ordination between arms by allowing large segments of the chromosome to segregate together. Interestingly, both condensins are required to maintain these domains.

Deletion of condensins also affects segregation of the entire chromosome. Deletion of MksB resulted in delaying the segregation of the entire chromosome, whereas, deletion of SMC accelerated segregation. Different roles of condensins in chromosome segregation can be attributed to their different localization pattern. Our results demonstrate that while SMC co-localizes with the *oriC* locus, MksB forms clusters at a distal location on chromosome. This may also indicate that these two condensins play opposite role in global chromosome organization, where MksB promotes condensation of the chromosome, SMC causes relaxation. These results suggest that MksB and SMC play separate roles in global chromosome organization, as well as in chromosome segregation.

Another well-known aspect of bacterial chromosome dynamics is the concurrent nature of replication and segregation. In *E. coli*, both replication and

segregation initiate from *oriC*, progress bidirectionally and end at the terminus. The *Ter*-Tus system located in this region prevents over-replication. However, it is still unknown how chromosome segregation ends in this region. Our results indicate that, in the PAO1 chromosome, segregation ends at the *dif* site, while replication ends at a location opposite to the origin. This asymmetric pattern suggests that there is no obvious coordination between replication and segregation. Notably, in *E. coli*, *dif* is also located at the terminus region, suggesting a common role of *dif* during chromosome segregation.

Finally, we uncovered a novel correlation between condensin mediated global chromosome organization and chromosome partitioning. Cells lacking MksB, SMC and ParB failed to survive. To determine that this lethality is due to the absence of all three proteins, we used two different cell viability assays. Using a recombination based cell viability assay and a degron mediated degradation of condensins, we showed that at least one of these three proteins is required for cell viability. According to the entropic model of chromosome segregation, newly replicated chromosomes can separate themselves by virtue of their intrinsic polymeric properties. Strikingly, our results suggest that entropy is not sufficient for cell viability in the absence of condensin and ParB. This lethality may be caused by the impairment of *oriC* segregation in the absence of both condensins and ParB

Similar to prokaryotes, condensins play vital a role in proper chromosome organization and segregation in eukaryotic cells. In higher eukaryotes, two different isoforms of condensins are found: condensin I and condensin II. Both

condensins share the same SMC proteins SMC2 and SMC4. Understanding the biochemical activity of eukaryotic condensin will shed light as to their activity within the cell. We expressed full-length human SMC2 protein using a eukaryotic expression system. This protein can bind DNA in vitro, suggesting that the DNA binding activity of condensins lies in its head domain. Failure to express SMC4 suggest that interaction with SMC2 is not sufficient for the stability of SMC4.

Table 1. List of plasmids used in studying *P. aeruginosa* chromosome segregation

Plasmids	Description	Source or reference
pP30D-FRT-TetO-0069	For inserting *tetO* repeats at PA0069	[149]
pP30D-FRT-TetO-0981	For inserting *tetO* repeats at PA0981	[149]
pP30D-FRT-TetO-2258	For inserting *tetO* repeats at PA2258	[149]
pP30D-FRT-TetO-3573	For inserting *tetO* repeats at PA3573	[149]
pP30D-FRT-parST1-0069	For inserting $parS^{pMT1}$ sequence at PA3573	[149]
pP30D-FRT-TetO-2910	For inserting *tetO* repeats at PA2910	This study
pP30D-FRT-TetO-4457	For inserting *tetO* repeats at PA4457	This study
pP30D-FRT-TetO-0460	For inserting *tetO* repeats at PA0460	This study
pP30D-FRT-TetO-5099	For inserting *tetO* repeats at PA5099	This study
pP30D-FRT-TetO-3267	For inserting *tetO* repeats at PA3267	This study
pP30D-FRT-TetO-1905	For inserting *tetO* repeats at PA1905	This study
pP30D-FRT-TetO-0716	For inserting *tetO* repeats at PA0716	This study
pP30D-FRT-TetO-1436	For inserting *tetO* repeats at PA1436	This study
pP30D-FRT-TetO-1673	For inserting *tetO* repeats at PA1673	This study
pP30D-FRT-TetO-3035	For inserting *tetO* repeats at PA3035	This study
pPSV35Ap-TetR-CFP-yGFP-ParBT1	Expressing TetR-CFP and GFP-ParBT1 chimera	[149]
pPSV35Ap-TetR-CFP	Expressing TetR-CFP chimera	This study
pPSV35Ap-TetR-mCherry	Expressing TetR-mCherry chimera	This study
pFLP2	Site-specific excision vector	[161]

pEX-Δ*smc*	SMC deletion plasmid	[17]
pEX-Δ*mksB*	MksB deletion plasmid	[17]
pEXG2	Scarless deletion plasmid	[149]
pEXG2-Δ*parB*	ParB deletion plasmid	This study
pEX18AP-*smc*-DAS4	ClpXP mediated Degradation of SMC protein	This study
pEX18AP-*mksB*-Das4	ClpXP mediated Degradation of MksB protein	This study
pPSPK-*sspB*	IPTG inducible sspB expression plasmid.	[162]
pEXG2-*sspB*	*sspB* deletion plasmid	[162]
pPSPK	Derived from pPSV37	[162]
pEX18AP	Deletion plasmid	[161]

Table 2. List of strains used in studying *P. aeruginosa* chromosome segregation

Strain	Relevant genotype or description	Source or reference
SM10 (λ pir)	thi thr leu tonA lacY supE recA::RP4-2-Tc::Mu Km λpir	[161]
DH5α	supE44 DlacU169 hsdR17 recA1 endA1 gyrA96 thi-1 relA1	Novagen
PAO1-LAC	lacIq+ delta(lacZ)M15+ tetA+ tetR+	ATCC 47085
BKB143	PAO1-LAC-Δ*smc*	[17]
BKB144	PAO1-LAC-Δ*mksB*	[17]
BKB156	PAO1-LAC-Δ*smc* Δ*mksB*	[17]
BKB295	PAO1-LAC-Δ*parB*	This study
BKB158	PAO1-LAC-tetO-PA0069 + pPSV35Ap-TetR-CFP	This study

BKB242	PAO1-LAC-tetO-PA0460 + pPSV35Ap-TetR-CFP	This study
BKB259	PAO1-LAC-tetO-PA0716 + pPSV35Ap-TetR-CFP	This study
BKB139	PAO1-LAC-tetO-PA00981 + pPSV35Ap-TetR-CFP	This study
BKB270	PAO1-LAC-tetO-PA1436 + pPSV35Ap-TetR-CFP	This study
BKB253	PAO1-LAC-tetO-PA1905 + pPSV35Ap-TetR-CFP	This study
BKB140	PAO1-LAC-tetO-PA2258 + pPSV35Ap-TetR-CFP	This study
BKB216	PAO1-LAC-tetO-PA2910 + pPSV35Ap-TetR-CFP	This study
BKB291	PAO1-LAC-tetO-PA3035 + pPSV35Ap-TetR-CFP	This study
BKB237	PAO1-LAC-tetO-PA3267 + pPSV35Ap-TetR-CFP	This study
BKB217	PAO1-LAC-tetO-PA4457 + pPSV35Ap-TetR-CFP	This study
BKB278	PAO1-LAC-tetO-PA5099 + pPSV35Ap-TetR-CFP	This study
BKB170	PAO1-LAC-Δ*mksB*-tetO-PA0069 + pPSV35Ap-TetR-CFP	This study
BKB243	PAO1-LAC-Δ*mksB*-tetO-PA0460 + pPSV35Ap-TetR-CFP	This study
BKB260	PAO1-LAC-Δ*mksB*-tetO-PA0716 + pPSV35Ap-TetR-CFP	This study
BKB175	PAO1-LAC-Δ*mksB*-tetO-PA0981 + pPSV35Ap-TetR-CFP	This study
BKB271	PAO1-LAC-Δ*mksB*-tetO-PA1436 + pPSV35Ap-TetR-CFP	This study
BKB286	PAO1-LAC-Δ*mksB*-tetO-PA1673 + pPSV35Ap-TetR-CFP	This study
BKB250	PAO1-LAC-Δ*mksB*-tetO-PA1905 + pPSV35Ap-TetR-CFP	This study
BKB174	PAO1-LAC-Δ*mksB*-tetO-PA2258 + pPSV35Ap-TetR-CFP	This study
BKB212	PAO1-LAC-Δ*mksB*-tetO-PA2910 + pPSV35Ap-TetR-CFP	This study

BKB287	PAO1-LAC-Δ*mksB*-tetO-PA3035 + pPSV35Ap-TetR-CFP	This study
BKB238	PAO1-LAC-Δ*mksB*-tetO-PA3267 + pPSV35Ap-TetR-CFP	This study
BKB171	PAO1-LAC-Δ*mksB*-tetO-PA3573 + pPSV35Ap-TetR-CFP	This study
BKB213	PAO1-LAC-Δ*mksB*-tetO-PA4457 + pPSV35Ap-TetR-CFP	This study
BKB279	PAO1-LAC-Δ*mksB*-tetO-PA5099 + pPSV35Ap-TetR-CFP	This study
BKB326	PAO1-LAC-Δ*smc*-tetO-PA0069 + pPSV35Ap-TetR-mCherry	This study
BKB336	PAO1-LAC-Δ*smc*-tetO-PA0460 + pPSV35Ap-TetR-mCherry	This study
BKB328	PAO1-LAC-Δ*smc*-tetO-PA0716 + pPSV35Ap-TetR-mCherry	This study
BKB329	PAO1-LAC-Δ*smc*-tetO-PA0981 + pPSV35Ap-TetR-mCherry	This study
BKB337	PAO1-LAC-Δ*smc*-tetO-PA1436 + pPSV35Ap-TetR-mCherry	This study
BKB338	PAO1-LAC-Δ*smc*-tetO-PA1905 + pPSV35Ap-TetR-mCherry	This study
BKB315	PAO1-LAC-Δ*smc*-tetO-PA2258 + pPSV35Ap-TetR-mCherry	This study
BKB314	PAO1-LAC-Δ*smc*-tetO-PA2910 + pPSV35Ap-TetR-mCherry	This study
BKB320	PAO1-LAC-Δ*smc*-tetO-PA3267 + pPSV35Ap-TetR-mCherry	This study
BKB321	PAO1-LAC-Δ*smc*-tetO-PA3573 + pPSV35Ap-TetR-mCherry	This study
BKB312	PAO1-LAC-Δ*smc*-tetO-PA4457 + pPSV35Ap-TetR-mCherry	This study
BKB339	PAO1-LAC-Δ*smc*-tetO-PA5099 + pPSV35Ap-TetR-mCherry	This study
BKB172	PAO1-LAC-Δ*mksB* Δ*smc* -tetO-PA0069 + pPSV35Ap-TetR-CFP	This study

BKB332	PAO1-LAC-Δ*parB*-tetO-PA0069 + pPSV35Ap-TetR-mCherry	This study
BKB080	PAO1-LAC-*smc-gfp*	This study
BKB147	PAO1-LAC-*mksB-gfp*	This study
BKB191	PAO1-LAC-*smc-gfp*- Δ*mksB*	This study
BKB220	PAO1-LAC-*mksB-gfp*-tetO-PA0069 + pPSV35Ap-TetR-mCherry	This study
BKB228	PAO1-LAC-*mksB-gfp*- Δ*parB*	This study
BKB229	PAO1-LAC-*smc-gfp*- Δ*parB*	This study
BKB274	PAO1-LAC-*smc-gfp*-tetO-PA0069 + pPSV35Ap-TetR-mCherry	This study
BKB302	PAO1-LAC-Δ*smc*- Δ*parB*	This study
BKB308	PAO1-LAC-Δ*mksB*- Δ*parB*	This study
BKB324	PA01-LAC-parST1-PA4457-tetO-PA1436 + pTetR-CFP-ParBT1-mCherry	This study
BKB335	PAO1-LAC-*mksB-gfp*- Δ*smc*	This study
BKB348	PAO1-LAC-Δ*sspB*-Δ*smc*-Δ*parB*	This study
BKB353	PA01-LAC-parST1-PA3267-tetO-PA1905 + pTetR-CFP-ParBT1-mCherry	This study
BKB366	PA01-LAC-Δ*smc*Δ*parB*Δ*sspB*-Δ*mksB-C1 (merodeploid)*	This study
BKB369	PA01-LAC-Δ*smc*Δ*parB*Δ*sspB*-Δ*mksB*-C2 (merodeploid)	This study
BKB370	PA01-LAC-Δ*smc*Δ*parB*Δ*sspB*-Δ*mksB*-C3 (merodeploid)	This study
BKB371	PA01-LAC-Δ*smc*Δ*parB*Δ*sspB*-Δ*mksB*-C4 (merodeploid)	This study
BKB372	PA01-LAC-Δ*mksB*Δ*parB*Δ*sspB*-Δ*smc*-C1 (merodeploid)	This study

BKB373	PA01-LAC-Δ*mksB*Δ*parB*Δ*sspB*-Δ*smc*-C2 (merodeploid)	This study
BKB374	PA01-LAC-Δ*mksB*Δ*parB*Δ*sspB*-Δ*smc*-C3 (merodeploid)	This study
BKB377	PA01-LAC-Δ*mksB*Δ*parB*Δ*sspB*-Δ*smc*-C4 (merodeploid)	This study
BKB390	PAO1-LAC-Δ*sspB*Δ*mksB*Δ*parB*-*smc*-DAS4	This study
BKB307	PAO1-LAC-Δ*sspB*Δ*smc*Δ*parB*-*mksB*-DAS4	This study
BKB396	PAO1-LAC-Δ*sspB*Δ*mksB*Δ*parB*-*smc*-DAS4 + pPSPK	This study
BKB397	PAO1-LAC-Δ*sspB*Δ*smc*Δ*parB*-*mk*sB-DAS4 + pPSPK	This study
BKB398	PAO1-LAC-Δ*sspB*Δ*parB*-*smc*-DAS4-MksB-DAS4 + pPSPK	This study

Table 3: List of plasmids and strains used for expressing human condensins

Plasmids	Description	Source or reference
pFastBacDual	Expression vector for insect cell line	Invitrogen
pFastBac Dual-Gus/CAT	Control vector expressing β-glucuronidase and chloramphenicol acetyltransferase	Invitrogen
pFastBacDual-SMC2-pH	Native SMC2 expressed from pH promoter	This study
pFastBacDual-N-His-SMC4-pH	N-terminal His tagged SMC4 expressed from pH promoter	This study

pFastBacDual-SMC4-pH	C-terminal His tagged SMC4 expressed from pH promoter	This study
pFastBacDual-SMC2-His-C-pH	Native SMC4 expressed from pH promoter	This study
pFastBacDual-SMC2-p10	C-terminal His tagged SMC2 expressed from pH promoter	This study
pFastBacDual-SMC2-pH	Native SMC2 expressed from p10 promoter	This study
pFastBacDual-SMC4-TEV-STREP-pH	Native SMC2 expressed from pH promoter	This study
pFastBacDual-SMC4-His-MBP-pH	C-terminal Strep tagged SMC4 expressed from pH promoter	This study
pFastBacDual-SMC4-His(N-Truncated)-pH	C-terminal 9XHis and MBP tagged SMC4 expressed from pH promoter	This study
pFastBacDual-SMC4-GFP-pH	N-terminal truncated SMC4, with 9XHis-tag on C-terminal	This study
pFastBacDual-SMC2(p10)-SMC4-HIS(pH)	C-terminal 9XHis and GFP tagged SMC4 expressed from pH promoter	This study
pFastBacDual-SMC2(P10)-SMC4-HIS(PH)-N	Native SMC2 expressed from p10 and C-terminal His tagged SMC4 expressed from pH promoter.	This study
pFastBacDual-SMC4-MBP-pH	Native SMC2 expressed from p10 and C-terminal His tagged SMC4 with truncated N-terminal	This study

pFastBacDual-SMC4-MBP-p10	C-terminal MBP tagged SMC4 expressed from pH promoter	This study
pFastBacDual-SMC2(pH)-SMC4-HTG(p10)	C-terminal MBP tagged SMC4 expressed from p10 promoter	This study
pFastBacDual-SMC2-His(pH)-SMC4 (p10)	Native SMC2 expressed from pH promoter and C-terminal HTG- tagged SMC4 expressed from p10 promoter.	This study
pFastBacDual-SMC2-His(pH)-SMC4 (p10)	C-terminal 9XHis tagged SMC2 expressed from pH promoter and native SMC4 expressed from p10 promoter	This study

Strains	Description	Source or reference
*Sf*9	Clonal isolate derived from Spodoptera frugiperda cell line	Invitrogen
DH10Bac	F^- *mcr*A Δ(*mrr*-hsdRMS-*mcr*BC) Φ80*lacZ*ΔM15 Δ*lacX*74 *rec*A1 *end*A1 *ara*D139 Δ(*ara*, leu)7697 *gal*U *gal*K λ^- *rps*L *nup*G/pMON14272/pMON7124	Invitrogen

Table 4: Primers used in studying *P. aeruginosa* chromosome segregation

Plasmid	Primers used to amplify and clone chromosomal segments	Location on *P. aeruginosa* chromosome
pP30D-FRT-tetO-0460	GCACTGAAGCTTGGCAACGATTATTCGCAACTGG GTACGTGGTACCACCCATCTCGTAGGGCGAAT	PA0460 (520737 bp)
pP30D-FRT-tetO-0716	GCACTGAAGCTTGGATTGGTAGAGGTCTCTGCAAAGG GTACGTGGTACCAACATGAGAATTGCGATGACT	PA0716 (786928 bp)
pP30D-FRT-tetO-0981	GCACTGAAGCTTGGTGTTGAGCCATATGGCGGATC GTACGTGGTACCGCGGTTCATCTTTCCTCATAA	PA0981 (1062921 bp)
pP30D-FRT-tetO-1436	GCACTGAAGCTTGTGTACATCATCCTCGGCGTGC GTACGTGGTACCCCGATCCTCTGTTCGCCTTCG	PA1436 (1563967 bp)
pP30D-FRT-tetO-1673	GCACTGAAGCTTGGAAATGCGCCATTCTGCTTCC GTACGTGGTACCCCATCAGGGTTTCCTCGAAG	PA1673 (1824969 bp)
pP30D-FRT-tetO-1905	GCACTGAAGCTTCCTGGAGTCGGTGGAGTTCTGG GTACGTGGTACCCGAGCTGATCATCCACCAGA	PA1905 (2076311 bp)
pP30D-FRT-tetO-2910	GCACTGAAGCTTTTCGGCGCAGGAATGTCG GTACGTGGTACCCCGGCTCGCTCCCGCCCA	PA2910 (2999192 bp)
pP30D-FRT-tetO-3035	GCACTGAAGCTTCCTTGAACCGCTCTGCGTCG GTACGTGGTACCCAGCGCCGGGTAGTGGTCC	PA3035 (3398104 bp)
pP30D-FRT-tetO-3267	GCACTGAAGCTTCTACAGGATCTTCTCACTGCCG GTACGTGGTACCGCACCGTAAAATGGTTCAACG	PA3267 (3653937 bp)
pP30D-FRT-tetO-4457	GCACTGAAGCTTGATGTTGTCGAAAATCGC GTACGTGGTACCTGTTCAACGAATGTGGCG	PA4457 (4989305 bp)
pP30D-FRT-tetO-5099	GTACGTGGTACCGTTCCTGCTGACCTTCTTCACC GCACTGAAGCTTCGATGATGTTCTCGACACAGG	PA5099 (5741524 bp)

Table 5: Primers used to construct PAO1-LAC mutants

Primer name	Nucleotide sequence
BB106	ACCTGGTACCAACCTGGATGACGGCGACGTC
BB107	CCAGTGAAGAGTTCTTCTCCTTTGCTAGCACCCCCGTGGTGAT GGTGGTGATGATGGTGGTGCGCCGGTTCGCCGGC
BB108	GCCGGCGAACCGGCGCACCACCATCATCACCACCATCACCAC GGGGGTGCTAGCAAAGGAGAAGAACTCTTCACTGG
BB109	GTCGGTGCTCAGCTTAGTTGTACAGTTCATCCATGCCATGTG
BB110	ACCTGGTACCAACCTGGATGACGG
BB111	GTCGGTGCTCAGCTTAGTTGTACAGTTCATC
BB143	ACAGGGTACCGAAGCGCTGGATAGCATGG
BB144	CCAGTGAAGAGTTCTTCTCCTTTGCTAGCACCCCCGTGGTGAT GGTGGTGATGATGGTGGTGGGCTTCAGCCAATGCGACC
BB145	GGTCGCATTGGCTGAAGCCCACCACCATCATCACCACCATCAC CACGGGGGTGCTAGCAAAGGAGAAGAACTCTTCACTGG
BB146	GTCGGTGCTCAGCTTAGTTGTACAGTTCATCCATGCCATGTG
BB147	ACAGGGTACCGAAGCGCTG
BB148	GTCGGTGCTCAGCTTAGTTGTACAGTTC
BB329	ACTGCTAAGCTTAAATGGACATGAAGGAAAATCGC
BB330	AGCAGTCTGCAGGCGGGTTCCTTATGCGGTTG
BB331	AGCAGTCTGCAGCACACTTTGGGTTGTAGCGG
BB332	TGACGTGGATCCAGCTGACCATCAGGGTCAGC

BB321	CGTTGCCTCTGTCCTTAATAAGG
BB323	CGATTGAGAGCAGAAAGCAGCC
BB324	CTTTCTGTGGCTTGTGCAGATG
BB510	GCTGAAACTCTTGCGTGGACAG

References:

1. Maeshima, K., M. Eltsov, and U.K. Laemmli, Chromosome structure: improved immunolabeling for electron microscopy. Chromosoma, 2005. 114(5): p. 365-375.
2. Kornberg, R.D. and Y. Lorch, Twenty-Five Years of the Nucleosome, Fundamental Particle of the Eukaryote Chromosome. Cell, 1999. 98(3): p. 285-294.
3. Gasser, S.M., et al., Metaphase chromosome structure. Journal of Molecular Biology, 1986. 188(4): p. 613-629.
4. Robinow, C. and E. Kellenberger, The bacterial nucleoid revisited. Microbiological Reviews, 1994. 58(2): p. 211-232.
5. Dame, R.T., The role of nucleoid-associated proteins in the organization and compaction of bacterial chromatin. Molecular Microbiology, 2005. 56(4): p. 858-870.
6. Dillon, S.C. and C.J. Dorman, Bacterial nucleoid-associated proteins, nucleoid structure and gene expression. Nature Reviews Microbiology, 2010. 8: p. 185.
7. Rybenkov, V.V., et al., MukBEF, a chromosomal organizer. Journal of molecular microbiology and biotechnology, 2014. 24(0): p. 371-383.
8. Wang, X. and D.Z. Rudner, Spatial organization of bacterial chromosomes. Current opinion in microbiology, 2014. 22: p. 66-72.
9. Wang, X., P.M. Llopis, and D.Z. Rudner, Organization and segregation of bacterial chromosomes. Nature Reviews Genetics, 2013. 14: p. 191.
10. Lagage, V., F. Boccard, and I. Vallet-Gely, Regional Control of Chromosome Segregation in Pseudomonas aeruginosa. PLOS Genetics, 2016. 12(11): p. e1006428.
11. Gruber, S., et al., Interlinked Sister Chromosomes Arise in the Absence of Condensin during Fast Replication in B. subtilis. Current Biology, 2014. 24(3): p. 293-298.
12. Niki, H., et al., The new gene mukB codes for a 177 kd protein with coiled-coil domains involved in chromosome partitioning of *E. coli*. The EMBO Journal, 1991. 10(1): p. 183-193.
13. Yamanaka, K., et al., Identification of two new genes, mukE and mukF, involved in chromosome partitioning in *Escherichia coli*. Molecular and General Genetics MGG, 1996. 250(3): p. 241-251.
14. Hirsch, E.B. and V.H. Tam, Impact of multidrug-resistant Pseudomonas aeruginosa infection on patient outcomes. Expert review of pharmacoeconomics & outcomes research, 2010. 10(4): p. 441-451.

15. Aloush, V., et al., Multidrug-Resistant Pseudomonas aeruginosa: Risk Factors and Clinical Impact. Antimicrobial Agents and Chemotherapy, 2006. 50(1): p. 43-48.

16. Petrushenko, Z.M., W. She, and V.V. Rybenkov, A new family of bacterial condensins. Molecular Microbiology, 2011. 81(4): p. 881-896.

17. Zhao, H., et al., *Pseudomonas aeruginosa* Condensins Support Opposite Differentiation States. Journal of Bacteriology, 2016. 198(21): p. 2936-2944.

18. Stover, C.K., et al., Complete genome sequence of *Pseudomonas aeruginosa* PAO1, an opportunistic pathogen. Nature, 2000. 406(6799): p. 959-964.

19. Li, Y., K. Sergueev, and S. Austin, The segregation of the *Escherichia coli* origin and terminus of replication. Molecular Microbiology, 2002. 46(4): p. 985-996.

20. Pavlendová, N., K. Muchová, and I. Barák, Chromosome segregation in *Bacillus subtilis*. Folia Microbiologica, 2007. 52(6): p. 563-572.

21. Badrinarayanan, A., T.B.K. Le, and M.T. Laub, Bacterial Chromosome Organization and Segregation. Annual Review of Cell and Developmental Biology, 2015. 31(1): p. 171-199.

22. Thanbichler, M. and L. Shapiro, Chromosome organization and segregation in bacteria. Journal of Structural Biology, 2006. 156(2): p. 292-303.

23. Sullivan, N.L., K.A. Marquis, and D.Z. Rudner, Recruitment of SMC by ParB-parS Organizes the Origin Region and Promotes Efficient Chromosome Segregation. Cell. 137(4): p. 697-707.

24. Gruber, S. and J. Errington, Recruitment of Condensin to Replication Origin Regions by ParB/SpoOJ Promotes Chromosome Segregation in *B. subtilis*. Cell, 2009. 137(4): p. 685-696.

25. Onn, I., et al., Reconstitution and subunit geometry of human condensin complexes. The EMBO Journal, 2007. 26(4): p. 1024-1034.

26. Baker, J.R., The cell-theory: a restatement, history, and critique. Part V. The multiplication of nuclei. Quarterly Journal of Microscopical Science, 1955. 96: p. 449-481.

27. Piekarski, G., Cytologische Untersuchungen an Paratyphus-und Colibakterien. Archiv für Mikrobiologie, 1937. 8(1): p. 428-439.

28. Stille, B., Zytologische Untersuchungen an Bakterien mit Hilfe der Feulgenschen Nuclealreaktion. Archiv für Mikrobiologie, 1937. 8(1): p. 125-148.

29. Yamazaki, K.-i., et al., Isolation and characterization of nucleoid proteins from Escherichia coli. Molecular and General Genetics MGG, 1984. 196(2): p. 217-224.

30. Delius, H. and A. Worcel, Letter: Electron microscopic visualization of the folded chromosome of Escherichia coli. J Mol Biol, 1974. 82(1): p. 107-9.

31. Kavenoff, R. and O.A. Ryder, Electron microscopy of membrane-associated folded chromosomes of *Escherichia coli*. Chromosoma, 1976. 55(1): p. 13-25.

32. Webb, C.D., et al., Bipolar Localization of the Replication Origin Regions of Chromosomes in Vegetative and Sporulating Cells of *B. subtilis*. Cell, 1997. 88(5): p. 667-674.

33. Sharpe, M.E. and J. Errington, A fixed distance for separation of newly replicated copies of *oriC* in *Bacillus subtilis*: implications for co-ordination of chromosome segregation and cell division. Molecular Microbiology, 1998. 28(5): p. 981-990.

34. Ueguchi, C. and T. Mizuno, The *Escherichia coli* nucleoid protein H-NS functions directly as a transcriptional repressor. The EMBO Journal, 1993. 12(3): p. 1039-1046.

35. Azam, T.A. and A. Ishihama, Twelve Species of the Nucleoid-associated Protein from *Escherichia coli* : SEQUENCE RECOGNITION SPECIFICITY AND DNA BINDING AFFINITY. Journal of Biological Chemistry, 1999. 274(46): p. 33105-33113.

36. Claret, L. and J. Rouviere-Yaniv, Variation in HU composition during growth of *Escherichia co*li: the heterodimer is required for long term survival11Edited by M. Gottesman. Journal of Molecular Biology, 1997. 273(1): p. 93-104.

37. Pettijohn, D.E., Histone-like proteins and bacterial chromosome structure. Journal of Biological Chemistry, 1988. 263(26): p. 12793-12796.

38. Pontiggia, A., et al., Protein HU binds specifically to kinked DNA. Molecular Microbiology, 1993. 7(3): p. 343-350.

39. Castaing, B., et al., HU Protein of Escherichia coli Binds Specifically to DNA That Contains Single-strand Breaks or Gaps. Journal of Biological Chemistry, 1995. 270(17): p. 10291-10296.

40. Kamashev, D., A. Balandina, and J. Rouviere-Yaniv, The binding motif recognized by HU on both nicked and cruciform DNA. The EMBO Journal, 1999. 18(19): p. 5434-5444.

41. Swinger, K.K., et al., Flexible DNA bending in HU–DNA cocrystal structures. The EMBO Journal, 2003. 22(14): p. 3749.

42. van Noort, J., et al., Dual architectural roles of HU: Formation of flexible hinges and rigid filaments. Proceedings of the National Academy of Sciences of the United States of America, 2004. 101(18): p. 6969-6974.

43. Skoko, D., et al., Micromechanical Analysis of the Binding of DNA-Bending Proteins HMGB1, NHP6A, and HU Reveals Their Ability To Form Highly Stable DNA−Protein Complexes. Biochemistry, 2004. 43(43): p. 13867-13874.

44. Broyles, S.S. and D.E. Pettijohn, Interaction of the *Escherichia coli* HU protein with DNA. Journal of Molecular Biology, 1986. 187(1): p. 47-60.

45. Swinger, K.K. and P.A. Rice, IHF and HU: flexible architects of bent DNA. Current Opinion in Structural Biology, 2004. 14(1): p. 28-35.

46. Mangan, M.W., et al., The integration host factor (IHF) integrates stationary-phase and virulence gene expression in *Salmonella enterica* serovar Typhimurium. Molecular Microbiology, 2006. 59(6): p. 1831-1847.

47. Travers, A., DNA–protein interactions: IHF - the master bender. Current Biology, 1997. 7(4): p. R252-R254.

48. Nozaki, S., Y. Yamada, and T. Ogawa, Initiator titration complex formed at datA with the aid of IHF regulates replication timing in *Escherichia coli*. Genes to Cells, 2009. 14(3): p. 329-341.

49. Macchi, R., et al., Recruitment of σ54-RNA Polymerase to the Pu Promoter of *Pseudomonas putida* through Integration Host Factor-mediated Positioning Switch of α Subunit Carboxyl-terminal Domain on an UP-like Element. Journal of Biological Chemistry, 2003. 278(30): p. 27695-27702.

50. Sheridan, S.D., C.J. Benham, and G.W. Hatfield, Activation of Gene Expression by a Novel DNA Structural Transmission Mechanism That Requires Supercoiling-induced DNA Duplex Destabilization in an Upstream Activating Sequence. Journal of Biological Chemistry, 1998. 273(33): p. 21298-21308.

51. Skoko, D., et al., Mechanism of Chromosome Compaction and Looping by the Escherichia coli Nucleoid Protein Fis. Journal of Molecular Biology, 2006. 364(4): p. 777-798.

52. Cho, B.-K., et al., Genome-wide analysis of Fis binding in Escherichia coli indicates a causative role for A-/AT-tracts. Genome Research, 2008. 18(6): p. 900-910.

53. Schneider, R., et al., An architectural role of the Escherichia coli chromatin protein FIS in organising DNA. Nucleic Acids Research, 2001. 29(24): p. 5107-5114.

54. Pan, C.Q., et al., Variable Structures of Fis-DNA Complexes Determined by Flanking DNA – Protein Contacts. Journal of Molecular Biology, 1996. 264(4): p. 675-695.

55. Zhang, J., et al., Multiple Site-Specific Binding of Fis Protein to Escherichia coli nuoA-N Promoter DNA and its Impact on DNA Topology Visualised by Means of Scanning Force Microscopy. ChemBioChem, 2004. 5(9): p. 1286-1289.

56. Schnetz, K., Fine-tuned growth phase control of dps, encoding a DNA protection protein, by FIS and H-NS. Molecular Microbiology, 2008. 68(6): p. 1345-1347.

57. McLeod, S.M., et al., The C-terminal domains of the RNA polymerase α subunits: contact site with fis and localization during co-activation with CRP at the Escherichia coli proP P2 promoter1. Journal of Molecular Biology, 2002. 316(3): p. 517-529.

58. Ali Azam, T., et al., Growth Phase-Dependent Variation in Protein Composition of the Escherichia coli Nucleoid. Journal of Bacteriology, 1999. 181(20): p. 6361-6370.

59. Hirsch, M. and T. Elliott, Fis Regulates Transcriptional Induction of RpoS in Salmonella enterica. Journal of Bacteriology, 2005. 187(5): p. 1568-1580.

60. Ball, C.A., et al., Dramatic changes in Fis levels upon nutrient upshift in Escherichia coli. Journal of Bacteriology, 1992. 174(24): p. 8043-8056.

61. Finkel, S.E. and R.C. Johnson, The Fis protein: it's not just for DNA inversion anymore. Molecular Microbiology, 1992. 6(22): p. 3257-3265.

62. Nilsson, L., et al., FIS-dependent trans activation of stable RNA operons of Escherichia coli under various growth conditions. Journal of Bacteriology, 1992. 174(3): p. 921-929.

63. Hommais, F., et al., Large-scale monitoring of pleiotropic regulation of gene expression by the prokaryotic nucleoid-associated protein, H-NS. Molecular Microbiology, 2001. 40(1): p. 20-36.

64. Dorman, C.J., J.C.D. Hinton, and A. Free, Domain organization and oligomerization among H-NS-like nucleoid-associated proteins in bacteria. Trends in Microbiology, 1999. 7(3): p. 124-128.

65. Oliver Schröder, R.W., The bacterial regulatory protein H-NS--a versatile modulator of nucleic acid structures. Biological Chemistry, 2002. 383(6): p. 945-960.

66. Spassky, A., et al., H1a, an E. coli DNA-binding protein which accumulates in stationary phase, strongly compacts DNA in vitro. Nucleic Acids Research, 1984. 12(13): p. 5321-5340.

67. Badaut, C., et al., The Degree of Oligomerization of the H-NS Nucleoid Structuring Protein Is Related to Specific Binding to DNA. Journal of Biological Chemistry, 2002. 277(44): p. 41657-41666.

68. Bloch, V., et al., The H-NS dimerization domain defines a new fold contributing to DNA recognition. Nat Struct Mol Biol, 2003. 10(3): p. 212-218.

69. Smyth, C.P., et al., Oligomerization of the chromatin-structuring protein H-NS. Molecular Microbiology, 2000. 36(4): p. 962-972.

70. Dame, R.T., C. Wyman, and N. Goosen, H-NS mediated compaction of DNA visualised by atomic force microscopy. Nucleic Acids Research, 2000. 28(18): p. 3504-3510.

71. Hinton, J.C.D., et al., Expression and mutational analysis of the nucleoid-associated protein H-NS of Salmonella typhimurium. Molecular Microbiology, 1992. 6(16): p. 2327-2337.

72. Zhang, A., et al., Escherichia coli protein analogs StpA and H-NS: regulatory loops, similar and disparate effects on nucleic acid dynamics. The EMBO Journal, 1996. 15(6): p. 1340-1349.

73. Vivero, A., et al., Modulation of Horizontally Acquired Genes by the Hha-YdgT Proteins in Salmonella enterica Serovar Typhimurium. Journal of Bacteriology, 2008. 190(3): p. 1152-1156.

74. Madrid, C., et al., The novel Hha/YmoA family of nucleoid-associated proteins: use of structural mimicry to modulate the activity of the H-NS family of proteins. Molecular Microbiology, 2007. 63(1): p. 7-14.

75. Cho, B.-K., et al., Genome-scale reconstruction of the Lrp regulatory network in Escherichia coli. Proceedings of the National Academy of Sciences, 2008. 105(49): p. 19462-19467.

76. Calvo, J.M. and R.G. Matthews, The leucine-responsive regulatory protein, a global regulator of metabolism in Escherichia coli. Microbiological Reviews, 1994. 58(3): p. 466-490.

77. E B Newman, a. and R. Lin, Leucine-Responsive Regulatory Protein: A Global Regulator of Gene Expression in E. Coli. Annual Review of Microbiology, 1995. 49(1): p. 747-775.

78. Tapias, A., G. López, and S. Ayora, Bacillus subtilis LrpC is a sequence-independent DNA-binding and DNA-bending protein which bridges DNA. Nucleic Acids Research, 2000. 28(2): p. 552-559.

79. Beloin, C., et al., Contribution of DNA Conformation and Topology in Right-handed DNA Wrapping by the Bacillus subtilis LrpC Protein. Journal of Biological Chemistry, 2003. 278(7): p. 5333-5342.

80. Jafri, S., et al., An Lrp-type transcriptional regulator from Agrobacterium tumefaciens condenses more than 100 nucleotides of DNA into globular nucleoprotein complexes1. Journal of Molecular Biology, 1999. 288(5): p. 811-824.

81. Wang, Q. and J.M. Calvo, Lrp, a major regulatory protein in Escherichia coli, bends DNA and can organize the assembly of a higher-order nucleoprotein structure. The EMBO Journal, 1993. 12(6): p. 2495-2501.

82. Strunnikov, A.V., V.L. Larionov, and D. Koshland, SMC1: an essential yeast gene encoding a putative head-rod-tail protein is required for nuclear division and defines a new ubiquitous protein family. The Journal of Cell Biology, 1993. 123(6): p. 1635.

83. Saka, Y., et al., Fission yeast cut3 and cut14, members of a ubiquitous protein family, are required for chromosome condensation and segregation in mitosis. The EMBO Journal, 1994. 13(20): p. 4938-4952.

84. Hirano, T. and T.J. Mitchison, A heterodimeric coiled-coil protein required for mitotic chromosome condensation in vitro. Cell, 1994. 79(3): p. 449-458.

85. Localization of topoisomerase II in mitotic chromosomes. The Journal of Cell Biology, 1985. 100(5): p. 1716-1725.

86. Saitoh, N., et al., ScII: an abundant chromosome scaffold protein is a member of a family of putative ATPases with an unusual predicted tertiary structure. The Journal of Cell Biology, 1994. 127(2): p. 303.

87. Nolivos, S. and D. Sherratt, The bacterial chromosome: architecture and action of bacterial SMC and SMC-like complexes. FEMS Microbiology Reviews, 2014. 38(3): p. 380-392.

88. Haering, K.N.a.C.H., THE STRUCTURE AND FUNCTION OF SMC AND KLEISIN COMPLEXES. Annual Review of Biochemistry, 2005. 74: p. 595-648.

89. Melby, T.E., et al., The Symmetrical Structure of Structural Maintenance of Chromosomes (SMC) and MukB Proteins: Long, Antiparallel Coiled Coils, Folded at a Flexible Hinge. The Journal of Cell Biology, 1998. 142(6): p. 1595-1604.

90. Anderson, D.E., et al., Condensin and cohesin display different arm conformations with characteristic hinge angles. The Journal of Cell Biology, 2002. 156(3): p. 419-424.

91. Palecek, Jan J. and S. Gruber, Kite Proteins: a Superfamily of SMC/Kleisin Partners Conserved Across Bacteria, Archaea, and Eukaryotes. Structure, 2015. 23(12): p. 2183-2190.

92. Ezaki, B., et al., Partitioning of a mini-F plasmid into anucleate cells of the mukB null mutant. Journal of Bacteriology, 1991. 173(20): p. 6643-6646.

93. Hiraga, S., et al., Bidirectional migration of SeqA-bound hemimethylated DNA clusters and pairing of oriC copies in Escherichia coli. Genes to Cells, 2000. 5(5): p. 327-341.

94. Mascarenhas, J., et al., Cell cycle-dependent localization of two novel prokaryotic chromosome segregation and condensation proteins in Bacillus subtilis that interact with SMC protein. The EMBO Journal, 2002. 21(12): p. 3108-3118.

95. Soppa, J., et al., Discovery of two novel families of proteins that are proposed to interact with prokaryotic SMC proteins, and characterization of the Bacillus subtilis family members ScpA and ScpB. Molecular Microbiology, 2002. 45(1): p. 59-71.

96. Cobbe, N. and M.M.S. Heck, The Evolution of SMC Proteins: Phylogenetic Analysis and Structural Implications. Molecular Biology and Evolution, 2004. 21(2): p. 332-347.

97. Hirano, T., Condensins: universal organizers of chromosomes with diverse functions. Genes & Development, 2012. 26(15): p. 1659-1678.

98. Hirano, T., Chromosome Cohesion, Condensation, and Separation. Annual Review of Biochemistry, 2000. 69(1): p. 115-144.

99. Michaelis, C., R. Ciosk, and K. Nasmyth, Cohesins: Chromosomal Proteins that Prevent Premature Separation of Sister Chromatids. Cell, 1997. 91(1): p. 35-45.

100. Fousteri, M.I. and A.R. Lehmann, A novel SMC protein complex in Schizosaccharomyces pombe contains the Rad18 DNA repair protein. The EMBO Journal, 2000. 19(7): p. 1691-1702.

101. Taylor, E.M., et al., Characterization of a Novel Human SMC Heterodimer Homologous to the Schizosaccharomyces pombe Rad18/Spr18 Complex. Molecular Biology of the Cell, 2001. 12(6): p. 1583-1594.

102. Stephan, A.K., et al., Roles of Vertebrate Smc5 in Sister Chromatid Cohesion and Homologous Recombinational Repair. Molecular and Cellular Biology, 2011. 31(7): p. 1369-1381.

103. Petrushenko, Z.M., et al., Mechanics of DNA bridging by bacterial condensin MukBEF in vitro and in singulo. The EMBO Journal, 2010. 29(6): p. 1126-1135.

104. Petrushenko, Z.M., C.-H. Lai, and V.V. Rybenkov, Antagonistic Interactions of Kleisins and DNA with Bacterial Condensin MukB. Journal of Biological Chemistry, 2006. 281(45): p. 34208-34217.

105. Shin, H.-C., et al., Focal localization of MukBEF condensin on the chromosome requires the flexible linker region of MukF. FEBS Journal, 2009. 276(18): p. 5101-5110.

106. Ohsumi, K., M. Yamazoe, and S. Hiraga, Different localization of SeqA-bound nascent DNA clusters and MukF–MukE–MukB complex in Escherichia coli cells. Molecular Microbiology, 2001. 40(4): p. 835-845.

107. She, W., et al., MukEF Is Required for Stable Association of MukB with the Chromosome. Journal of Bacteriology, 2007. 189(19): p. 7062-7068.

108. Minnen, A., et al., SMC is recruited to oriC by ParB and promotes chromosome segregation in Streptococcus pneumoniae. Molecular Microbiology, 2011. 81(3): p. 676-688.

109. Wang, X., P.M. Llopis, and D.Z. Rudner, Organization and segregation of bacterial chromosomes. Nature reviews. Genetics, 2013. 14(3): p. 10.1038/nrg3375.

110. Niki, H., Y. Yamaichi, and S. Hiraga, Dynamic organization of chromosomal DNA in Escherichia coli. Genes & Development, 2000. 14(2): p. 212-223.

111. Valens, M., et al., Macrodomain organization of the Escherichia coli chromosome. The EMBO Journal, 2004. 23(21): p. 4330.

112. Duigou, S. and F. Boccard, Long range chromosome organization in Escherichia coli: The position of the replication origin defines the non-structured regions and the Right and Left macrodomains. PLOS Genetics, 2017. 13(5): p. e1006758.

113. Mercier, R., et al., The MatP/matS Site-Specific System Organizes the Terminus Region of the E. coli Chromosome into a Macrodomain. Cell, 2008. 135(3): p. 475-485.

114. Dupaigne, P., et al., Molecular Basis for a Protein-Mediated DNA-Bridging Mechanism that Functions in Condensation of the E. coli Chromosome. Molecular Cell, 2012. 48(4): p. 560-571.

115. Espéli, O., et al., A MatP–divisome interaction coordinates chromosome segregation with cell division in <em>E. coli</em&gt. The EMBO Journal, 2012. 31(14): p. 3198.

116. Valens, M., A. Thiel, and F. Boccard, The MaoP/maoS Site-Specific System Organizes the Ori Region of the E. coli Chromosome into a Macrodomain. PLOS Genetics, 2016. 12(9): p. e1006309.

117. Viollier, P.H., et al., Rapid and sequential movement of individual chromosomal loci to specific subcellular locations during bacterial DNA replication. Proceedings of the National Academy of Sciences of the United States of America, 2004. 101(25): p. 9257-9262.

118. Le, T.B.K. and M.T. Laub, New approaches to understanding the spatial organization of bacterial genomes. Current opinion in microbiology, 2014. 22: p. 15-21.

119. Umbarger, Mark A., et al., The Three-Dimensional Architecture of a Bacterial Genome and Its Alteration by Genetic Perturbation. Molecular Cell, 2011. 44(2): p. 252-264.

120. Harms, A., et al., Tracking of Chromosome and Replisome Dynamics in Myxococcus xanthus Reveals a Novel Chromosome Arrangement. PLOS Genetics, 2013. 9(9): p. e1003802.

121. Fogel, M.A. and M.K. Waldor, Distinct segregation dynamics of the two Vibrio cholerae chromosomes. Molecular Microbiology, 2005. 55(1): p. 125-136.

122. Nielsen, H.J., et al., The Escherichia coli chromosome is organized with the left and right chromosome arms in separate cell halves. Molecular Microbiology, 2006. 62(2): p. 331-338.

123. Wang, X., P. Montero Llopis, and D.Z. Rudner, Bacillus subtilis chromosome organization oscillates between two distinct patterns. Proceedings of the National Academy of Sciences, 2014. 111(35): p. 12877-12882.

124. Fogel, M.A. and M.K. Waldor, A dynamic, mitotic-like mechanism for bacterial chromosome segregation. Genes & Development, 2006. 20(23): p. 3269-3282.

125. Ireton, K., N.W. Gunther, and A.D. Grossman, spo0J is required for normal chromosome segregation as well as the initiation of sporulation in Bacillus subtilis. Journal of Bacteriology, 1994. 176(17): p. 5320-5329.

126. Lin, D.C.-H. and A.D. Grossman, Identification and Characterization of a Bacterial Chromosome Partitioning Site. Cell, 1998. 92(5): p. 675-685.

127. Mohl, D.A., J. Easter, and J.W. Gober, The chromosome partitioning protein, ParB, is required for cytokinesis in Caulobacter crescentus. Molecular Microbiology, 2001. 42(3): p. 741-755.

128. Livny, J., Y. Yamaichi, and M.K. Waldor, Distribution of Centromere-Like parS Sites in Bacteria: Insights from Comparative Genomics. Journal of Bacteriology, 2007. 189(23): p. 8693-8703.

129. Bartosik, A.A., et al., ParB of Pseudomonas aeruginosa: Interactions with Its Partner ParA and Its Target parS and Specific Effects on Bacterial Growth. Journal of Bacteriology, 2004. 186(20): p. 6983-6998.

130. Dubarry, N., F. Pasta, and D. Lane, ParABS Systems of the Four Replicons of Burkholderia cenocepacia: New Chromosome Centromeres Confer Partition Specificity. Journal of Bacteriology, 2006. 188(4): p. 1489-1496.

131. Shebelut, C.W., et al., Caulobacter chromosome segregation is an ordered multistep process. Proceedings of the National Academy of

Sciences of the United States of America, 2010. 107(32): p. 14194-14198.

132. Ptacin, J.L., et al., A spindle-like apparatus guides bacterial chromosome segregation. Nature cell biology, 2010. 12(8): p. 791-798.

133. Gerdes, K., M. Howard, and F. Szardenings, Pushing and Pulling in Prokaryotic DNA Segregation. Cell, 2010. 141(6): p. 927-942.

134. Jun, S. and B. Mulder, Entropy-driven spatial organization of highly confined polymers: Lessons for the bacterial chromosome. Proceedings of the National Academy of Sciences of the United States of America, 2006. 103(33): p. 12388-12393.

135. Jun, S. and A. Wright, Entropy as the driver of chromosome segregation. Nature reviews. Microbiology, 2010. 8(8): p. 600-607.

136. Fisher, J.K., et al., Four dimensional imaging of E. coli nucleoid organization and dynamics in living cells. Cell, 2013. 153(4): p. 882-895.

137. Yazdi, N.H., et al., Variation of the folding and dynamics of the Escherichia coli chromosome with growth conditions. Molecular Microbiology, 2012. 86(6): p. 1318-1333.

138. Kleckner, N., et al., The Bacterial Nucleoid: Nature, Dynamics and Sister Segregation. Current opinion in microbiology, 2014. 22: p. 127-137.

139. Lemon, K.P. and A.D. Grossman, Localization of Bacterial DNA Polymerase: Evidence for a Factory Model of Replication. Science, 1998. 282(5393): p. 1516.

140. Lyczak, J.B., C.L. Cannon, and G.B. Pier, Establishment of Pseudomonas aeruginosa infection: lessons from a versatile opportunist1*Address for correspondence: Channing Laboratory, 181 Longwood Avenue, Boston, MA 02115, USA. Microbes and Infection, 2000. 2(9): p. 1051-1060.

141. Hidron, A.I., et al., Antimicrobial-Resistant Pathogens Associated With Healthcare-Associated Infections: Annual Summary of Data Reported to the National Healthcare Safety Network at the Centers for Disease Control and Prevention, 2006–2007. Infection Control; Hospital Epidemiology, 2008. 29(11): p. 996-1011.

142. Chastre, J. and J.-Y. Fagon, Ventilator-associated Pneumonia. American Journal of Respiratory and Critical Care Medicine, 2002. 165(7): p. 867-903.

143. Winsor, G.L., et al., Enhanced annotations and features for comparing thousands of Pseudomonas genomes in the Pseudomonas genome database. Nucleic Acids Research, 2016. 44(D1): p. D646-D653.

144. Silby, M.W., et al., Pseudomonas genomes: diverse and adaptable. FEMS Microbiology Reviews, 2011. 35(4): p. 652.

145. Yee, T.W. and D.W. Smith, Pseudomonas chromosomal replication origins: a bacterial class distinct from Escherichia coli-type origins. Proceedings of the National Academy of Sciences of the United States of America, 1990. 87(4): p. 1278-1282.

146. Jiang, Y., et al., Functional analysis of two putative chromosomal replication origins from Pseudomonas aeruginosa. Plasmid, 2006. 55(3): p. 194-200.

147. Mathee, K., et al., Dynamics of Pseudomonas aeruginosa genome evolution. Proceedings of the National Academy of Sciences of the United States of America, 2008. 105(8): p. 3100-3105.

148. Jecz, P., et al., A Single parS Sequence from the Cluster of Four Sites Closest to oriC Is Necessary and Sufficient for Proper Chromosome Segregation in Pseudomonas aeruginosa. PLOS ONE, 2015. 10(3): p. e0120867.

149. Vallet-Gely, I. and F. Boccard, Chromosomal Organization and Segregation in Pseudomonas aeruginosa. PLOS Genetics, 2013. 9(5): p. e1003492.

150. Klockgether, J., et al., Genome Diversity of Pseudomonas aeruginosa PAO1 Laboratory Strains. Journal of Bacteriology, 2010. 192(4): p. 1113-1121.

151. Hmelo, L.R., et al., Precision-engineering the Pseudomonas aeruginosa genome with two-step allelic exchange. Nat. Protocols, 2015. 10(11): p. 1820-1841.

152. Wang, Q., et al., Chromosome Condensation in the Absence of the Non-SMC Subunits of MukBEF. Journal of Bacteriology, 2006. 188(12): p. 4431-4441.

153. Edelstein, A.D., et al., Advanced methods of microscope control using μManager software. 2014, 2014.

154. Schneider, C.A., W.S. Rasband, and K.W. Eliceiri, NIH Image to ImageJ: 25 years of image analysis. Nat Meth, 2012. 9(7): p. 671-675.

155. Levchenko, I., et al., A Specificity-Enhancing Factor for the ClpXP Degradation Machine. Science, 2000. 289(5488): p. 2354-2356.

156. Wah, D.A., et al., Flexible Linkers Leash the Substrate Binding Domain of SspB to a Peptide Module that Stabilizes Delivery Complexes with the AAA+ ClpXP Protease. Molecular Cell, 2003. 12(2): p. 355-363.

157. McGinness, K.E., T.A. Baker, and R.T. Sauer, Engineering Controllable Protein Degradation. Molecular Cell, 2006. 22(5): p. 701-707.

158. Zhao, H., Unpublished data. Unpublished Article, 2017.

159. Petrushenko, Z.M., et al., DNA Reshaping by MukB RIGHT-HANDED KNOTTING, LEFT-HANDED SUPERCOILING. Journal of Biological Chemistry, 2006. 281(8): p. 4606-4615.

160. Donovan, C., et al., A synthetic Escherichia coli system identifies a conserved origin tethering factor in Actinobacteria. Molecular Microbiology, 2012. 84(1): p. 105-116.

161. Hoang, T.T., et al., A broad-host-range Flp-FRT recombination system for site-specific excision of chromosomally-located DNA sequences: application for isolation of unmarked Pseudomonas aeruginosa mutants. Gene, 1998. 212(1): p. 77-86.

162. Castang, S., et al., H-NS family members function coordinately in an opportunistic pathogen. Proceedings of the National Academy of Sciences, 2008. 105(48): p. 18947-18952.